Loss of Insulin Receptor Substrates 1 and 2 Suppresses Kras-Driven Non-Small Cell Lung Cancer

Permanent link

Terms of Use

Share Your Story

The Harvard community has made this article openly available.
Please share how this access benefits you. Submit a story .

Accessibility

HARVARD UNIVERSITY
Graduate School of Arts and Sciences

DISSERTATION ACCEPTANCE CERTIFICATE

The undersigned, appointed by the

Division of Medical Sciences

in the subject of Biological and Biomedical Sciences

have examined a dissertation entitled

Loss of Insulin Receptor Substrates 1 and 2 Suppresses Kras-driven Non-Small Cell Lung Cancer

presented by He (Clare) Xu

candidate for the degree of Doctor of Philosophy and hereby
certify that it is worthy of acceptance.

Signature: _____

Typed Name: Dr. Alex Toker

Signature: _____
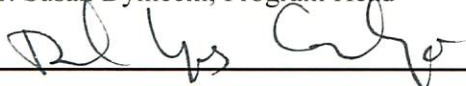
Typed Name: Dr. Kevin Haigis

Signature: _____

Typed Name: Dr. Richard Possemato

_____
Dr. Susan Dymecki, Program Head

Date: June 01, 2017

_____
Dr. David Lopes Cardozo, Director of Graduate Studies

Loss of Insulin Receptor Substrates 1 and 2 Suppresses *Kras*-driven Non-Small Cell Lung

Cancer

A dissertation presented

by

He (Clare) Xu

to

The Division of Medical Sciences

in partial fulfillment of the requirements

for the degree of

Doctor of Philosophy

in the subject of

Biological and Biomedical Sciences

Harvard University

Cambridge, Massachusetts

June 2017

Dissertation Advisor: Professor Nada Kalaany   He (Clare) Xu

Loss of Insulin Receptor Substrates 1 and 2 Suppresses *Kras*-driven Non-Small Cell

Lung Cancer

Abstract

Lung cancer remains the leading cause of cancer death worldwide, with non-small cell lung cancer (NSCLC) being the majority of diagnosed cases of lung cancer. Mutant *KRAS* is found in about 25% of all NSCLC and has proved to be extraordinarily difficult to directly target for therapeutic purposes. It has been demonstrated that mutant *KRAS* directly binds to and activates PI3K, and this interaction is required for the initiation and maintenance of NSCLC in mice. However, it has remained controversial whether signaling from upstream insulin receptor (IR) and insulin-like growth factor 1 receptor (IGF-1R) contributes to tumorigenesis in the context of activated *KRAS*, and whether the upstream signaling represents a potential strategy for therapeutic targeting.

Using a conditional mouse model of lung tumorigenesis driven by activated *Kras* and loss of tumor suppressor *p53*, I have demonstrated that concomitant lung-specific genetic ablation of insulin receptor substrates 1 and 2 (*Irs1* and *Irs2*), which mediate signaling from IR and IGF-1R, inhibits *Kras*-driven tumor development and significantly extends the survival of mice. However, mice eventually overcome the loss of *Irs1* and *Irs2* and succumb to lung cancer with a varied but significantly longer latency. Through proteomic characterizations of mouse cell lines established from these tumors, I discovered that tumor cells with loss of *Irs1* and *Irs2* demonstrate severely suppressed Akt and downstream effector

signaling. Metabolic profiling also revealed that loss of *Irs1* and *Irs2* results in dramatically decreased levels of intracellular amino acids. Similar signaling and metabolic alterations were found in human *KRAS*-mutant NSCLC cells with double knockout or double knockdown of *IRS1* and *IRS2*, accompanied by enhanced basal autophagy and sensitivity to autophagy and proteasome inhibitors. Acute pharmacological inhibition of IR/IGF-1R signaling in both murine and human *KRAS*-mutant lung cancer cells also results in decreased intracellular amino acid levels and increased basal autophagy. Therefore, my research demonstrated that Irs1 and Irs2-mediated IR/IGF-1R signaling is essential to *KRAS*-driven lung tumorigenesis. More importantly, these studies identified amino acid metabolism as a vulnerability in cells that overcome IR/IGF-1R inhibition. Consequently, combinatorial targeting of IR/IGF-1R with autophagy or proteasome inhibitors may represent a viable therapeutic strategy in *KRAS*-mutant NSCLC.

<u>**TABLE OF CONTENTS**</u>

LIST OF FIGURES

ACKNOWLEDGMENT

CHAPTER 1: INTRODUCTION

1.1 NON-SMALL CELL LUNG CANCER

1.1.1 Histological subtypes of lung cancer

Lung cancer remains the leading cause of cancer-related deaths worldwide, with more than 85% of all lung cancers being diagnosed as non-small cell lung cancer (NSCLC) (Siegel, Miller, and Jemal 2017; Ettinger et al. 2017). NSCLC is a highly lethal disease with a dismal 5-year survival rate of 17.7% (Ettinger et al. 2017). Clinically, NSCLC is classified as two dominant histological types upon diagnosis, adenocarcinoma (ADC; ~ 50%) and squamous cell carcinoma (SCC; ~ 40%). ADCs generally arise in more distal airways, have glandular histology and express biomarkers associated with the distal lung, such as thyroid transcription factor (TTF1, also known as NKX2-1) and keratin 7 (KRT7) (Davidson, Gazdar, and Clarke, 2013; Langer et al. 2010). By contrast, SCCs arise in more proximal airways and are more strongly associated with smoking and chronic inflammation. SCCs have histology similar to the pseudostratified columnar epithelium that lines trachea and the upper airways. SCCs express biomarkers including cytokeratin 5, cytokeratin 6, the transcription factor SOX2 and p63 (Davidson, Gazdar, and Clarke, 2013; Langer et al. 2010; Lu et al. 2010). A small subset of NSCLC is large cell carcinoma, which is diagnosed by exclusion of both ADC and SCC based on histology and biomarker expression (M. R. Davidson, Gazdar, and Clarke 2013).

1.1.2 Genetic complexity of NSCLC

Although histological features and biomarker expression remain the basis of clinical tumor diagnosis, recent advances in high-throughput genomic sequencing have allowed researchers to examine the breadth of genetic mutations in lung cancers. NSCLC is a genetically complex disease, with a number of oncogenes and tumor suppressor genes

affected in majority of cases. Mutant *KRAS* is the most common oncogene, found in about 25% of all NSCLC cases as a dominant driver of tumorigenesis (Ettinger et al. 2017). *EGFR* mutations are also frequently encountered as a driver oncogene in NSCLC, found in about 10% of Caucasian patients and 35% of East Asian patients (Lynch et al. 2004; J. G. Paez et al. 2004; Pao et al. 2004). Other mutations that are commonly found in oncogenes include *BRAF, PIK3CA*, *MET* and the small GTPase *RIT1* (Collisson et al. 2014; Lynch et al. 2004; J Guillermo Paez et al. 2004; Pao et al. 2004; J. A. Engelman et al. 2007). Further recurrent mutations and amplifications have been identified in *HER2* (also knowns as *ERBB2*), fibroblast growth factor receptor 1 (*FGFR1*) and *FGFR2*, as well as fusion oncogenes involving anaplastic lymphoma kinase (*ALK*), the *ROS1* receptor tyrosine kinase, neuregulin 1 (*NRG1)*, neurotrophic tyrosine kinase receptor type 1 (*NTRK1*) and *RET* (Fernandez-Cuesta et al. 2014; Kohno et al. 2012; Soda et al. 2007; Vaishnavi et al. 2013; Stephens et al. 2004; Weiss et al. 2010; Ding et al. 2008; Imielinski et al. 2012; Heist and Engelman 2012). *TP53* is the most commonly mutated tumor suppressor in NSCLC, occurring in about 46% of all cases. Other tumor suppressors that have been reported to be mutated in NSCLC include *STK11*, *KEAP1*, *NF1*, *RB1* and *CDKN2A* (Collisson et al. 2014). An important challenge that remains in the field is to understand how each of these oncogenes and tumor suppressors contributes to lung tumorigenesis and disease progression, as well as how they can be best exploited for therapeutic purposes. One of these oncogenes, *KRAS*, has been the subject of intense research due to its prevalence in human cancers and its potent oncogenic effects.

1.2 <u>MUTANT *KRAS* IN HUMAN CANCERS</u>

1.2.1 The RAS signaling pathways

The *RAS* gene family (*HRAS*, *KRAS* and *NRAS*) is the most frequently mutated

oncogene family in human cancers with *KRAS* accounting for 86% of all *RAS*-driven cancers

(Cox et al. 2014). RAS is a membrane-associated small GTP-binding protein that regulates

cell proliferation, survival, motility and metabolism in response to extracellular stimuli

through upstream growth factor receptors, such as activation of epidermal growth factor

receptor (EGFR) or T-cell receptor (TCR) (Cox et al. 2014). When bound to GDP, RAS

proteins are inactive. Upon exchange of GDP to GTP, RAS is activated and stimulates

multiple downstream effector pathways (Fig. 1.1). The RAF-MEK-ERK pathway is the

prototypical mitogen-activated protein kinase (MAPK) cascade that culminates in

transcription of pro-survival, mitogenic genes (Cox et al. 2014). The PI3K-AKT-mTOR

pathway also contributes to cell growth, proliferation as well as protein synthesis downstream

of *RAS*, though there has been evidence suggesting that basal signaling from upstream

receptor tyrosine kinases (RTKs) is necessary for RAS-mediated activation of this pathway

(Molina-Arcas et al. 2013). A third major effector pathway is the Ral GTPase pathway that

results in increased endocytosis and activation of transcription factors Jun and Fos (Stephen et

al. 2014). GTP-bound RAS becomes deactivated by its intrinsic GTPase activity shortly after

activation. However, the intrinsic GTPase activity of RAS is rather low and needs to be

activated by GTPase-activating proteins (GAPs) such as neurofibromin, encoded by the NF1

gene, and p120GAP (Boguski and McCormick 1993; Donovan, Shannon, and Bollag 2002).

Activation of RAS occurs through guanine nucleotide exchange factors (GEFs) such as SOS

and RasGRP1, which catalyze the exchange of RAS-bound GDP with free GTP (Schubbert,

Shannon, and Bollag 2007). Oncogenic mutations in *RAS* render the proteins unresponsive to the action of GAPs and hence constitutively GTP-bound and active.
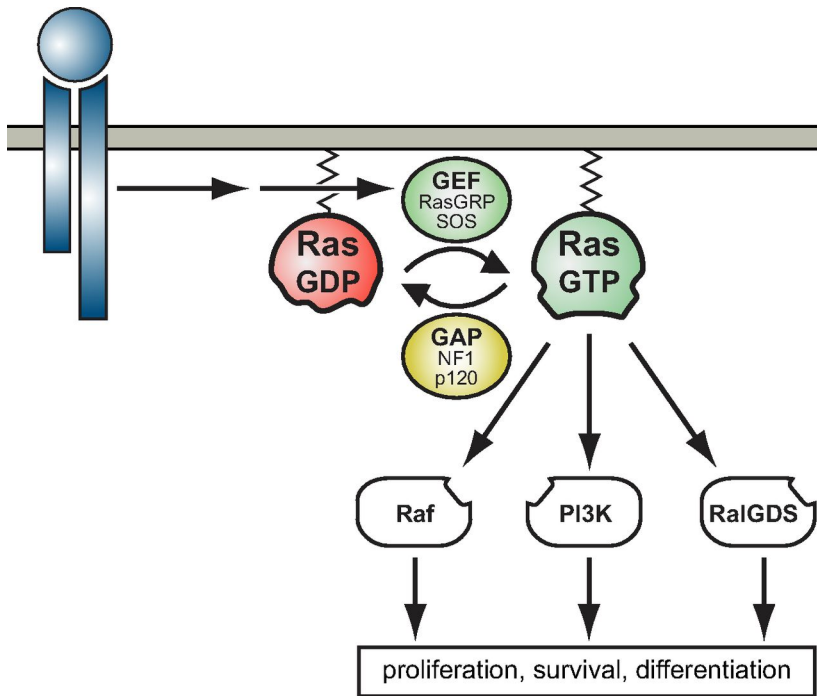
Figure 1.1. The RAS switch.

The RAS proteins oscillate between a GDP-bound, inactive state and a GTP-bound, active state. Transmembrane receptor signaling recruits RAS guanine nucleotide exchange factors (GEFs) such as SOS and RasGRP1 to the cell membrane, where they catalyze the exchange of GDP for GTP and activate RAS, which in turn activates multiple downstream signaling pathways that regulate cell proliferation, survival and differentiation. RAS possesses low intrinsic GTP hydrolysis activity that needs to be accelerated by GTPase activating proteins (GAPs) such as NF1 and p120GAP. Figure reprinted from Ward, Braun, and Shannon 2012.

1.2.2 *KRAS* mutations in NSCLC

KRAS mutations are found in about 30% of ADCs and about 5% of SCCs (Korpanty et al. 2014). They are more frequently present in patients with smoking history than in never-smokers, as well as in Caucasian patients than in Asian patients (Riely et al. 2008; Roberts and Der 2007). Most *KRAS* mutations in NSCLC are single base pair substitutions in codon 12 (80%), and to a lesser extent codon 13 and 61, which result in the substitution of a single amino acid in the protein (Prior, Lewis, and Mattos 2012). In patients with smoking history, *KRAS* mutations are usually transversions (G $\rightarrow$ T or G $\rightarrow$ C), whereas in never-smokers transitions (G $\rightarrow$ A and C$\rightarrow$ T) are more common (Riely et al. 2008). *KRAS* mutations are almost always mutually exclusive with *EGFR* and *BRAF* mutations as they are part of the same signal transduction pathway (Schmid et al. 2009; Eberhard et al. 2005).

Despite decades of advancement in our understanding of the molecular etiology of NSCLC, particularly the role of *KRAS* mutations in driving tumor formation, treatment options for patients with *KRAS*-mutant NSCLC are still very limited. KRAS has proven to be an elusive target for direct inhibition by small molecules (Cox et al. 2014; Ostrem and Shokat 2016). Most efforts currently focus on inhibiting signaling cascades downstream of activated *KRAS* such as the RAF-MEK-ERK pathway and the PI3K-AKT pathway (Engelman et al. 2008; Roberts and Der 2007; Jänne et al. 2013; Gandara et al. 2017; Hanna et al. 2004). However, the clinical benefits of MEK inhibitors, even in combination with other agents, are somewhat modest and are associated with inevitably acquired resistance (Duncan et al. 2012; Hata et al. 2014; Little et al. 2011, 2012; Pettazzoni et al. 2015; Scagliotti et al. 2009). Therefore novel targets and pathways that could improve treatment outcome for patients with *KRAS*-mutant NSCLC are in critical need.

1.3 IR/IGF-1R AND DOWNSTREAM EFFECTOR SIGNALING

1.3.1 Overview

IR/IGF-1R signaling is an evolutionarily conserved system that regulates cellular metabolism, survival, proliferation, motility and differentiation. In *Caenorhabditis elegans*, signaling molecules related to IR and IGF-1R regulate cell fate and lifespan in relation to nutrient availability (Dong et al. 2007). In zebrafish, *ir* is required for normal embryogenesis (Toyoshima et al. 2008). In humans, insulin was first discovered as a "cure" for diabetes in 1922 (Banting et al. 1922). Other functions such as the pro-survival, anti-apoptotic and mitogenic signaling by the insulin and IGF system have since emerged. This section touches on 1) the signaling cascade of insulin/IGF signaling; 2) its relation to mutant *KRAS*; 3) its involvement in tumorigenesis; 4) targeted IGF-1 therapies as treatment for NSCLC; 5) the specific roles of insulin receptor substrates (IRS) 1 and 2 in mediating signaling in cancer.

1.3.2 Insulin/IGF-1 signaling

The insulin/IGF signaling pathway consists of three ligands - insulin, IGF-1 and IGF-2; three receptor tyrosine kinases - insulin receptor (IR), IGF-1 receptor (IGF-1R) and IGF-2 receptor (IGF-2R); and six serum IGF binding proteins (IGFBP 1-6). Insulin, IGF-1 and IGF-2 are structurally similar peptides that bind to receptors to activate downstream signaling. Insulin functions mostly as a classic hormone. It is mainly produced by pancreatic β-cells in response to circulating glucose, and signals peripheral metabolic tissues such as muscle and adipose tissue to take up glucose. IGF-1 and IGF-2, on the other hand, are widely expressed by many cell types, and autocrine expression and signaling by transformed cells is common (Pollak 2008). Systemically, IGF-1 and IGF-2 are mainly produced by the liver. Hepatic

production of IGF-1 is stimulated by growth hormone (GH) secreted from the pituitary gland, and is kept in homeostasis via negative feedback that inhibits pituitary GH production. Therefore, IGF-1 functions both as a hormone and as a tissue growth factor as cells can respond to locally produced ligands and to ligands delivered by general circulation.

Insulin and IGF receptors are dimers comprised of two hemireceptors (Fig. 1.2). Each hemireceptor is comprised of an extracellular α subunit that binds to the ligand and a membrane-associated β subunit that functions as a tyrosine kinase. The insulin hemireceptor exists in two splice variant isoforms, IR-A and IR-B, with the former but not the latter, lacking exon 11. The IR-A isoform is known to preferentially mediate the mitogenic effects of insulin signaling while the IR-B isoform mainly mediates the metabolic outcome of insulin signaling (Belfiore et al. 2009). Each insulin receptor (IR) can therefore be formed from two IR-A hemireceptors or two IR-B hemireceptors, and insulin binds to both types of IR. IGF-1 binds to either IGF-1R, which is formed by two IGF-1R hemireceptors, or hybrid receptors that are comprised of one IGF-1R hemireceptor and one insulin hemireceptor (either IR-A or IR-B). IGF-2, on the other hand, binds to both IGF-1R as well as hybrid receptors and IRs that contain IR-A. IGF-2R is a non-signal transducing receptor that mainly serves to bind to and sequester IGF-2, and hence is considered a negative regulator of IGF-2 signaling (Gallagher and LeRoith 2010).
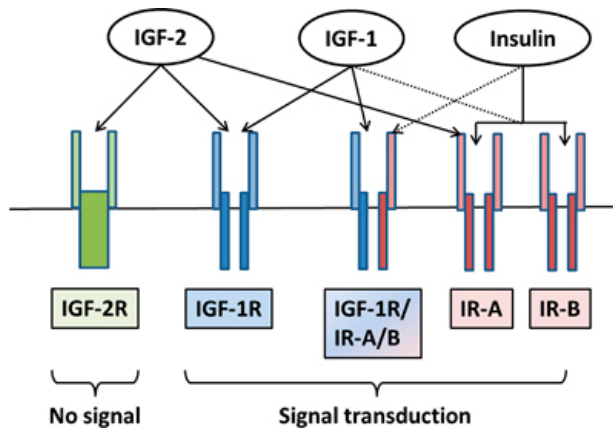
Figure 1.2. Insulin/IGF receptor binding.

IR and IGF receptors consist of two hemireceptors, each of which is comprised of an extracellular ligand-binding domain and a membrane-associated tyrosine kinase domain. Insulin hemireceptors exist in either of two splice variant isoforms, IR-A and IR-B. Insulin binds to both types of IR as well as weakly to hybrid receptors. IGF-1 binds to IGF-1R, hybrid receptors, and weakly to IR. IGF-2, on the other hand, binds to IGF-1R, IR and hybrid receptors containing the IR-A isoform, as well as IGF-2R that does not transduce signal. IR shares about 50% and 80% homology with the ligand-binding and tyrosine kinase domain, respectively, of the IGF-1R (Belfiore et al. 2009). Solid lines indicate high binding affinity and dashed lines indicate low binding affinity. Figure reprinted from Klement and Fink 2016.

The bioactivity of IGFs is modulated by IGFBPs, which bind to both IGF-1 and IGF-2 with high affinity. Of the 6 serum IGFBPs, IGFBP-3 is the most prevalent (Pollak 2008). IGFBPs extend the half-life of IGF-1 and IGF-2 in circulation while making them unavailable to receptor-mediated signaling. Therefore, IGFBPs are generally considered to negatively regulate IGF-1R signaling. Secretion of IGFBPs has been found to be enhanced by the tumor

suppressor p53, as well as other growth inhibitors such as vitamin D, anti-oestrogens, retinoids, and transforming growth factor-β (TGF-β) (Firth and Baxter 2002; Buckbinder et al. 1995; Rozen et al. 1997; Huynh, Yang, and Pollak 1996; Gucev et al. 1996).

Upon binding of ligand to the α subunit of insulin/IGF-1 receptors, the β subunit becomes autophosphorylated on tyrosine residues, which then act as docking sites for signaling adaptor proteins such as insulin receptor substrates (IRS) 1- 4, as well as SHC, phospholipase C (PLC) γ1 and GAB1 (GRB2-associated binding protein 1). These adaptor proteins subsequently activate downstream pathways including the PI3K/AKT/mTOR pathway and the RAF/MEK/ERK pathway among others. Receptor-bound IRS-1 recruits PI3K to the membrane through its p85 regulatory subunit by binding to the Src-homology 2 (SH2) domain on the latter. Binding of p85 to IRS-1 relieves p85 inhibition of the PI3K catalytic subunit p110α, which then converts phosphatidylinositol 4,5-bisphosphate (PIP2) to phosphatidylinositol 3,4,5-trisphosphate (PIP3) at the membrane. PIP3 provides a docking site at the membrane for pleckstrin homology (PH) domain-containing proteins, including AKT and PDK1. AKT is phosphorylated by PDK-1 at T308 and by mTORC2 at S473, achieving full activation by both phosphorylation events. Activated AKT has well over 100 substrates, among which are Forkhead transcription factors (FKHR), p27, MDM2, BAD and BCL-2. AKT phosphorylation of these substrates leads to promotion of cell cycle progression and inhibition of apoptosis (Fig. 1.3, Manning and Toker 2017).

Many of the downstream effects of AKT on cellular growth and metabolism are carried out through the mTORC1 complex. AKT indirectly activates mTORC1 by phosphorylating and inhibiting TSC2, relieving its inhibition of RHEB, a GTPase protein essential for mTORC1 activation. GTP-bound RHEB then activates mTORC1 after the latter

has been recruited to the outer lysosomal membrane following amino acid sensing and regulation by the Rag GTPases (Issam Ben-Sahra and Manning 2017; Bar-Peled and Sabatini 2014). Activated mTORC1 subsequently promotes cell growth by activating a variety of anabolic processes including protein, lipid and nucleotide synthesis (Issam Ben-Sahra and Manning 2017). Active mTORC1 promotes protein synthesis by direct phosphorylation of S6 kinases and 4E-BP1 and 2 (the eukaryotic translation initiation factor 4E, or eIF4E - binding proteins), and by enhancing ribosome biogenesis (Issam Ben-Sahra and Manning 2017; Iadevaia, Liu, and Proud 2014). Lipid synthesis is promoted by activated mTORC1 through its regulation of SREBP transcription factors (Issam Ben-Sahra and Manning 2017). mTORC1 activation acutely stimulates de novo pyrimidine synthesis through S6K1-dependent phosphorylation of CAD, a multifunctional enzyme involving carbamoyl-phosphate synthetase 2, aspartate transcarbamylase, and dihydro-orotase that catalyzes the first three steps in pyrimidine synthesis (Ben-Sahra et al. 2013; Robitaille et al. 2013). mTORC1 activation also enhances de novo purine synthesis by transcriptionally promoting enzymes involved in pentose phosphate pathway (PPP), serine and glycine synthesis, as well as the mitochondrial tetrahydrofolate (mTHF) pathway (Ben-Sahra et al. 2016). Conversely, activated mTORC1 inhibits catabolic processes such as autophagy and lysosomal degradation through its effects on ULK1/2, other proteins involved in autophagosome formation, as well as the master regulator of lysosomal biogenesis TFEB (D. Egan et al. 2011; J. Kim et al. 2011; Puente, Hendrickson, and Jiang 2016; Yuan, Russell, and Guan 2013; Nazio et al. 2013; Peña-Llopis et al. 2011; Settembre et al. 2012; Martina et al. 2012; Settembre et al. 2011; Roczniak-Ferguson et al. 2012).
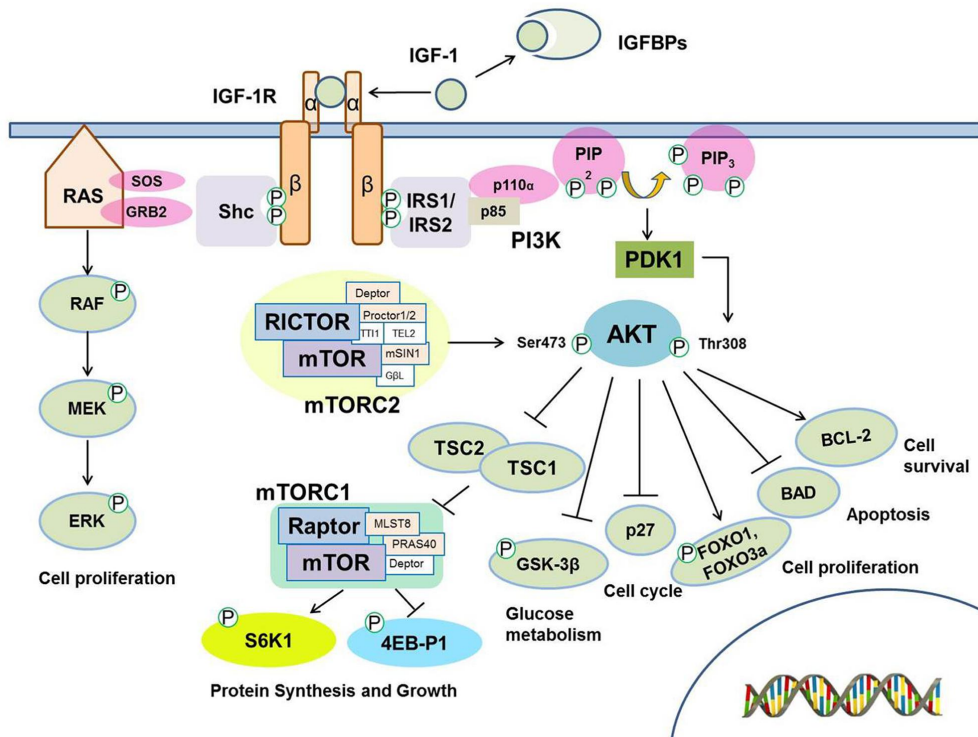
Figure 1.3. The insulin/IGF-1 signaling pathway.

IGFBPs modulate the bioavailability of IGF-1 by binding to it, thus preventing it from engaging with the receptors. Upon binding of ligand to the α subunit of receptors, the β subunit becomes autophosphorylated on tyrosine residues, which then act as docking sites for signaling adaptor proteins including IRS1/2 and Shc that contain phosphotyrosine binding (PTB) domains. These adaptor proteins subsequently activate downstream pathways including the PI3K/AKT/mTOR pathway and the RAF/MEK/ERK pathway among others. Activated AKT phosphorylates large numbers of substrates to promote cell survival, catabolic metabolism, cell proliferation and to inhibit apoptosis. Figure reprinted from Jung and Suh 2015.

1.3.3 KRAS and PI3K/AKT signaling

In addition to the activation of PI3K/AKT signaling and its downstream effectors, insulin and IGF-1 also cross-activate RAS signaling. Phosphorylation of IRS-1 and SHC leads to recruitment of other adaptor proteins such as GRB2 and SOS to the membrane, which bind to and activate RAS and its downstream RAF/MEK/ERK pathway that promotes cell proliferation and growth (Fig. 1.3). Conversely, activated RAS protein directly binds to the catalytic subunit p110 of class I PI3K and activates it (P Rodriguez-Viciana et al. 1997; Pablo Rodriguez-Viciana et al. 1994; Pacold et al. 2000). This interaction has been found to be critical for RAS signaling in normal development and oncogenesis. *Hras*-induced transformation is inhibited in mouse embryonic fibroblasts (MEFs) that express mutant p110α with point mutations in its RAS binding domain (RBD) (Gupta et al. 2007). Transformation by mutant *EGFR*, which activates RAS signaling downstream, is similarly inhibited (Gupta et al. 2007). Same p110α mutants impede *Kras*-driven lung tumorigenesis as well as *Hras*-driven skin carcinogenesis *in vivo* when expressed from the endogenous locus of *pik3ca* (Gupta et al. 2007). Moreover, this p110α-RAS interaction was found to be required for maintenance of established *Kras*-mutant lung tumors. When this interaction is inhibited in an inducible *in vivo* model, *Kras*-mutant lung tumors experience partial regression and sustained tumor stasis in a cell-autonomous manner (Castellano et al. 2013). Notably the ability of RAS to activate PI3K depends on upstream signaling of IGF-1R. In the presence of IGF-1R inhibitors, oncogenic signaling of mutant *KRAS* does not lead to AKT activation in NSCLC cells (Molina-Arcas et al. 2013). Additionally both *RAS*-mutant NSCLC and colorectal cancer cell lines are more sensitive to IGF-1R inhibitors and dependent on IGF-1R-mediated signaling than *RAS*-wild type cell lines *in vitro* (Molina-Arcas et al. 2013). However, whether

upstream IR/IGF-1R signaling is required for *RAS*-mutant tumors to grow *in vivo* has remained controversial and unexplored.

In addition to RAS-PI3K interaction, cross-talk between the RAS-MAPK pathway and the PI3K/AKT pathway also occurs at other signaling nodes. Mutant RAS can induce ERK and its downstream target RSK-mediated phosphorylation of TSC2 and RAPTOR, part of mTORC1 complex, resulting in activation of mTORC1 independent of AKT (Roux et al. 2004; Carriere et al. 2011; Foster et al. 2010). Conversely, activated AKT can negatively regulate ERK activation by phosphorylating inhibitory sites in the Raf N-terminus (Zimmermann and Moelling 1999; Dhillon et al. 2002; Guan et al. 2000). Activated ERK can also phosphorylate GAB1 and inhibit GAB1-mediated recruitment of PI3K to EGFR, hence attenuating PI3K/AKT signaling (Yu, Liu, and Cantley 2002; Lehr et al. 2004).

1.3.4 IR/IGF-1R signaling and tumorigenesis

IR/IGF-1R signaling has been implicated in various diseases including obesity, type 2 diabetes, and cancer. As a result, intense efforts have been devoted to develope viable therapeutic strategies that target this pathway. Epidemiological studies have shown that obesity and type-2 diabetes (T2DM) increase the risk of cancer-associated deaths (Sciacca et al. 2013; Vigneri et al. 2009; Calle 2007; Calle et al. 2003; Calle and Kaaks 2004). Conversely, caloric restriction (CR) leads to reduced tumor burden and decreased tumor progression in a number of different experimental contexts, including xenograft studies and autochthonous models of NSCLC (Kopeina, Senichkin, and Zhivotovsky 2017; Curry et al. 2013). Obesity is characterized by increased circulating levels of insulin and IGF-1, whereas caloric restriction results in decreased circulating levels of both (Dunn et al. 1997; Lashinger

et al. 2011, 2013, 2016; Curry et al. 2013; Dawson et al. 2013). Hence, it has been proposed that the anti-apoptotic, mitogenic effects of IR/IGF-1R signaling promote tumor growth, and may contribute partially to obesity-associated cancer risk (Calle and Kaaks 2004; Calle 2007).

IR/IGF-1R signaling pathway is frequently altered in human tumors, including osteosarcomas, gynecological, gastrointestinal, breast, prostate, and lung cancer (Pollak 2008; Gallagher and LeRoith 2010). Individuals with congenital IGF-1 deficiency are protected from cancer development compared to their relatives without the hormonal deficiency (Gallagher and LeRoith 2010; Pollak 2008). Transgenic mice with liver-specific IGF-1 deficiency (LID) have decreased growth and metastasis of transplanted colon or mammary tumors. Administration of IGF-1 reverses the suppressive effect of IGF-1 deficiency on tumor growth (Wu et al. 2002, 2003). IGF-1R and the IR-A isoform of IR are often overexpressed in human cancers to promote mitogenic signaling of IGF-1/IR-A hybrid receptors as well as IR-A homodimer receptors (Belfiore 2007; Frasca et al. 2008). Specifically, higher circulating levels of IGF-1 in humans is associated with increased risk of lung cancer (H. Yu et al. 1999; Spitz et al. 2002). IGF-1R protein levels have been shown to be high in NSCLC cell lines and patient samples, both in ADCs and SCCs (Tran et al. 2014; Reinmuth et al. 2014) . In addition, IGF-1R expression is associated with poor prognosis in NSCLC patients (Gately et al. 2014). Therefore, various efforts have been undertaken to develop targeted therapies against IR/IGF-1R signaling as a treatment strategy for human cancers including NSCLC.

1.3.5 Targeted IR/IGF-1R therapies in treating NSCLC

Therapeutic strategies to target IGF-1R signaling have included three main classes: antibodies that target the receptor, anti-ligands that bind to and sequester the ligands, as well

as receptor tyrosine kinase inhibitors (TKIs) that inhibit the kinase activity of IR and IGF-1R (Nurwidya et al. 2016). Of the three classes, anti-receptor antibodies have been most widely tested in clinical studies. Success in early-phase clinical trials quickly turned into disappointing outcomes in multiple Phase II and III trials that were terminated early due to lack of efficacy and in some cases severe adverse effects (Langer et al. 2014; Goto et al. 2012; Ramalingam et al. 2011). One of the main challenges to clinical applications of targeted IR/IGF-1R therapies is the lack of predictive biomarkers that can be used to identify patient populations most likely to benefit from such therapies. Tumor expression of IGF-1R protein has not consistently demonstrated predictive value in patients with NSCLC (Kurzrock et al. 2010). However, more recent data have shown that improved disease control and overall survival are associated with elevated pretreatment serum total IGF-1 (Langer et al. 2014; Goto et al. 2012). Active research is under way to identify alternative pathway activation and gene expression profiles associated with IGF-1R signaling dependence in tumors.

In addition to the lack of predictive biomarkers, IGF-1R inhibition often leads to compensatory signaling from IR as well as other RTKs including growth hormone receptor (GHR) and EGFR. In the case of compensatory IR signaling, IGF-1R signaling is no longer needed and downstream AKT activation is restored. Notably, high IR to IGF-1R ratio is associated with increased resistance to IGF-1R inhibitors and tumors resistant to IGF-1R inhibition demonstrate elevated expression of IR and insulin binding to IR (Thariat et al. 2012; Ulanet et al. 2010). Therefore, it stands to reason that therapies that inhibit both IR and IGF-1R signaling, leading to a complete blockade of downstream effector activation might achieve greater efficacy and reduce the risk of resistance in patients.

Systemic IGF-1R inhibition can lead to compensatory pituitary secretion of GH, as it is no longer suppressed via negative feedback by active IGF-1R signaling, which results in increased serum GH levels (Haluska et al. 2010; Moody et al. 2014). GH can lead to activation of PI3K/AKT and MAPK pathways independent of IGF-1R (Felice et al. 2013). Increased serum GH levels also stimulate hepatic production of IGF-1, resulting in higher circulating levels of IGF-1 in patients that may paradoxically increase IGF-1R signaling as well as EGFR signaling (Haluska et al. 2007; Tolcher et al. 2009). Additionally, high serum GH levels have also been linked to insulin resistance due to increased release of hepatic free fatty acids and lipids, hence contributing to hyperglycemic incidences in patients (Møller and Jørgensen 2009).

EGFR signaling is also partially redundant with IGF-1R signaling, leading to activation of AKT and MAPK pathways independent from IGF-1R. EGFR has been shown to heterodimerize with IGF-1R in response to IGF-1 stimulation, and IGF-1 can induce phosphorylation of EGFR (Barnes et al. 2007). As mentioned above, circulating levels of IGF-1 have been observed to increase as a result of IGF-1R inhibition. This can paradoxically result in activation of IGF-1R downstream effectors via EGFR signaling.

Alternative means to block signaling through both IR and IGR-1R without generating the above-mentioned compensatory pathway activation may provide better efficacy and survival benefits for patients. IRS1 and IRS2, as the predominant adaptor proteins that mediate signaling through all forms of IR, IGF-1R, IR/IGF-1R hybrid receptors as well as some signaling through GHR and EGFR, may represent a more effective targeting strategy. Notably, one study has demonstrated that increased expression of IRS2 was associated with figitumumab (anti-IGF-1R antibody) sensitivity (Huang et al. 2015). Independently, cells that

express high levels of both IGF-1R and IRS1 are more sensitive to IGF-1R inhibition (Mukohara et al. 2009). These observations suggest that IRS1 and IRS2 proteins may serve as not only biomarkers indicating dependence on IGF-1R signaling, but also functionally relevant targets to completely inhibit IR/IGF-1R signaling while circumventing the caveats of monotherapies targeting IGF-1R.

1.3.6 IRS1 and IRS2 functions and roles in cancer

Insulin receptor substrates (IRS) are a family of six structurally similar intracellular signaling adaptor proteins that integrate and coordinate extracellular stimuli within the cell (Dearth et al. 2007). Of the six IRSs, IRS1 and IRS2 are widely expressed by different tissues. IRS3 is only expressed in rodents and a human equivalent has not yet been identified. IRS4 expression is limited to the brain and thymus (Dearth et al. 2007). IRS5 and IRS6 are more distantly related to the rest of the IRS family and do not bind to PI3K following insulin induction (Cai et al. 2003). Therefore IRS1 and IRS2 are the predominant adaptor proteins for IR/IGF-1R signaling in the majority of human tissues including the lungs, and hence will remain the focus of this section. IRS1 and IRS2 bind to ligand-phosphorylated IR, IGF-1R or hybrid receptors and become rapidly phosphorylated themselves. In turn they become docking sites for multiple SH2-containing proteins including p85, the regulatory subunit of PI3K, as well as GRB2, the adaptor protein for RAS/MAPK cascade (Taniguchi, Emanuelli, and Kahn 2006).

In addition to their role in relaying PI3K/AKT and RAS/MAPK signal transductions, IRS1 and IRS2 also interact with cytokines, integrins and several hormones in a noncanonical manner. IRS1 and IRS2 mediate cytokine-induced proliferation and protection from apoptosis

via phosphorylation by the Janus cytoplasmic tyrosine kinase family (JAK1, JAK2, JAK3, Tyk2) (Burfoot et al. 1997; Jiang, Harris, and Rothman 2000; Knoops and Renauld 2004; Yenush and White 1997). Activated IRS2 also promotes cellular motility by altering integrin expression through a mechanism involving the small G protein RHOA, focal adhesion kinase (FAK) and Rho-kinase (ROCK) (Lebrun et al. 1998, 2000). Growth hormone (GH), important in human development, and prolactin (PRL), critical for normal mammary gland development, have both been shown to activate IRS1 and IRS2 via growth hormone receptor (GHR) and prolactin receptor (PRLR) and JAK2, inducing downstream PI3K and RAS/MAPK pathway signaling (Yamauchi et al. 1998; L. Liang, Jiang, and Frank 2000; Berlanga et al. 1997). IRS1 and IRS2 are also found in the nucleus and have a variety of nuclear functions including association with the estrogen receptor α (ERα) on estrogen-responsive promoters, as well as binding to upstream binding factor 1 (UBF-1) to regulate RNA polymerase 1 activity (Tu et al. 2002; Sun et al. 2003; Morelli et al. 2004).

IRS1 and IRS2 have been found to be regulated via several negative feedback control loops. IRS proteins contain over 20 serine phosphorylation sites that are direct targets of serine/threonine kinases that inhibit tyrosine phosphorylation. Protein tyrosine phosphatases like SHP2 have been shown to dephosphorylate and inactivate IRS1 (Noguchi et al. 1994). Additionally, IRS1 is phosphorylated by activated p70 S6K downstream of mTORC1 on serine residues that leads to its proteasomal degradation (Haruta et al. 2000). Conversely, pharmacological inhibition of mTORC1, which inhibits downregulation of IRS1, has been shown to upregulate AKT activity through increased IGF-1R and IRS1 (Shi et al. 2005).

IRS1 and IRS2 have been demonstrated to have transforming capabilities and can act as or cooperate with oncogenes. IRS1 overexpression can transform MEFs and is required for

SV40 T antigen-induced transformation (D'Ambrosio et al. 1995; DeAngelis et al. 2006). IRS2 was also able to transform NIH3T3 cells in a foci formation assay (Dearth et al. 2007). In human cancers, IRS1 and IRS2 have been shown to be overexpressed in hepatocellular carcinoma, an extremely aggressive liver cancer characterized by hyperactivation of IR/IGF-1R signaling (Nishiyama and Wands 1992; Nehrbass, Klimek, and Bannasch 1998; Boissan et al. 2005). In addition, IRS1 and IRS2 are found to be involved in cellular survival, proliferation and tumor metastasis in breast cancer (Dearth et al. 2007). IRS levels have also been reported to be increased in pancreatic cancer and IRS1-mediated mitogenic signaling enhances tumor cell proliferation (Bergmann et al. 1996; Bergmann et al. 1996b; Kornmann et al. 1998).

Given the importance of IRS1 and IRS2 in mediating IR/IGF-1R signaling and their role as proto-oncogenes and oncogenic collaborators in multiple cancers, researchers have investigated the therapeutic potential of targeting IRS1 and IRS2. Genetic ablation of *Irs2* has been demonstrated to suppress tumor progression in a mouse model of *Pten*$^{+/-}$ prostate cancer (Szabolcs et al. 2009). Notably, small molecule inhibitors of IRS1 and IRS2 have been developed (Reuveni et al. 2013). This class of compounds is found to bind allosterically to IGF-1R and induce a conformational change, which leads to dissociation of IRS1 and 2 from the receptor. This strengthens the interaction between IGF-1R and SHC, resulting in enhanced MAPK signaling and ERK activation. Activated ERK then promotes serine phosphorylation of IRS1 and 2 and their proteasomal degradation. These compounds are capable of inhibiting growth of *BRAF*$^{V600E/K}$ tumors that are resistant to targeted therapy (Reuveni et al. 2013). They also suppress growth and invasion of osteosarcoma cells *in vitro*, as well as both androgen-

responsive and -independent prostate cancer cell growth *in vitro* and *in vivo* (Garofalo et al. 2015; Ibuki et al. 2014).

Taken together, these studies have demonstrated the critical role of IRS1 and IRS2 in mediating IR/IGF-1R signaling, their involvement in other signaling pathways as well as in driving and supporting oncogenesis in a variety of contexts, providing compelling rationale to investigate the effects of genetic ablation of IRS1 and IRS2 on lung tumorigenesis, as well as to evaluate the therapeutic potential of targeting IRS1 and IRS2 in NSCLC.

1.4 <u>AMINO ACID METABOLISM IN CANCER</u>

1.4.1 Overview of altered metabolism in *Kras*-driven tumors

Altered metabolism has emerged as a hallmark of cancer cells (Hanahan and Weinberg 2011). It has been shown that genetic mutations, tumor microenvironment, as well as tissue of origin all contribute to rewiring metabolism in cancer cells in order to adapt to their anabolic and energetic needs for rapid proliferation, and their limited access to nutrient (Vander Heiden and DeBerardinis 2017; Pavlova and Thompson 2016). Specifically *Kras*-driven pancreatic cancer tumors have upregulated glycolytic flux into non-oxidative pentose phosphate pathway to produce ribose for nucleotide synthesis and into the hexosamine biosynthesis pathway to produce glycosylation precursors (Ying et al. 2012). Mutant *Kras* also rewires glutamine metabolism to maximize NADPH production for maintaining redox balance (Son et al. 2013; Lyssiotis et al. 2013). Moreover, *Kras*-mutant cancer cells demonstrate reliance on alternative, scavenging pathways such as macropinocytosis and autophagy to acquire or generate nutrient to meet their various anabolic demands (Commisso et al. 2013; Kamphorst et al. 2013, 2015; Guo et al. 2011; Yang et al. 2011; Davidson et al.

2016). What has been increasingly appreciated over the past decade of cancer metabolism research is that rewired metabolism does not stop at the "Warburg effect", or aerobic glycolysis. All aspects of cellular metabolism are subject to alterations that favor tumor survival and progression, chief among which is amino acid metabolism. Various amino acids have been demonstrated to play an important role in oncogenesis.

1.4.2 Serine and glycine metabolism contributes to tumorigenesis

Cancer cells often display increased need for nucleotide synthesis and glutathione production due to their rapid rate of proliferation and consequently their need to maintain redox balance. As a result, serine and glycine have been found to play a critical role in supporting tumor growth due to their contribution to purine synthesis and one carbon metabolism. Serine biosynthesis was found to be essential to the growth of breast cancer cells both *in vitro* and *in vivo*, by providing α-ketoglutarate (αKG) for TCA cycle anaeplerosis (Possemato et al. 2011). 3-phosphoglycerate dehydrogenase (PHGDH), the enzyme that catalyzes the first step in serine synthesis from 3-phosphoglycerate (3PG), is frequently amplified, resulting in increased mRNA and protein levels in majority of estrogen receptor (ER) negative breast cancers (Possemato et al. 2011). Similarly, another group found PHGDH to be frequently amplified in melanoma cells, and is essential to cell proliferation (Locasale et al. 2011). One study found a strong correlation between the rate of proliferation and the rate of glycine consumption and expression of glycine biosynthetic genes across cancer cells (Jain et al. 2012). Fast-growing cancers cells are found to be more dependent on de novo purine synthesis supported by glycine metabolism for their proliferation than less proliferative cancer cells (Jain et al. 2012). Serine hydroxymethyltransferase (SHMT2), the enzyme that converts

serine to glycine in the mitochondria, is required for glioblastoma cells to adapt to hypoxic

tumor microenvironment by inhibiting pyruvate kinase (PKM2) activity and hence reducing

oxygen consumption (D. Kim et al. 2015). Notably, inhibition of downstream glycine

decarboxylase (GLDC) in SHMT2-high cells leads to accumulation of glycine and its

conversion to toxic molecules aminoacetone and methylglyoxal, and impairs cell survival (D.

Kim et al. 2015). Interestingly, GLDC is also reported to be overexpressed in NSCLC tumor-

initiating cells (TICs), to regulate TIC proliferation through pyrimidine metabolism, and to be

a prognostic marker for mortality in NSCLC patients (Zhang et al. 2012). In *Kras*-driven,

Lkb1-null pancreatic cancer, serine-glycine synthesis and one-carbon metabolism are induced

via activated mTORC1 to promote S-adenosylmethionine generation and DNA methylation.

As a result, *Lkb1* loss confers sensitivity to inhibition of these pathways (Kottakis et al. 2016).

In a study that investigated serine biosynthetic pathway in NSCLC cells, proliferation and

tumor growth for some cells are highly dependent on serine - glycine biosynthesis due to its

role in glutathione and nucleotide production. In addition, expression of key enzyme genes

involved in this pathway such as *PHGDH*, *PSAT1* and *SHMT2* confers poor prognosis in

human NSCLC patients (DeNicola et al. 2015). Although serine and glycine can be

interconverted by the cytosolic and mitochondrial SHMT1 and 2, their roles in cell

metabolism are not interchangeable. In particular, exogenous glycine cannot replace serine to

support cancer cell proliferation. In contrast, high glycine level inhibits proliferation of cancer

cells in the absence of serine as glycine is converted to serine, thereby depleting the one-

carbon pool (Labuschagne et al. 2014). More recently it was shown that a serine- and glycine-

free diet extends survival in genetically engineered mouse models (GEMMs) of intestinal

cancer and lymphoma (Maddocks et al. 2017). However, mutant *Kras* in a conditional mouse

model of pancreatic cancer confers resistance to dietary depletion of serine and glycine through upregulation of de novo serine biosynthesis, emphasizing the ability of genetic mutations to modulate amino acid metabolism in cancer (Maddocks et al. 2017).

1.4.3 Glutamine, glutamate and aspartate contribute to tumorigenesis

In addition to serine and glycine, glutamine also plays an essential and versatile role in supporting tumor growth, both as a nitrogen donor for amino acid and de novo nucleotide synthesis, as well as an indirect modulator of tumor cell epigenetics. Glutamine can also contribute to NADPH production and is required for glutathione synthesis, and hence critical for maintaining cellular redox balance. *Pten*-null glioblastoma and breast cancer cells display enhanced proliferation that is dependent on glutamine flux through de novo pyrimidine synthesis, and tumor growth is suppressed by inhibition of dihydroorotate dehydrogenase (DHODH), a rate-limiting enzyme for pyrimidine ring synthesis (Mathur et al. 2017). Differential levels of glutamine in core regions and peripheral regions of solid tumors are found to result in differences in α-ketoglutarate and hence histone hypermethylation in tumor core that leads to cancer cell dedifferentiation and resistance to targeted therapy (Pan et al. 2016). *Kras*-mutant pancreatic cancer cells demonstrate increased glutamine uptake and flux to form aspartate, whose metabolism ultimately generates NADPH to maintain cellular redox balance (Son et al. 2013). Similarly, proliferating breast cancer cells also increase transamination of glutamate for non-essential amino acid synthesis, and inhibition of transaminases suppresses the proliferative state (Coloff et al. 2016). Glutamine anaeplerosis also provides a means for cells to escape glycolysis dependency, therefore conferring

metabolic flexibility to tumors cells undergoing therapies targeting glucose metabolism (Pusapati et al. 2016).

Aspartate is required as a nitrogen donor to both pyrimidine and purine synthesis, and has also been found to promote tumor growth. Deficiency of the aspartate catabolic enzyme argininosuccinate synthase (ASS1) increases cytosolic aspartate levels, which increases pyrimidine synthesis via CAD (carbamoyl-phosphate synthase 2, aspartate transcarbamylase, and dihydroorotase complex) and proliferation in cancer cells (Rabinovich et al. 2015). Consistently, it was demonstrated that a major function of mitochondrial respiration is to supply aspartate for nucleotide synthesis, and proliferation of respiration-deficient cells can be rescued by the supplementation with aspartate or pyruvate, which can be used to synthesize aspartate (Birsoy et al. 2015; Sullivan et al. 2015).

1.4.4 Other aspects of amino acid metabolism in cancer

Recently the roles of other amino acids in supporting tumor growth have also emerged. Branched chain amino acids (BCAA, leucine, isoleucine and valine) have been found instrumental in supporting *Kras*-mutant lung tumor growth. In contrast to *Kras*-driven pancreatic cancer that displays decreased BCAA uptake, *Kras*-mutant lung tumors increase their uptake of BCAAs to use as a nitrogen source and inhibition of BCAA catabolism impairs NSCLC tumor formation (Mayers et al. 2016). A subset of cancer cells is found to be dependent on exogenous proline for proliferation, which alleviates ER stress induced by hyperactive mTORC1-4EBP1 signaling (Sahu et al. 2016). In *EGFR*-mutant human mammary epithelial cells, cystine is essential to cell survival and protects cells from hydrogen

peroxide-induced synchronous ferroptosis. Depletion of cystine also suppresses *EGFR*-mutant NSCLC growth *in vivo* (Poursaitidis et al. 2017).

Consistent with the studies that demonstrate amino acids' importance in supporting cancer cell growth, it has been shown that amino acids (other than glutamine) contribute to the majority of cellular mass in proliferating cells, despite the vastly larger amounts of glucose and glutamine they consume (Hosios et al. 2016). Moreover, the majority of glutamine-derived carbons end up in amino acids and proteins, suggesting that glutamine is mainly used to synthesize other amino acids. Cells also demonstrate serine uptake to an appreciable extent, which contributes significantly to the biomass of nucleotides, corroborating other findings of the essential role of serine in supporting nucleotide synthesis in various cancer cells (Hosios et al. 2016).

Given the essentiality of amino acids in supporting many facets of tumor metabolism and in making up the bulk of cellular biomass, tumor cells have found alternative ways to replenish amino acids when deprived of them. Specifically *Kras*-mutant pancreatic cancer, which is poorly vascularized and therefore often limited in their exposure to nutrients, upregulates macropinocytosis to actively scavenge for and catabolize extracellular proteins (Commisso et al. 2013; Kamphorst et al. 2015; Davidson et al. 2016). Additionally, mutant *Kras* also promotes autophagy to recycle intracellular contents as another means to replenish cellular amino acid pool, which will be discussed in detail in the next section.

1.5 MULTIFACETED ROLE OF AUTOPHAGY IN CANCER

1.5.1 Overview

Autophagy is the catabolic process of "self-eating" through which intracellular contents such as proteins, organelles as well as bulk cytoplasm are sequestered and degraded in the lysosome to regenerate macromolecules and components for cellular metabolic, energetic and homeostatic purposes (Kimmelman and White 2017). Autophagy is essential to maintaining cellular energetic and nutrient homeostasis during starvation and hence is activated by nutritional stress such as amino acid starvation or high AMP/ATP ratio (Kim and Lee 2014). Additionally, a constitutive, basal level of autophagy is important for protein and organelle quality control (Kim and Lee 2014). There are three broad categories of autophagy: macroautophagy, microautophagy and chaperone-mediated autophagy (Kaur and Debnath 2015). Macroautophagy involves the formation of double-membraned vesicles known as autophagosomes that engulf cytoplasmic proteins and organelles and traffic them to lysosomes for degradation. In microautophagy, substrates are directly engulfed by lysosomal or endosomal membrane invagination. On the other hand, chaperone-mediated autophagy only selectively targets and degrades substrates that contain the pentapeptide motif KFERQ. These proteins are recognized by the heat shock cognate 70kDa protein (HSC70) chaperone and translocated to lysosomes via the lysosomal-associated membrane protein 2A (LAMP2A) receptor (Cuervo and Wong 2014). From here on the discussion will focus on macroautophagy (hereafter referred to as autophagy) and its role in NSCLC.

1.5.2 Autophagosome formation and maturation in mammals

Studies in yeast have identified more than 30 autophagy-related proteins (ATGs), many of which have mammalian orthologues (Ktistakis and Tooze 2016). In mammalian cells, autophagosome formation consists of three distinct steps: initiation, elongation and closure, and fusion with lysosome (Fig. 1.4) (Kenific and Debnath 2015). Autophagosome formation is initiated at the phagophore assembly site (PAS) by the UNC51-like kinase (ULK) complex, composed of ULK1 or ULK2, ATG13, FAK family kinase interacting protein of 200kDa (FIP200) and ATG101 (Mizushima 2010). Under nutrient-replete conditions, the ULK complex is inactive as ULK1/2 is phosphorylated and inactivated by mTORC1 (Chan 2009). Upon starvation or absence of growth factor signaling, mTORC1 is inactivated, which leads to its dissociation from and the activation of the ULK complex. The activated ULK complex then targets a class III PI3K complex - consisting of Beclin 1, p150, VPS34 and ATG14 - to produce a local pool of phosphatidylinositol 3 - phosphate (PI3P) that serves to recruit additional ATGs that will subsequently mediate elongation and closure of the autophagosome membrane (Itakura et al. 2008). Finally, elongation and closure of autophagosome is regulated by two ubiquitin-like conjugation pathways that conjugate ATG12 to ATG5 and microtubule-associated protein 1 light chain (LC3) to the lipid phosphatidylethanolamine (PE) (Geng and Klionsky 2008). ATG7 and ATG10 regulate the conjugation of ATG12 to ATG5. The ATG12-ATG5 complex then associates with ATG16 and localizes to the outer autophagosomal membrane to facilitate the lipidation of LC3 by PE. LC3 is conjugated to PE by ATG7 and ATG3. PE is inserted into the elongating autophagosome membrane, and as a result LC3 is localized to both the inner and outer autophagosomal membranes (Kaur and Debnath 2015). LC3-PE (also termed LC3-II) is

28

required for the expansion of autophagic membranes, recognition of cargoes and the fusion of autophagosomes with lysosomes (Kim and Lee 2014; Kenific and Debnath 2015). It is also commonly used as a marker of autophagosome to monitor induction or inhibition of autophagy (Klionsky et al. 2016). Ultimately, the autophagosome fuses with endosomes and lysosomes, forming autolysosomes. Lysosomal proteases then degrade the autophagic cargo to regenerate building blocks and macromolecules for energy production and biosynthesis (Kaur and Debnath 2015).
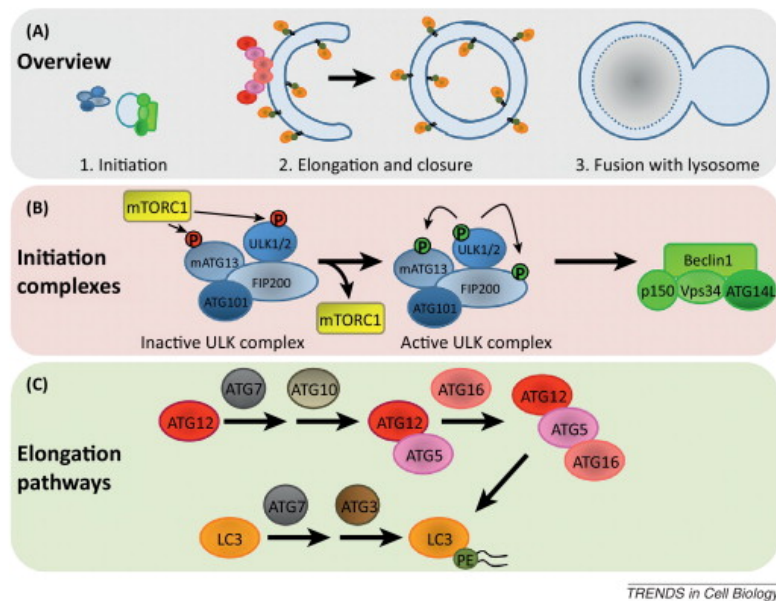
Figure 1.4. Autophagosome formation and maturation in mammals.

(**A**) Overview of autophagosome formation and maturation process. (**B**) Initiation of autophagosome formation by the ULK complex. (**C**) Elongation of autophagosome is mediated by two ubiquitin-like conjugation pathways that conjugate ATG12 to ATG5 and microtubule-associated protein 1 light chain (LC3) to the lipid phosphatidylethanolamine (PE). Figure reprinted from Kenific and Debnath 2015.

1.5.3 Nutrient, energy sensing and regulation of autophagy

Autophagy is a dynamic process that is regulated by many cellular effectors including transcription factors, noncoding microRNAs, protein kinases, acetyltransferases and deacetylases (Feng, Yao, and Klionsky 2015). Two predominant regulators of autophagy are mTORC1 complex and AMPK, both of which modulate autophagy in response to growth factor signaling, cellular nutrient and energy states, and have opposing effects on autophagy. In the presence of active growth factor signaling and abundant intracellular amino acids, mTORC1 complex is recruited to and activated at the outer lysosomal surface. Activated mTORC1 inhibits ULK1 and ATG13 in the ULK complex by phosphorylation (He and Klionsky 2009). This phosphorylation of ULK1 also disrupts its interaction with AMPK, preventing ULK1 activation by the latter. mTORC1 seems to be a dominant regulator of autophagy, as mTORC1 inhibition is sufficient to induce autophagy and its constitutive activation is sufficient to block the latter (Thoreen et al. 2009; Efeyan et al. 2013). In addition to the regulation of autophagy initiation, mTORC1 activity is required for autophagy termination. Free amino acids as end products of autophagy result in an increase in mTORC1 activity and the reformation of lysosomes (L. Yu et al. 2010).

Conversely, under low cellular energy state with a high AMP:ATP ratio, AMPK is activated and phosphorylates ULK1 to activate the ULK complex and initiate autophagosome formation (D. F. Egan et al. 2011; J. Kim et al. 2011). Active AMPK also stimulates autophagy by suppressing mTORC1, both indirectly and directly. AMPK activates TSC2, a negative regulator of mTORC1 activity. It also phosphorylates mTOR binding partner RAPTOR and reduces mTOR kinase activity (Inoki, Zhu, and Guan 2003; Gwinn et al. 2008). Additionally, AMPK activates the FOXO transcription factors, which transcriptionally

promote autophagy by increasing expression of genes of the core autophagy machinery involved in autophagosome formation (Mammucari et al. 2007).

In addition to post-translational regulation of autophagy through mTORC1 activity, amino acids can modulate autophagy at the transcriptional level as well. During low levels of amino acids, uncharged tRNAs accumulate and are detected by general control nonderepressible 2 (GCN2), a serine/threonine kinase that senses amino acid abundance (J. Dong et al. 2000). GCN2, upon binding to an uncharged tRNA, is activated and inhibits protein synthesis by phosphorylating eIF2α (Berlanga, Santoyo, and De Haro 1999). Active GCN2 also induces transcription of autophagy-related genes via the eIF2α - ATF4 axis (B'chir et al. 2013). Moreover, during amino acid deprivation, TFEB, a master regulator of lysosomal biogenesis, translocates into the nucleus to induce expression of autophagy and lysosomal genes (C. Settembre et al. 2011).

Therefore, the cellular process of autophagy is exquisitely controlled in response to cellular nutrient status, in particular amino acid levels. Its role has been extensively studied in normal physiology and in diseased states including cancer.

1.5.4 Autophagy in NSCLC

Analysis of human cancer genome and transcriptome showed that the core autophagy genes are generally not mutated genetically in human cancer and their expression are largely invariable, suggesting that core autophagy machinery may be somewhat essential and protected from alterations in human cancers (Lebovitz et al. 2015). Early studies showed that loss of a copy of the Beclin1 gene results in increased tumorigenesis in mice, suggesting that Beclin1 acts as a haploinsufficient tumor suppressor and autophagy has tumor-suppressive

roles (Aita et al. 1999; X. H. Liang et al. 1999; Qu et al. 2003; Yue et al. 2003). However, preclinical studies have increasingly demonstrated that autophagy can be neutral, tumor-suppressive or tumor-promoting in different contexts, depending on nutrient availability, tumor microenvironment, tumor stage as well as the presence of immune system effectors (Amaravadi, Kimmelman, and White 2016). Expression of *Hras*^{V12} or *Kras*^{V12} oncogenes in immortalized baby mouse kidney epithelial (iBMK) cells upregulates basal autophagy in nutrient-replete conditions, which is required for survival in starvation and tumor growth *in vivo*. Mutant *Ras* also induces dependency on autophagy-mediated mitochondrial oxidative metabolism during starvation (Guo et al. 2011). Specifically in lung cancer there has been abundant evidence pointing to the tumor-promoting effects of autophagy in various mouse models. In a conditional *Kras*-driven lung cancer model, concomitant lung-specific genetic deletion of *Atg7* at the onset of tumor initiation leads to reduced tumor progression and formation of benign oncocytomas (Guo et al. 2013). Tumor cells display accumulation of defective mitochondria, which leads to growth arrest and cell death. Interestingly, mice do not experience overall survival benefit in this case but instead succumb to fatal pneumonia, indicating that lack of autophagy leads to activation of proinflammatory pathways and immune infiltration into the tumor microenvironment. Similarly, in *Kras*-mutant lung cancer with loss of *p53*, genetic ablation of *Atg7* in the lungs leads to increased survival, suppressed tumor progression and development of oncocytomas (Guo et al. 2013). Lung tumor cells display accumulation of defective mitochondria, impaired mitochondrial respiration and fatty acid oxidation that leads to lipid accumulation. In the same *Kras*-driven lung cancer model genetic ablation of *Atg5* in the lungs markedly impairs tumor progression and significantly extends survival of mice (Rao et al. 2014). Intriguingly, loss of *Atg5* accelerates tumor

initiation, revealing the dual effect of autophagy in tumorigenesis. More recent studies have demonstrated that mechanistically autophagy is required in *Kras*-mutant, *p53*-null lung tumor cells to supply glutamine for mitochondrial respiration and for maintaining nucleotide pool and energy stasis (Guo et al. 2016). Therefore autophagy promotes metabolic robustness and malignancy of *Kras*-driven lung cancer through maintenance of mitochondrial function. Similar findings have been established in mouse models of $Braf^{V600E}$-driven lung cancer (A. M. Strohecker et al. 2013; Anne M Strohecker and White 2014). Taken together, these studies suggest that autophagy may play distinct roles in *Kras*-driven lung tumor initiation and progression. While inhibition of autophagy may contribute to the onset of tumorigenesis, it may have clinical value in the treatment of established NSCLC and may stall tumor progression.

The therapeutic potential of autophagy inhibition in NSCLC has been tested. Systemic deletion of *Atg7* in adult mice leads to adipose loss, muscle wasting, liver damage, and eventual death from neurodegeneration after 2 - 3 months (Karsli-Uzunbas et al. 2014). However, other tissues including the lungs are relatively unaffected, underscoring the distinct metabolic demands of various tissues and the differential importance of autophagy in maintaining tissue homeostasis. Systemic knockout of *Atg*7 does not affect the initiation of *Kras*-driven, *p53*-deficient lung tumors, but does cause significant tumor regression in established tumors. Loss of *Atg7* results in increased apoptosis, decreased proliferation, suppressed MAPK signaling that all contribute to reduced tumor burden and tumor transition to benign oncocytomas (Karsli-Uzunbas et al. 2014). Intriguingly, greater tumor regression is observed in mice with whole-body rather than lung-specific autophagy inhibition, suggesting that both tumor cell-autonomous and host autophagy play a role in tumor maintenance

(Karsli-Uzunbas et al. 2014; Guo et al. 2013). Moreover, whole-body inhibition of autophagy acutely suppresses tumor growth while the adverse systemic effects only occur after chronic autophagy inhibition, hence presenting a therapeutic window (Karsli-Uzunbas et al. 2014). In addition, these findings indicate that newly transformed lung epithelial cells have distinct metabolic needs from established tumor cells, and reinforce the notion that autophagy plays differential roles in tumor initiation versus tumor maintenance and progression.

Given the established critical role of autophagy in maintaining *Kras*-driven, *p53*-deficient NSCLC, it is therefore exciting that my research implicates autophagy in NSCLC with the loss of IRS1 and IRS2. Autophagy has emerged as a potential metabolic adaptation of cells under suppression of insulin/IGF-1 signaling. Therefore, its concomitant targeting may provide clinical benefits in treating NSCLC.

1.6 <u>OVERVIEW OF THE DISSERTATION</u>

Oncogenic *KRAS* is well documented to be prevalent in human NSCLC, and the essential role of KRAS direct interaction with PI3K regulatory subunit p110α in the initiation and maintenance of NSCLC has been established. However, much controversy remains about whether this KRAS-p110α binding is sufficient in driving NSCLC, as well as whether upstream IR/IGF-1R signaling merits as a potential therapeutic target in the presence of mutant *KRAS*. In this dissertation, using a conditional mouse model of NSCLC, I provide robust genetic evidence demonstrating the requirement for *Irs1* and *Irs2* in *Kras*-driven lung tumor initiation.

In Chapter 2, I establish a genetically engineered mouse model (GEMM) with conditionally activated *Kras*, loss of *p53*, and concomitant loss of *Irs1* and *Irs2* to investigate

the effects of genetic ablation of *Irs1* and *Irs2* on lung tumorigenesis. I present evidence showing altered signaling and metabolism in both human and mouse tumor cells with loss of *Irs1* and *Irs2*, and identify amino acid metabolism as a metabolic vulnerability that could be targeted via autophagy and/or proteasome inhibition.

In Chapter 3, I present additional findings demonstrating the functional redundancy between *Irs1* and *Irs2* in mediating Ir/Igf-1r signaling. I also present preliminary results showing that *Foxo* transcription factors contribute partially to tumor suppression conferred by loss of *Irs1* and *Irs2*. Additionally, hypothesis-generating studies on how loss of *Irs1* and *Irs2* could impact amino acid metabolism and autophagy is discussed. Implications from my research, potential caveats as well as important future work are also outlined.

In sum, my study highlights the essential role of *Irs1* and *Irs2* in *Kras*-driven lung cancer and points to the promise of combinatorial therapies targeting IR/IGF-1R and protein catabolic pathways such as autophagy and proteasomal degradation in treating NSCLC.

REFERENCES

Aita VM, Liang XH, Murty VV, Pincus DL, Yu W, Cayanis E, Kalachikov S, Gilliam TC, and Levine B. 1999. "Cloning and Genomic Organization of Beclin 1, a Candidate Tumor Suppressor Gene on Chromosome 17q21." *Genomics* 59 (1): 59–65.

Amaravadi R, Kimmelman AC, and White E. 2016. "Recent Insights into the Function of Autophagy in Cancer." *Genes & Development* 30 (17): 1913–30.

B'chir W, Maurin AC, Carraro V, Averous J, Jousse C, Muranishi Y, Parry L, Stepien G, Fafournoux P, and Bruhat A. 2013. "The eIF2α/ATF4 Pathway Is Essential for Stress-Induced Autophagy Gene Expression." *Nucleic Acids Research* 41 (16): 7683–99.

Banting FG, Best CH, Collip JB, Campbell WR, and Fletcher AA. 1922. "Pancreatic Extracts in the Treatment of Diabetes Mellitus." *Canadian Medical Association Journal* 12 (3): 141–46.

Bar-Peled L, and Sabatini DM. 2014. "Regulation of mTORC1 by Amino Acids." *Trends in Cell Biology* 24 (7): 400–406.

Barnes CJ , Kazufumi O, Rayala SK, El-Naggar AK, and Kumar R. 2007. "Insulin-like Growth Factor Receptor as a Therapeutic Target in Head and Neck Cancer." *Clinical Cancer Research : An Official Journal of the American Association for Cancer Research* 13 (14): 4291–99.

Belfiore A. 2007. "The Role of Insulin Receptor Isoforms and Hybrid insulin/IGF-I Receptors in Human Cancer." *Current Pharmaceutical Design* 13 (7): 671–86.

Belfiore A, Frasca F, Pandini G, Sciacca L, and Vigneri R. 2009. "Insulin Receptor Isoforms and Insulin Receptor/Insulin-Like Growth Factor Receptor Hybrids in Physiology and Disease." *Endocrine Reviews* 30 (6): 586–623.

Ben-Sahra I, Hoxhaj G, Ricoult SJH, Asara JM, and Manning BD. 2016. "mTORC1 Induces Purine Synthesis through Control of the Mitochondrial Tetrahydrofolate Cycle." *Science* 351 (6274): 728–33.

Ben-Sahra I, Howell JJ, Asara JM, and Manning BD. 2013. "Stimulation of de Novo
Pyrimidine Synthesis by Growth Signaling through mTOR and S6K1." *Science (New
York, N.Y.)* 339 (6125): 1323–28.

Ben-Sahra I and Manning BD. 2017. "mTORC1 Signaling and the Metabolic Control of Cell
Growth." *Current Opinion in Cell Biology* 45 (April): 72–82.

Bergmann U, Funatomi H, Kornmann M, Beger HG, and Korc M. 1996. "Increased
Expression of Insulin Receptor Substrate-1 in Human Pancreatic Cancer." *Biochemical
and Biophysical Research Communications* 220 (3): 886–90.

Bergmann U, Funatomi H, Kornmann M, Ishiwata T, Beger H, and Korc M. 1996. "Insulin-
like Growth Factor II Activates Mitogenic Signaling in Pancreatic Cancer Cells via IRS-
1." *International Journal of Oncology* 9 (3): 487–92.

Berlanga JJ, Gualillo O, Buteau H, Applanat M, Kelly PA, and Edery M. 1997. "Prolactin
Activates Tyrosyl Phosphorylation of Insulin Receptor Substrate 1 and
Phosphatidylinositol-3-OH Kinase." *The Journal of Biological Chemistry* 272 (4): 2050–
52.

Berlanga JJ, Santoyo J, and De Haro C. 1999. "Characterization of a Mammalian Homolog of
the GCN2 Eukaryotic Initiation Factor 2alpha Kinase." *European Journal of
Biochemistry* 265 (2): 754–62.

Birsoy K, Wang T, Chen WW, Freinkman E, Abu-Remaileh M, and Sabatini DM. 2015. "An
Essential Role of the Mitochondrial Electron Transport Chain in Cell Proliferation Is to
Enable Aspartate Synthesis." *Cell* 162 (3): 540–51.

Boguski MS and McCormick F. 1993. "Proteins Regulating Ras and Its Relatives." *Nature*
366 (6456): 643–54.

Boissan M, Beurel E, Wendum D, Rey C, Lécluse Y, Housset C, Lacombe ML, and Desbois-
Mouthon C. 2005. "Overexpression of Insulin Receptor Substrate-2 in Human and
Murine Hepatocellular Carcinoma." *The American Journal of Pathology* 167 (3): 869–
77.

Buckbinder L, Talbott R, Velasco-Miguel S, Takenaka I, Faha B, Seizinger BR, and Kley N. 1995. "Induction of the Growth Inhibitor IGF-Binding Protein 3 by p53." *Nature* 377 (6550): 646–49.

Burfoot MS, Rogers NC, Watling D, Smith JM, Pons S, Paonessaw G, Pellegrini S, White MF, and Kerr IM. 1997. "Janus Kinase-Dependent Activation of Insulin Receptor Substrate 1 in Response to Interleukin-4, Oncostatin M, and the Interferons." *The Journal of Biological Chemistry* 272 (39): 24183–90.

Cai D, Dhe-Paganon S, Melendez PA, Lee J, and Shoelson SE. 2003. "Two New Substrates in Insulin Signaling, IRS5/DOK4 and IRS6/DOK5." *The Journal of Biological Chemistry* 278 (28): 25323–30.

Calle EE. 2007. "Obesity and Cancer." *BMJ* 335 (7630): 1107–8.

Calle EE and Kaaks R. 2004. "Overweight, Obesity and Cancer: Epidemiological Evidence and Proposed Mechanisms." *Nature Reviews Cancer* 4 (8): 579–91.

Calle EE, Rodriguez C, Walker-Thurmond K and Thun MJ. 2003. "Overweight, Obesity, and Mortality from Cancer in a Prospectively Studied Cohort of U.S. Adults." *New England Journal of Medicine* 348 (17): 1625–38.

Carriere A, Romeo Y, Acosta-Jaquez HA, Moreau J, Bonneil E, Thibault P, Fingar DC and Roux PP. 2011. "ERK1/2 Phosphorylate Raptor to Promote Ras-Dependent Activation of mTOR Complex 1 (mTORC1)." *The Journal of Biological Chemistry* 286 (1): 567–77.

Castellano E, Sheridan C, Thin MZ, Nye E, Spencer-Dene B, Diefenbacher ME, Moore C, et al. 2013. "Requirement for Interaction of PI3-Kinase p110α with RAS in Lung Tumor Maintenance." *Cancer Cell* 24 (5): 617–30.

Chan EY. 2009. "mTORC1 Phosphorylates the ULK1-mAtg13-FIP200 Autophagy Regulatory Complex." *Science Signaling* 2 (84): pe51.

Collisson EA, Campbell JD, Brooks AN, Berger AH, Lee W, Chmielecki J, Beer DG, et al. 2014. "Comprehensive Molecular Profiling of Lung Adenocarcinoma." *Nature* 511 (7511): 543–50.

Coloff JL, Murphy JP, Braun CR, Harris IS, Shelton LM, Kami K, Gygi SP, Selfors LM, and
Brugge JS. 2016. "Differential Glutamate Metabolism in Proliferating and Quiescent
Mammary Epithelial Cells." *Cell Metabolism* 23 (5): 867–80.

Commisso C, Davidson SM, Soydaner-Azeloglu RG, Parker SJ, Kamphorst JJ, Hackett S,
Grabocka E, et al. 2013. "Macropinocytosis of Protein Is an Amino Acid Supply Route
in Ras-Transformed Cells." *Nature* 497 (7451): 633–37.

Cox AD, Fesik SW, Kimmelman AC, Luo J, and Der CJ. 2014. "Drugging the Undruggable
RAS: Mission Possible?" *Nature Reviews. Drug Discovery* 13 (11): 828–51.

Cuervo AM and Wong E. 2014. "Chaperone-Mediated Autophagy: Roles in Disease and
Aging." *Cell Research* 24 (1): 92–104.

Curry NL, Mino-Kenudson M, Oliver TG, Yilmaz OH, Yilmaz VO, Moon JY, Jacks T,
Sabatini DM, and Kalaany NY. 2013. "Pten-Null Tumors Cohabiting the Same Lung
Display Differential AKT Activation and Sensitivity to Dietary Restriction." *Cancer
Discovery* 3 (8): 908–21.

D'Ambrosio C, Keller DT, Morrione A, Lienhard GE, Baserga R, and Surmacz E. 1995.
"Transforming Potential of the Insulin Receptor Substrate 1." *Cell Growth &
Differentiation : The Molecular Biology Journal of the American Association for Cancer
Research* 6 (5): 557–62.

Davidson MR, Gazdar AF and Clarke BE. 2013. "The Pivotal Role of Pathology in the
Management of Lung Cancer." *Journal of Thoracic Disease* 5 Suppl 5 (October): S463-
78.

Davidson SM, Jonas O, Keibler MA, Hou HW, Luengo A, Mayers JR, Wyckoff J, et al. 2016.
"Direct Evidence for Cancer-Cell-Autonomous Extracellular Protein Catabolism in
Pancreatic Tumors." *Nature Medicine* 23 (2): 235–41.

Dawson DW, Hertzer K, Moro A, Donald G, Chang HH, Go VL, Pandol SJ, et al. 2013.
"High-Fat, High-Calorie Diet Promotes Early Pancreatic Neoplasia in the Conditional
KrasG12D Mouse Model." *Cancer Prevention Research (Philadelphia, Pa.)* 6 (10):
1064–73.

DeAngelis T, Chen J, Wu A, Prisco M, and Baserga R. 2006. "Transformation by the Simian Virus 40 T Antigen Is Regulated by IGF-I Receptor and IRS-1 Signaling." *Oncogene* 25 (1): 32–42.

Dearth RK, Cui X, Kim HJ, Hadsell DL, and Lee AV. 2007. "Oncogenic Transformation by the Signaling Adaptor Proteins Insulin Receptor Substrate (IRS)-1 and IRS-2." *Cell Cycle* 6 (6): 705–13.

DeNicola GM, Chen PH, Mullarky E, Sudderth JA, Hu Z, Wu D, Tang H, et al. 2015. "NRF2 Regulates Serine Biosynthesis in Non–small Cell Lung Cancer." *Nature Genetics* 47 (12): 1475–81.

Dhillon AS, Meikle S, Yazici Z, Eulitz M, and Kolch W. 2002. "Regulation of Raf-1 Activation and Signalling by Dephosphorylation." *The EMBO Journal* 21 (1–2): 64–71.

Ding L, Getz G, Wheeler DA, Mardis ER, McLellan MD, Cibulskis K, Sougnez C, et al. 2008. "Somatic Mutations Affect Key Pathways in Lung Adenocarcinoma." *Nature* 455 (7216): 1069–75.

Dong J, Qiu H, Garcia-Barrio M, Anderson J and Hinnebusch AG. 2000. "Uncharged tRNA Activates GCN2 by Displacing the Protein Kinase Moiety from a Bipartite tRNA-Binding Domain." *Molecular Cell* 6 (2): 269–79.

Dong MQ, Venable JD, Au N, Xu T, Park SK, Cociorva D, Johnson JR, Dillin A, and Yates JR. 2007. "Quantitative Mass Spectrometry Identifies Insulin Signaling Targets in C. Elegans." *Science (New York, N.Y.)* 317 (5838): 660–63.

Donovan S, Shannon KM and Bollag G. 2002. "GTPase Activating Proteins: Critical Regulators of Intracellular Signaling." *Biochimica et Biophysica Acta* 1602 (1): 23–45.

Duncan JS, Whittle MC, Nakamura K, Abell AN, Midland AA, Zawistowski JS, Johnson NL, et al. 2012. "Dynamic Reprogramming of the Kinome in Response to Targeted MEK Inhibition in Triple-Negative Breast Cancer." *Cell* 149 (2): 307–21.

Dunn SE, Kari FW, French J, Leininger JR, Travlos G, Wilson R and Barrett JC. 1997. "Dietary Restriction Reduces Insulin-like Growth Factor I Levels, Which Modulates Apoptosis, Cell Proliferation, and Tumor Progression in p53-Deficient Mice." *Cancer Research* 57 (21): 4667–72.

Eberhard DA, Johnson BE, Amler LC, Goddard AD, Heldens SL, Herbst RS, Ince WL, et al. 2005. "Mutations in the Epidermal Growth Factor Receptor and in KRAS Are Predictive and Prognostic Indicators in Patients With Non–Small-Cell Lung Cancer Treated With Chemotherapy Alone and in Combination With Erlotinib." *Journal of Clinical Oncology* 23 (25): 5900–5909.

Efeyan A, Zoncu R, Chang S, Gumper I, Snitkin H, Wolfson RL, Kirak O and Sabatini DM. 2013. "Regulation of mTORC1 by the Rag GTPases Is Necessary for Neonatal Autophagy and Survival." *Nature* 493 (7434): 679–83.

Egan D, Kim J, Shaw RJ and Guan KL. 2011. "The Autophagy Initiating Kinase ULK1 Is Regulated via Opposing Phosphorylation by AMPK and mTOR." *Autophagy* 7 (6): 643–44.

Egan DF, Shackelford DB, Mihaylova MM, Gelino S, Kohnz RA, Mair W, Vasquez DS, et al. 2011. "Phosphorylation of ULK1 (hATG1) by AMP-Activated Protein Kinase Connects Energy Sensing to Mitophagy." *Science (New York, N.Y.)* 331 (6016): 456–61.

Engelman JA, Zejnullahu K, Mitsudomi T, Song Y, Hyland C, Park JO, Lindeman N, et al. 2007. "MET Amplification Leads to Gefitinib Resistance in Lung Cancer by Activating ERBB3 Signaling." *Science* 316 (5827): 1039–43.

Engelman JA, Chen L, Tan X, Crosby K, Guimaraes AR, Upadhyay R, Maira M, et al. 2008. "Effective Use of PI3K and MEK Inhibitors to Treat Mutant Kras G12D and PIK3CA H1047R Murine Lung Cancers." *Nature Medicine* 14 (12): 1351–56.

Ettinger DS, Wood DE, Aisner DL, Akerley W, Bauman J, Chirieac LR, D'Amico TA, et al. 2017. "Non-Small Cell Lung Cancer, Version 5.2017, NCCN Clinical Practice Guidelines in Oncology." *Journal of the National Comprehensive Cancer Network : JNCCN* 15 (4): 504–35.

Felice DL, El-Shennawy L, Zhao S, Lantvit DL, Shen Q, Unterman TG, Swanson SM and Frasor J. 2013. "Growth Hormone Potentiates 17β-Estradiol-Dependent Breast Cancer Cell Proliferation Independently of IGF-I Receptor Signaling." *Endocrinology* 154 (9): 3219–27.

Feng Y, Yao Z and Klionsky DJ. 2015. "How to Control Self-Digestion: Transcriptional, Post-Transcriptional, and Post-Translational Regulation of Autophagy." *Trends in Cell Biology* 25 (6): 354–63.

Fernandez-Cuesta L, Plenker D, Osada H, Sun R, Menon R, Leenders F, Ortiz-Cuaran S, et al. 2014. "CD74-NRG1 Fusions in Lung Adenocarcinoma." *Cancer Discovery* 4 (4): 415–22.

Firth SM and Baxter RC. 2002. "Cellular Actions of the Insulin-Like Growth Factor Binding Proteins." *Endocrine Reviews* 23 (6): 824–54.

Foster KG, Acosta-Jaquez HA, Romeo Y, Ekim B, Soliman GA, Carriere A, Roux PP, Ballif BA and Fingar DC. 2010. "Regulation of mTOR Complex 1 (mTORC1) by Raptor Ser [863] and Multisite Phosphorylation." *Journal of Biological Chemistry* 285 (1): 80–94.

Frasca F, Pandini G, Sciacca L, Pezzino V, Squatrito S, Belfiore A and Vigneri R. 2008. "The Role of Insulin Receptors and IGF-I Receptors in Cancer and Other Diseases." *Archives of Physiology and Biochemistry* 114 (1): 23–37.

Gallagher EJ and LeRoith D. 2010. "The Proliferating Role of Insulin and Insulin-like Growth Factors in Cancer." *Trends in Endocrinology & Metabolism* 21 (10): 610–18.

Gandara DR, Leighl N, Delord JP, Barlesi F, Bennouna J, Zalcman G, Infante JR, et al. 2017. "A Phase 1/1b Study Evaluating Trametinib Plus Docetaxel or Pemetrexed in Patients With Advanced Non-Small Cell Lung Cancer." *Journal of Thoracic Oncology : Official Publication of the International Association for the Study of Lung Cancer* 12 (3): 556–66.

Garofalo C, Capristo M, Mancarella C, Reunevi H, Picci P and Scotlandi K. 2015. "Preclinical Effectiveness of Selective Inhibitor of IRS-1/2 NT157 in Osteosarcoma Cell Lines." *Frontiers in Endocrinology* 6 (May): 74.

Gately K, Forde L, Cuffe S, Cummins R, Kay EW, Feuerhake F and J O'Byrne K. 2014. "High Coexpression of Both EGFR and IGF1R Correlates with Poor Patient Prognosis in Resected Non-Small-Cell Lung Cancer." *Clinical Lung Cancer* 15 (1): 58–66.

Geng J and Klionsky DJ. 2008. "The Atg8 and Atg12 Ubiquitin-like Conjugation Systems in Macroautophagy. 'Protein Modifications: Beyond the Usual Suspects' Review Series." *EMBO Reports* 9 (9): 859–64.

Goto Y, Sekine I, Tanioka M, Shibata T, Tanai C, Asahina H, Nokihara H, et al. 2012. "Figitumumab Combined with Carboplatin and Paclitaxel in Treatment-Naïve Japanese Patients with Advanced Non-Small Cell Lung Cancer." *Investigational New Drugs* 30 (4): 1548–56.

Guan KL, Figueroa C, Brtva TR, Zhu T, Taylor J, Barber TD and Vojtek AB. 2000. "Negative Regulation of the Serine/threonine Kinase B-Raf by Akt." *Journal of Biological Chemistry* 275 (35): 27354–59.

Gucev ZS, Oh Y, Kelley KM, and Rosenfeld RG. 1996. "Insulin-like Growth Factor Binding Protein 3 Mediates Retinoic Acid- and Transforming Growth Factor beta2-Induced Growth Inhibition in Human Breast Cancer Cells." *Cancer Research* 56 (7): 1545–50.

Guo JY, Chen HY, Mathew R, Fan J, Strohecker AM, Karsli-Uzunbas G, Kamphorst JJ, et al. 2011. "Activated Ras Requires Autophagy to Maintain Oxidative Metabolism and Tumorigenesis." *Genes & Development* 25 (5): 460–70.

Guo JY, Karsli-Uzunbas G, Mathew R, Aisner SC, Kamphorst JJ, Strohecker AM, Chen G, et al. 2013. "Autophagy Suppresses Progression of K-Ras-Induced Lung Tumors to Oncocytomas and Maintains Lipid Homeostasis." *Genes & Development* 27 (13): 1447–61.

Guo JY, Teng X, Laddha SV, Ma S, Van Nostrand SC, Yang Y, Khor S, Chan CS, Rabinowitz JD and White E. 2016. "Autophagy Provides Metabolic Substrates to Maintain Energy Charge and Nucleotide Pools in Ras-Driven Lung Cancer Cells." *Genes & Development* 30 (15): 1704–17.

Gupta S, Ramjaun AR, Haiko P, Wang Y, Warne PH, Nicke B, Nye E, Stamp G, Alitalo K and Downward J. 2007. "Binding of Ras to Phosphoinositide 3-Kinase p110alpha Is Required for Ras-Driven Tumorigenesis in Mice." *Cell* 129 (5): 957–68.

Gwinn DM, Shackelford DB, Egan DF, Mihaylova MM, Mery A, Vasquez DS, Turk BE and Shaw RH. 2008. "AMPK Phosphorylation of Raptor Mediates a Metabolic Checkpoint." *Molecular Cell* 30 (2): 214–26.

Haluska P, Shaw HM, Batzel GN, Yin D, Molina JR, Molife LR, Yap TA, et al. 2007. "Phase I Dose Escalation Study of the Anti Insulin-like Growth Factor-I Receptor Monoclonal Antibody CP-751,871 in Patients with Refractory Solid Tumors." *Clinical Cancer Research : An Official Journal of the American Association for Cancer Research* 13 (19): 5834–40.

Haluska P, Worden F, Olmos D, Yin D, Schteingart D, Batzel GN, Paccagnella ML, de Bono JS, Gualberto A and Hammer GD. 2010. "Safety, Tolerability, and Pharmacokinetics of the Anti-IGF-1R Monoclonal Antibody Figitumumab in Patients with Refractory Adrenocortical Carcinoma." *Cancer Chemotherapy and Pharmacology* 65 (4): 765–73.

Hanahan D and Weinberg RA. 2011. "Hallmarks of Cancer: The next Generation." *Cell* 144 (5): 646–74.

Hanna N, Shepherd FA, Fossella FV, Pereira JR, De Marinis F, von Pawel J, Gatzemeier U, et al. 2004. "Randomized Phase III Trial of Pemetrexed versus Docetaxel in Patients with Non-Small-Cell Lung Cancer Previously Treated with Chemotherapy." *Journal of Clinical Oncology : Official Journal of the American Society of Clinical Oncology* 22 (9): 1589–97.

Haruta T, Uno T, Kawahara J, Takano A, Egawa K, Sharma PM, Olefsky JM and Kobayashi M. 2000. "A Rapamycin-Sensitive Pathway Down-Regulates Insulin Signaling via Phosphorylation and Proteasomal Degradation of Insulin Receptor Substrate-1." *Molecular Endocrinology* 14 (6): 783–94.

Hata AN, Yeo A, Faber AC, Lifshits E, Chen Z, Cheng KA, Walton Z, et al. 2014. "Failure to Induce Apoptosis via BCL-2 Family Proteins Underlies Lack of Efficacy of Combined MEK and PI3K Inhibitors for KRAS-Mutant Lung Cancers." *Cancer Research* 74 (11): 3146–56.

He C and Klionsky DJ. 2009. "Regulation Mechanisms and Signaling Pathways of Autophagy." *Annual Review of Genetics* 43 (1): 67–93.

Vander Heiden MG and DeBerardinis RJ. 2017. "Understanding the Intersections between Metabolism and Cancer Biology." *Cell* 168 (4): 657–69.

Heist RS and Engelman JA. 2012. "SnapShot: Non-Small Cell Lung Cancer." *Cancer Cell* 21 (3): 448–448.e2.

Hosios AM, Hecht VC, Danai LV, Johnson MO, Rathmell JC, Steinhauser ML, Manalis SR, andVander Heiden MG. 2016. "Amino Acids Rather than Glucose Account for the Majority of Cell Mass in Proliferating Mammalian Cells." *Developmental Cell* 36 (5): 540–49.

Huang F, Chang H, Greer A, Hillerman S, Reeves KA, Hurlburt W, Cogswell J, et al. 2015. "IRS2 Copy Number Gain, KRAS and BRAF Mutation Status as Predictive Biomarkers for Response to the IGF-1R/IR Inhibitor BMS-754807 in Colorectal Cancer Cell Lines." *Molecular Cancer Therapeutics* 14 (2): 620–30.

Huynh H, Yang X and Pollak M. 1996. "Estradiol and Antiestrogens Regulate a Growth Inhibitory Insulin-like Growth Factor Binding Protein 3 Autocrine Loop in Human Breast Cancer Cells." *The Journal of Biological Chemistry* 271 (2): 1016–21.

Iadevaia V, Liu R and Proud CG. 2014. "mTORC1 Signaling Controls Multiple Steps in Ribosome Biogenesis." *Seminars in Cell & Developmental Biology* 36 (December): 113–20.

Ibuki N, Ghaffari M, Reuveni H, Pandey M, Fazli L, Azuma H, Gleave ME, Levitzki A and Cox ME. 2014. "The Tyrphostin NT157 Suppresses Insulin Receptor Substrates and Augments Therapeutic Response of Prostate Cancer." *Molecular Cancer Therapeutics* 13 (12): 2827–39.

Imielinski M, Berger AH, Hammerman PS, Hernandez B, Pugh TJ, Hodis E, Cho J, et al. 2012. "Mapping the Hallmarks of Lung Adenocarcinoma with Massively Parallel Sequencing." *Cell* 150 (6): 1107–20.

Inoki K, Zhu T and Guan KL. 2003. "TSC2 Mediates Cellular Energy Response to Control Cell Growth and Survival." *Cell* 115 (5): 577–90.

Itakura E, Kishi C, Inoue K and Mizushima N. 2008. "Beclin 1 Forms Two Distinct Phosphatidylinositol 3-Kinase Complexes with Mammalian Atg14 and UVRAG." *Molecular Biology of the Cell* 19 (12): 5360–72.

Jain M, Nilsson R, Sharma S, Madhusudhan N, Kitami T, Souza AL, Kafri R, Kirschner MW, Clish CB and Mootha VK. 2012. "Metabolite Profiling Identifies a Key Role for Glycine in Rapid Cancer Cell Proliferation." *Science (New York, N.Y.)* 336 (6084): 1040–44.

Jänne PA, Shaw AT, Pereira JR, Jeannin G, Vansteenkiste J, Barrios C, Franke FA, et al. 2013. "Selumetinib plus Docetaxel for KRAS-Mutant Advanced Non-Small-Cell Lung Cancer: A Randomised, Multicentre, Placebo-Controlled, Phase 2 Study." *The Lancet Oncology* 14 (1): 38–47.

Jiang H, Harris MB and Rothman P. 2000. "IL-4/IL-13 Signaling beyond JAK/STAT." *The Journal of Allergy and Clinical Immunology* 105 (6 Pt 1): 1063–70.

Jung HJ and Suh Y. 2015. "Regulation of IGF -1 Signaling by microRNAs." *Frontiers in Genetics* 5 (January): 472.

Kamphorst JJ, Cross JR, Fan J, de Stanchina E, Mathew R, White EP, Thompson CB and Rabinowitz JD. 2013. "Hypoxic and Ras-Transformed Cells Support Growth by Scavenging Unsaturated Fatty Acids from Lysophospholipids." *Proceedings of the National Academy of Sciences* 110 (22): 8882–87.

Kamphorst JJ, Nofal M, Commisso C, Hackett SR, Lu W, Grabocka E, Vander Heiden MG, et al. 2015. "Human Pancreatic Cancer Tumors Are Nutrient Poor and Tumor Cells Actively Scavenge Extracellular Protein." *Cancer Research* 75 (3): 544–53.

Karsli-Uzunbas G, Guo JY, Price S, Teng X, Laddha SV, Khor S, Kalaany NY, et al. 2014. "Autophagy Is Required for Glucose Homeostasis and Lung Tumor Maintenance." *Cancer Discovery* 4 (8): 914–27.

Kaur J and Debnath J. 2015. "Autophagy at the Crossroads of Catabolism and Anabolism." *Nature Reviews. Molecular Cell Biology* 16 (8): 461–72.

Kenific CM and Debnath J. 2015. "Cellular and Metabolic Functions for Autophagy in Cancer Cells." *Trends in Cell Biology* 25 (1): 37–45.

Kim D, Fiske BP, Birsoy K, Freinkman E, Kami K, Possemato RL, Chudnovsky Y, et al. 2015. "SHMT2 Drives Glioma Cell Survival in Ischaemia but Imposes a Dependence on Glycine Clearance." *Nature* 520 (7547): 363–67.

Kim J, Kundu M, Viollet B and Guan KL. 2011. "AMPK and mTOR Regulate Autophagy through Direct Phosphorylation of Ulk1." *Nature Cell Biology* 13 (2): 132–41.

Kim KH and Lee MS. 2014. "Autophagy—a Key Player in Cellular and Body Metabolism." *Nature Reviews Endocrinology* 10 (6): 322–37.

Kimmelman AC and White E. 2017. "Autophagy and Tumor Metabolism." *Cell Metabolism* 25 (5): 1037–43.

Klement RJ and Fink MK. 2016. "Dietary and Pharmacological Modification of the insulin/IGF-1 System: Exploiting the Full Repertoire against Cancer." *Oncogenesis* 5 (2): e193.

Klionsky DJ, Abdelmohsen K, Abe A, Abedin MJ, Abeliovich H, Arozena AA, Adachi H, et al. 2016. "Guidelines for the Use and Interpretation of Assays for Monitoring Autophagy (3rd Edition)." *Doi.org*, no. 1(January). Informa UK Limited: 1–222.

Knoops L and Renauld JC. 2004. "IL-9 and Its Receptor: From Signal Transduction to Tumorigenesis." *Growth Factors* 22 (4): 207–15.

Kohno T, Ichikawa H, Totoki Y, Yasuda K, Hiramoto M, Nammo T, Sakamoto H, et al. 2012. "KIF5B-RET Fusions in Lung Adenocarcinoma." *Nature Medicine* 18 (3): 375–77.

Kopeina GS, Senichkin VV and Zhivotovsky B. 2017. "Caloric Restriction - A Promising Anti-Cancer Approach: From Molecular Mechanisms to Clinical Trials." *Biochimica et Biophysica Acta (BBA) - Reviews on Cancer* 1867 (1): 29–41.

Kornmann M, Maruyama H, Bergmann U, Tangvoranuntakul P, Beger HG, White MF and Korc M. 1998. "Enhanced Expression of the Insulin Receptor Substrate-2 Docking Protein in Human Pancreatic Cancer." *Cancer Research* 58 (19): 4250–54.

Korpanty GJ, Graham DM, Vincent MD and Leighl NB. 2014. "Biomarkers That Currently Affect Clinical Practice in Lung Cancer: EGFR, ALK, MET, ROS-1, and KRAS." *Frontiers in Oncology* 4 (August): 204.

Kottakis F, Nicolay BN, Roumane A, Karnik R, Gu H, Nagle JM, Boukhali M, et al. 2016. "LKB1 Loss Links Serine Metabolism to DNA Methylation and Tumorigenesis." *Nature* 539 (7629): 390–95.

Ktistakis NT and Tooze SA. 2016. "Digesting the Expanding Mechanisms of Autophagy." *Trends in Cell Biology* 26 (8): 624–35.

Kurzrock R, Patnaik A, Aisner J, Warren T, Leong S, Benjamin R, Eckhardt SG, et al. 2010. "A Phase I Study of Weekly R1507, a Human Monoclonal Antibody Insulin-like Growth Factor-I Receptor Antagonist, in Patients with Advanced Solid Tumors." *Clinical Cancer Research : An Official Journal of the American Association for Cancer Research* 16 (8): 2458–65.

Labuschagne CF, van den Broek NJF, Mackay GM, Vousden KH and Maddocks ODK. 2014. "Serine, but Not Glycine, Supports One-Carbon Metabolism and Proliferation of Cancer Cells." *Cell Reports* 7 (4): 1248–58.

Langer CJ, Besse B, Gualberto A, Brambilla E and Soria JC. 2010. "The Evolving Role of Histology in the Management of Advanced Non-Small-Cell Lung Cancer." *Journal of Clinical Oncology : Official Journal of the American Society of Clinical Oncology* 28 (36): 5311–20.

Langer CJ, Novello S, Park K, Krzakowski M, Karp DD, Mok T, Benner RJ, Scranton JR, Olszanski AJ and Jassem J. 2014. "Randomized, Phase III Trial of First-Line Figitumumab in Combination with Paclitaxel and Carboplatin versus Paclitaxel and Carboplatin Alone in Patients with Advanced Non-Small-Cell Lung Cancer." *Journal of Clinical Oncology : Official Journal of the American Society of Clinical Oncology* 32 (19): 2059–66.

Lashinger LM, Harrison LM, Rasmussen AJ, Logsdon CD, Fischer SM, McArthur MJ, and Hursting SD. 2013. "Dietary Energy Balance Modulation of Kras- and Ink4a/Arf+/-- Driven Pancreatic Cancer: The Role of Insulin-like Growth Factor-I." *Cancer Prevention Research (Philadelphia, Pa.)* 6 (10): 1046–55.

Lashinger LM, Malone LM, McArthur MJ, Goldberg JA, Daniels EA, Pavone A, Colby JK, et al. 2011. "Genetic Reduction of Insulin-like Growth Factor-1 Mimics the Anticancer Effects of Calorie Restriction on Cyclooxygenase-2-Driven Pancreatic Neoplasia." *Cancer Prevention Research (Philadelphia, Pa.)* 4 (7): 1030–40.

Lashinger LM, O'Flanagan CH, Dunlap SM, Rasmussen AJ, Sweeney S, Guo JY, Lodi A, Tiziani S, White E and Hursting SD. 2016. "Starving Cancer from the Outside and inside: Separate and Combined Effects of Calorie Restriction and Autophagy Inhibition on Ras-Driven Tumors." *Cancer & Metabolism* 4 (1): 18.

Lebovitz CB, Robertson AG, Goya R, Jones SJ, Morin RD, Marra MA and Gorski SM. 2015. "Cross-Cancer Profiling of Molecular Alterations within the Human Autophagy Interaction Network." *Autophagy* 11 (9): 1668–87.

Lebrun P, Baron V, Hauck CR, Schlaepfer DD and Van Obberghen E. 2000. "Cell Adhesion and Focal Adhesion Kinase Regulate Insulin Receptor Substrate-1 Expression." *The Journal of Biological Chemistry* 275 (49): 38371–77.

Lebrun P, Mothe-Satney I, Delahaye L, Van Obberghen E and Baron V. 1998. "Insulin Receptor Substrate-1 as a Signaling Molecule for Focal Adhesion Kinase pp125(FAK) and pp60(src)." *The Journal of Biological Chemistry* 273 (48): 32244–53.

Lehr S, Kotzka J, Avci H, Sickmann A, Meyer HE, Herkner A and Muller-Wieland D. 2004. "Identification of Major ERK-Related Phosphorylation Sites in Gab1." *Biochemistry* 43 (38): 12133–40.

Liang L, Jiang J and Frank SJ. 2000. "Insulin Receptor Substrate-1-Mediated Enhancement of Growth Hormone-Induced Mitogen-Activated Protein Kinase Activation." *Endocrinology* 141 (9): 3328–36.

Liang XH, Jackson S, Seaman M, Brown K, Kempkes B, Hibshoosh H and Levine B. 1999. "Induction of Autophagy and Inhibition of Tumorigenesis by Beclin 1." *Nature* 402 (6762): 672–76.

Little AS, Balmanno K, Sale MJ, Newman S, Dry JR, Hampson M, Edwards PAW, Smith PD and Cook SJ. 2011. "Amplification of the Driving Oncogene, KRAS or BRAF, Underpins Acquired Resistance to MEK1/2 Inhibitors in Colorectal Cancer Cells." *Science Signaling* 4 (166): ra17.

Little AS, Balmanno K, Sale MJ, Smith PD and Cook SJ. 2012. "Tumour Cell Responses to MEK1/2 Inhibitors: Acquired Resistance and Pathway Remodelling." *Biochemical Society Transactions* 40 (1): 73–78.

Locasale JW, Grassian AR, Melman T, Lyssiotis CA, Mattaini KR, Bass AJ, Heffron G, et al. 2011. "Phosphoglycerate Dehydrogenase Diverts Glycolytic Flux and Contributes to Oncogenesis." *Nature Genetics* 43 (9): 869–74.

Lu Y, Futtner C, Rock JR, Xu X, Whitworth W, Hogan BLM and Onaitis MW. 2010. "Evidence That SOX2 Overexpression Is Oncogenic in the Lung." Edited by Alfons Navarro. *PloS One* 5 (6): e11022.

Lynch TJ, Bell DW, Sordella R, Gurubhagavatula S, Okimoto RA, Brannigan BW, Harris PL, et al. 2004. "Activating Mutations in the Epidermal Growth Factor Receptor Underlying Responsiveness of Non–Small-Cell Lung Cancer to Gefitinib." *New England Journal of Medicine* 350 (21): 2129–39.

Lyssiotis CA, Son J, Cantley LC and Kimmelman AC. 2013. "Pancreatic Cancers Rely on a Novel Glutamine Metabolism Pathway to Maintain Redox Balance." *Cell Cycle (Georgetown, Tex.)* 12 (13): 1987–88.

Maddocks ODK, Athineos D, Cheung EC, Lee P, Zhang T, van den Broek NJF, Mackay GM, et al. 2017. "Modulating the Therapeutic Response of Tumours to Dietary Serine and Glycine Starvation." *Nature* 544 (7650): 372–76.

Mammucari C, Milan G, Romanello V, Masiero E, Rudolf R, Del Piccolo P, Burden SJ, et al. 2007. "FoxO3 Controls Autophagy in Skeletal Muscle in Vivo." *Cell Metabolism* 6 (6): 458–71.

Manning BD and Toker A. 2017. "AKT/PKB Signaling: Navigating the Network." *Cell* 169 (3): 381–405.

Martina JA, Chen Y, Gucek M and Puertollano R. 2012. "MTORC1 Functions as a Transcriptional Regulator of Autophagy by Preventing Nuclear Transport of TFEB." *Autophagy* 8 (6): 903–14.

Mathur D, Stratikopoulos E, Ozturk S, Steinbach N, Pegno S, Schoenfeld S, Yong R, et al. 2017. "PTEN Regulates Glutamine Flux to Pyrimidine Synthesis and Sensitivity to Dihydroorotate Dehydrogenase Inhibition." *Cancer Discovery* 7 (4): 380–90.

Mayers JR, Torrence ME, Danai LV, Papagiannakopoulos T, Davidson SM, Bauer MR, Lau AN, et al. 2016. "Tissue of Origin Dictates Branched-Chain Amino Acid Metabolism in Mutant Kras-Driven Cancers." *Science* 353 (6304): 1161–65.

Mizushima N. 2010. "The Role of the Atg1/ULK1 Complex in Autophagy Regulation." *Current Opinion in Cell Biology* 22 (2): 132–39.

Molina-Arcas M, Hancock DC, Sheridan C, Kumar MS and Downward J. 2013. "Coordinate Direct Input of Both KRAS and IGF1 Receptor to Activation of PI3 Kinase in KRAS-Mutant Lung Cancer." *Cancer Discovery* 3 (5): 548–63.

Møller N and Jørgensen JOL. 2009. "Effects of Growth Hormone on Glucose, Lipid, and Protein Metabolism in Human Subjects." *Endocrine Reviews* 30 (2): 152–77.

Moody G, Beltran PJ, Mitchell P, Cajulis E, Chung YA, Hwang D, Kendall R, Radinsky R, Cohen P and Calzone FJ. 2014. "IGF1R Blockade with Ganitumab Results in Systemic Effects on the GH-IGF Axis in Mice." *The Journal of Endocrinology* 221 (1): 145–55.

Morelli C, Garofalo C, Sisci D, del Rincon S, Cascio S, Tu X, Vecchione A, Sauter ER, Miller WH and Surmacz E. 2004. "Nuclear Insulin Receptor Substrate 1 Interacts with Estrogen Receptor Alpha at ERE Promoters." *Oncogene* 23 (45): 7517–26.

Mukohara T, Shimada H, Ogasawara N, Wanikawa R, Shimomura M, Nakatsura T, Ishii G, et al. 2009. "Sensitivity of Breast Cancer Cell Lines to the Novel Insulin-like Growth Factor-1 Receptor (IGF-1R) Inhibitor NVP-AEW541 Is Dependent on the Level of IRS-1 Expression." *Cancer Letters* 282 (1): 14–24.

Nazio F, Strappazzon F, Antonioli M, Bielli P, Cianfanelli V, Bordi M, Gretzmeier C, et al. 2013. "mTOR Inhibits Autophagy by Controlling ULK1 Ubiquitylation, Self-Association and Function through AMBRA1 and TRAF6." *Nature Cell Biology* 15 (4): 406–16.

Nehrbass D, Klimek F and Bannasch P. 1998. "Overexpression of Insulin Receptor Substrate-1 Emerges Early in Hepatocarcinogenesis and Elicits Preneoplastic Hepatic Glycogenosis." *The American Journal of Pathology* 152 (2): 341–45.

Nishiyama M and Wands JR. 1992. "Cloning and Increased Expression of an Insulin Receptor Substrate-1-like Gene in Human Hepatocellular Carcinoma." *Biochemical and Biophysical Research Communications* 183 (1): 280–85.

Noguchi T, Matozaki T, Horita K, Fujioka Y and Kasuga M. 1994. "Role of SH-PTP2, a Protein-Tyrosine Phosphatase with Src Homology 2 Domains, in Insulin-Stimulated Ras Activation." *Molecular and Cellular Biology* 14 (10): 6674–82.

Nurwidya F, Andarini S, Takahashi F, Syahruddin E and Takahashi K. 2016. "Implications of Insulin-like Growth Factor 1 Receptor Activation in Lung Cancer." *The Malaysian Journal of Medical Sciences : MJMS* 23 (3): 9–21.

Ostrem JML and Shokat KM. 2016. "Direct Small-Molecule Inhibitors of KRAS: From Structural Insights to Mechanism-Based Design." *Nature Reviews. Drug Discovery* 15 (11): 771–85.

Pacold ME, Suire S, Perisic O, Lara-Gonzalez S, Davis CT, Walker EH, Hawkins PT, Stephens L, Eccleston JF, and Williams RL. 2000. "Crystal Structure and Functional Analysis of Ras Binding to Its Effector Phosphoinositide 3-Kinase Gamma." *Cell* 103 (6): 931–43.

Paez JG, Jänne PA, Lee JC, Tracy S, Greulich H, Gabriel S, Herman P, et al. 2004. "EGFR Mutations in Lung Cancer: Correlation with Clinical Response to Gefitinib Therapy." *Science* 304 (5676): 1497–1500.

Pan M, Reid MA, Lowman XH, Kulkarni RP, Tran TQ, Liu X, Yang Y, et al. 2016. "Regional Glutamine Deficiency in Tumours Promotes Dedifferentiation through Inhibition of Histone Demethylation." *Nature Cell Biology* 18 (10): 1090–1101.

Pao W, Miller V, Zakowski M, Doherty J, Politi K, Sarkaria I, Singh B, et al. 2004. "EGF Receptor Gene Mutations Are Common in Lung Cancers from "never Smokers" and Are Associated with Sensitivity of Tumors to Gefitinib and Erlotinib." *Proceedings of the National Academy of Sciences* 101 (36): 13306–11.

Pavlova NN and Thompson CB. 2016. "The Emerging Hallmarks of Cancer Metabolism." *Cell Metabolism* 23 (1): 27–47.

Peña-Llopis S, Vega-Rubin-de-Celis S, Schwartz JC, Wolff NC, Tran TAT, Zou L, Xie XJ, Corey DR and Brugarolas J. 2011. "Regulation of TFEB and V-ATPases by mTORC1." *The EMBO Journal* 30 (16): 3242–58.

Pettazzoni P, Viale A, Shah P, Carugo A, Ying H, Wang H, Genovese G, et al. 2015. "Genetic Events That Limit the Efficacy of MEK and RTK Inhibitor Therapies in a Mouse Model of KRAS-Driven Pancreatic Cancer." *Cancer Research* 75 (6): 1091–1101.

Pollak M. 2008. "Insulin and Insulin-like Growth Factor Signalling in Neoplasia." *Nature Reviews Cancer* 8 (12): 915–28.

Possemato R, Marks KM, Shaul YD, Pacold ME, Kim D, Birsoy K, Sethumadhavan S, et al. 2011. "Functional Genomics Reveal That the Serine Synthesis Pathway Is Essential in Breast Cancer." *Nature* 476 (7360): 346–50.

Poursaitidis I, Wang X, Crighton T, Labuschagne C, Mason D, Cramer SL, Triplett K, et al. 2017. "Oncogene-Selective Sensitivity to Synchronous Cell Death Following Modulation of the Amino Acid Nutrient Cystine." *Cell Reports* 18 (11): 2547–56.

Prior IA, Lewis PD and Mattos C. 2012. "A Comprehensive Survey of Ras Mutations in Cancer." *Cancer Research* 72 (10): 2457–67.

Puente C, Hendrickson RC and Jiang X. 2016. "Nutrient-Regulated Phosphorylation of ATG13 Inhibits Starvation-Induced Autophagy." *Journal of Biological Chemistry* 291 (11): 6026–35.

Pusapati RV, Daemen A, Wilson C, Sandoval W, Gao M, Haley B, Baudy AR, Hatzivassiliou G, Evangelista M and Settleman J. 2016. "mTORC1-Dependent Metabolic Reprogramming Underlies Escape from Glycolysis Addiction in Cancer Cells." *Cancer Cell* 29 (4): 548–62.

Qu X, Yu J, Bhagat G, Furuya N, Hibshoosh H, Troxel A, Rosen J, et al. 2003. "Promotion of Tumorigenesis by Heterozygous Disruption of the Beclin 1 Autophagy Gene." *The Journal of Clinical Investigation* 112 (12): 1809–20.

Rabinovich S, Adler L, Yizhak K, Sarver A, Silberman A, Agron S, Stettner N, et al. 2015. "Diversion of Aspartate in ASS1-Deficient Tumours Fosters de Novo Pyrimidine Synthesis." *Nature* 527 (7578): 379–83.

Ramalingam SS, Spigel DR, Chen D, Steins MB, Engelman JA, Schneider CP, Novello S, et al. 2011. "Randomized Phase II Study of Erlotinib in Combination with Placebo or R1507, a Monoclonal Antibody to Insulin-like Growth Factor-1 Receptor, for Advanced-Stage Non-Small-Cell Lung Cancer." *Journal of Clinical Oncology : Official Journal of the American Society of Clinical Oncology* 29 (34): 4574–80.

Rao S, Tortola L, Perlot T, Wirnsberger G, Novatchkova M, Nitsch R, Sykacek P, et al. 2014. "A Dual Role for Autophagy in a Murine Model of Lung Cancer." *Nature Communications* 5 (January): 3056.

Reinmuth N, Kloos S, Warth A, Risch A, Muley T, Hoffmann H, Thomas M and Meister M. 2014. "Insulin-like Growth Factor 1 Pathway Mutations and Protein Expression in Resected Non–small Cell Lung Cancer." *Human Pathology* 45 (6): 1162–68.

Reuveni H, Flashner-Abramson E, Steiner L, Makedonski K, Song R, Shir A, Herlyn M, Bar-Eli M and Levitzki A. 2013. "Therapeutic Destruction of Insulin Receptor Substrates for Cancer Treatment." *Cancer Research* 73 (14): 4383–94.

Riely GJ, Kris MG, Rosenbaum D, Marks J, Li A, Chitale DA, Nafa K, et al. 2008. "Frequency and Distinctive Spectrum of KRAS Mutations in Never Smokers with Lung Adenocarcinoma." *Clinical Cancer Research : An Official Journal of the American Association for Cancer Research* 14 (18): 5731–34.

Roberts PJ and Der CJ. 2007. "Targeting the Raf-MEK-ERK Mitogen-Activated Protein Kinase Cascade for the Treatment of Cancer." *Oncogene* 26 (22): 3291–3310.

Robitaille AM, Christen S, Shimobayashi M, Cornu M, Fava LL, Moes S, Prescianotto-Baschong C, Sauer, Jenoe P and Hall MN. 2013. "Quantitative Phosphoproteomics Rev Ueal mTORC1 Activates de Novo Pyrimidine Synthesis." *Science (New York, N.Y.)* 339 (6125): 1320–23.

Roczniak-Ferguson A, Petit CS, Froehlich F, Qian S, Ky J, Angarola B, Walther TC and Ferguson SM. 2012. "The Transcription Factor TFEB Links mTORC1 Signaling to Transcriptional Control of Lysosome Homeostasis." *Science Signaling* 5 (228): ra42.

Rodriguez-Viciana P, Warne PH, Dhand R, Vanhaesebroeck B, Gout I, Fry MJ, Waterfield MD and Downward J. 1994. "Phosphatidylinositol-3-OH Kinase Direct Target of Ras." *Nature* 370 (6490): 527–32.

Rodriguez-Viciana P, Warne PH, Khwaja A, Marte BM, Pappin D, Das P, Waterfield MD, Ridley A and Downward J. 1997. "Role of Phosphoinositide 3-OH Kinase in Cell Transformation and Control of the Actin Cytoskeleton by Ras." *Cell* 89 (3): 457–67.

Roux PP, Ballif BA, Anjum R, Gygi SP and Blenis J. 2004. "Tumor-Promoting Phorbol Esters and Activated Ras Inactivate the Tuberous Sclerosis Tumor Suppressor Complex via p90 Ribosomal S6 Kinase." *Proceedings of the National Academy of Sciences of the United States of America* 101 (37): 13489–94.

Rozen F, Yang XF, Huynh H and Pollak M. 1997. "Antiproliferative Action of Vitamin D-Related Compounds and Insulin-like Growth Factor-Binding Protein 5 Accumulation." *Journal of the National Cancer Institute* 89 (9): 652–56.

Sahu N, Cruz DD, Gao M, Sandoval W, Haverty PM, Liu J, Stephan JP, et al. 2016. "Proline Starvation Induces Unresolved ER Stress and Hinders mTORC1-Dependent Tumorigenesis." *Cell Metabolism* 24 (5): 753–61.

Scagliotti G, Hanna N, Fossella F, Sugarman K, Blatter J, Peterson P, Simms L and Shepherd FA. 2009. "The Differential Efficacy of Pemetrexed according to NSCLC Histology: A Review of Two Phase III Studies." *The Oncologist* 14 (3): 253–63.

Schmid K, Oehl N, Wrba F, Pirker R, Pirker C and Filipits M. 2009. "EGFR/KRAS/BRAF Mutations in Primary Lung Adenocarcinomas and Corresponding Locoregional Lymph Node Metastases." *Clinical Cancer Research* 15 (14): 4554–60.

Schubbert S, Shannon K and Bollag G. 2007. "Hyperactive Ras in Developmental Disorders and Cancer." *Nature Reviews Cancer* 7 (4): 295–308.

Sciacca L, Vigneri R, Tumminia A, Frasca F, Squatrito S, Frittitta L and Vigneri P. 2013. "Clinical and Molecular Mechanisms Favoring Cancer Initiation and Progression in Diabetic Patients." *Nutrition, Metabolism and Cardiovascular Diseases* 23 (9): 808–15.

Settembre C, Di Malta C, Polito VA, Arencibia MG, Vetrini F, Erdin S, Erdin SU, et al. 2011. "TFEB Links Autophagy to Lysosomal Biogenesis." *Science* 332 (6036): 1429–33.

Settembre C, Zoncu R, Medina DL, Vetrini F, Erdin S, Erdin SU, Huynh Y, et al. 2012. "A Lysosome-to-Nucleus Signalling Mechanism Senses and Regulates the Lysosome via mTOR and TFEB." *The EMBO Journal* 31 (5): 1095–1108.

Shi Y, Yan H, Frost P, Gera J and Lichtenstein A. 2005. "Mammalian Target of Rapamycin Inhibitors Activate the AKT Kinase in Multiple Myeloma Cells by up-Regulating the Insulin-like Growth Factor Receptor/insulin Receptor Substrate-1/phosphatidylinositol 3-Kinase Cascade." *Molecular Cancer Therapeutics* 4 (10): 1533–40.

Siegel RL, Miller KD and Jemal A. 2017. "Cancer Statistics, 2017." *CA: A Cancer Journal for Clinicians* 67 (1): 7–30.

Soda M, Choi YL, Enomoto M, Takada S, Yamashita Y, Ishikawa S, Fujiwara S, et al. 2007. "Identification of the Transforming EML4–ALK Fusion Gene in Non-Small-Cell Lung Cancer." *Nature* 448 (7153): 561–66.

Son J, Lyssiotis CA, Ying H, Wang X, Hua S, Ligorio M, Perera RM, et al. 2013. "Glutamine Supports Pancreatic Cancer Growth through a KRAS-Regulated Metabolic Pathway." *Nature* 496 (7443): 101–5.

Spitz MR, Barnett MJ, Goodman GE, Thornquist MD, Wu X and Pollak M 2002. "Serum Insulin-like Growth Factor (IGF) and IGF-Binding Protein Levels and Risk of Lung Cancer: A Case-Control Study Nested in the Beta-Carotene and Retinol Efficacy Trial Cohort." *Cancer Epidemiology, Biomarkers & Prevention : A Publication of the American Association for Cancer Research, Cosponsored by the American Society of Preventive Oncology* 11 (11): 1413–18.

Stephen AG, Esposito D, Bagni RK and McCormick F. 2014. "Dragging Ras Back in the Ring." *Cancer Cell* 25 (3): 272–81.

Stephens P, Hunter C, Bignell G, Edkins S, Davies H, Teague J, Stevens C, et al. 2004. "Lung Cancer: Intragenic ERBB2 Kinase Mutations in Tumours." *Nature* 431 (7008): 525–26.

Strohecker AM, Guo JY, Karsli-Uzunbas G, Price SM, Chen GJ, Mathew R, McMahon M, and White E. 2013. "Autophagy Sustains Mitochondrial Glutamine Metabolism and Growth of BrafV600E-Driven Lung Tumors." *Cancer Discovery* 3 (11): 1272–85.

Strohecke AM and White E. 2014. "Autophagy Promotes *Braf*[V600E]-Driven Lung Tumorigenesis by Preserving Mitochondrial Metabolism." *Autophagy* 10 (2): 384–85.

Sullivan LB, Gui DY, Hosios AM, Bush LN, Freinkman E and Vander Heiden MG. 2015. "Supporting Aspartate Biosynthesis Is an Essential Function of Respiration in Proliferating Cells." *Cell* 162 (3): 552–63.

Sun, HZ, Tu X, Prisco M, Wu A, Casiburi I and Baserga R. 2003. "Insulin-like Growth Factor I Receptor Signaling and Nuclear Translocation of Insulin Receptor Substrates 1 and 2." *Molecular Endocrinology (Baltimore, Md.)* 17 (3): 472–86.

Szabolcs M, Keniry M, Simpson L, Reid LJ, Koujak S, Schiff SC, Davidian G, et al. 2009. "Irs2 Inactivation Suppresses Tumor Progression in Pten+/- Mice." *The American Journal of Pathology* 174 (1): 276–86.

Taniguchi CM, Emanuelli B and Kahn CR. 2006. "Critical Nodes in Signalling Pathways: Insights into Insulin Action." *Nature Reviews Molecular Cell Biology* 7 (2): 85–96.

Thariat J, Bensadoun RJ, Etienne-Grimaldi MC, Grall D, Penault-Llorca F, Dassonville O, Bertucci F, et al. 2012. "Contrasted Outcomes to Gefitinib on Tumoral IGF1R Expression in Head and Neck Cancer Patients Receiving Postoperative Chemoradiation (GORTEC Trial 2004-02)." *Clinical Cancer Research* 18 (18): 5123–33.

Thoreen CC, Kang SA, Chang JW, Liu Q, Zhang J, Gao Y, Reichling LJ, Sim T, Sabatini DM and Gray NS. 2009. "An ATP-Competitive Mammalian Target of Rapamycin Inhibitor Reveals Rapamycin-Resistant Functions of mTORC1." *Journal of Biological Chemistry* 284 (12): 8023–32.

Tolcher AW, Sarantopoulos J, Patnaik A, Papadopoulos K, Lin CC, Rodon J, Murphy B, et al. 2009. "Phase I, Pharmacokinetic, and Pharmacodynamic Study of AMG 479, a Fully Human Monoclonal Antibody to Insulin-Like Growth Factor Receptor 1." *Journal of Clinical Oncology* 27 (34): 5800–5807.

Toyoshima Y, Monson C, Duan C, Wu Y, Gao C, Yakar S, Sadler KC and LeRoith D. 2008. "The Role of Insulin Receptor Signaling in Zebrafish Embryogenesis." *Endocrinology* 149 (12): 5996–6005.

Tran TN, Selinger CI, Yu B, Ng CC, Kohonen-Corish MRJ, McCaughan B, Kennedy C, O'Toole SA and Cooper WA. 2014. "Alterations of Insulin-like Growth Factor-1 Receptor Gene Copy Number and Protein Expression Are Common in Non-Small Cell Lung Cancer." *Journal of Clinical Pathology* 67 (11): 985–91.

Tu X, Batta P, Innocent N, Prisco M, Casaburi I, Belletti B and Baserga R. 2002. "Nuclear Translocation of Insulin Receptor Substrate-1 by Oncogenes and Igf-I. Effect on Ribosomal RNA Synthesis." *The Journal of Biological Chemistry* 277 (46): 44357–65.

Ulanet DB, Ludwig DL, Kahn CR and Hanahan D. 2010. "Insulin Receptor Functionally Enhances Multistage Tumor Progression and Conveys Intrinsic Resistance to IGF-1R Targeted Therapy." *Proceedings of the National Academy of Sciences of the United States of America* 107 (24): 10791–98.

Vaishnavi A, Capelletti M, Le AT, Kako S, Butaney M, Ercan D, Mahale S, et al. 2013. "Oncogenic and Drug-Sensitive NTRK1 Rearrangements in Lung Cancer." *Nature Medicine* 19 (11): 1469–72.

Vigneri P, Frasca F, Sciacca L, Pandini G and Vigneri R. 2009. "Diabetes and Cancer." *Endocrine Related Cancer* 16 (4): 1103–23.

Ward AF, Braun BS and Shannon KM. 2012. "Targeting Oncogenic Ras Signaling in Hematologic Malignancies." *Blood* 120 (17): 3397–3406.

Weiss J, Sos ML, Seidel D, Peifer M, Zander T, Heuckmann JM, Ullrich RT, et al. 2010. "Frequent and Focal FGFR1 Amplification Associates with Therapeutically Tractable FGFR1 Dependency in Squamous Cell Lung Cancer." *Science Translational Medicine* 2 (62): 62ra93-62ra93.

Wu, Y, Cui K, Miyoshi K, Hennighausen L, Green JE, Setser J, LeRoith D and Yakar S. 2003. "Reduced Circulating Insulin-like Growth Factor I Levels Delay the Onset of Chemically and Genetically Induced Mammary Tumors." *Cancer Research* 63 (15): 4384–88.

Wu Y, Yakar S, Zhao L, Hennighausen L and LeRoith D. 2002. "Circulating Insulin-like Growth Factor-I Levels Regulate Colon Cancer Growth and Metastasis." *Cancer Research* 62 (4): 1030–35.

Yamauchi T, Kaburagi Y, Ueki K, Tsuji Y, Stark GR, Kerr IM, Tsushima T, et al. 1998. "Growth Hormone and Prolactin Stimulate Tyrosine Phosphorylation of Insulin Receptor Substrate-1, -2, and -3, Their Association with p85 Phosphatidylinositol 3-Kinase (PI3-Kinase), and Concomitantly PI3-Kinase Activation via JAK2 Kinase." *The Journal of Biological Chemistry* 273 (25): 15719–26.

Yang S, Wang X, Contino G, Liesa M, Sahin E, Ying H, Bause A, et al. 2011. "Pancreatic Cancers Require Autophagy for Tumor Growth." *Genes & Development* 25 (7): 717–29.

Yenush L and White MF. 1997. "The IRS-Signalling System during Insulin and Cytokine Action." *BioEssays* 19 (6): 491–500.

Ying H, Kimmelman AC, Lyssiotis CA, Hua S, Chu GC, Fletcher-Sananikone E, Locasale JW, et al. 2012. "Oncogenic Kras Maintains Pancreatic Tumors through Regulation of Anabolic Glucose Metabolism." *Cell* 149 (3): 656–70.

Yu CF, Liu ZX and Cantley LG. 2002. "ERK Negatively Regulates the Epidermal Growth Factor-Mediated Interaction of Gab1 and the Phosphatidylinositol 3-Kinase." *Journal of Biological Chemistry* 277 (22): 19382–88.

Yu H, Spitz MR, Mistry J, Gu J, Hong WK and Wu X. 1999. "Plasma Levels of Insulin-like Growth Factor-I and Lung Cancer Risk: A Case-Control Analysis." *Journal of the National Cancer Institute* 91 (2): 151–56.

Yu L, McPhee CK, Zheng L, Mardones GA, Rong Y, Peng J, Mi N, et al. 2010. "Termination of Autophagy and Reformation of Lysosomes Regulated by mTOR." *Nature* 465 (7300): 942–46.

Yuan HX, Russell RC and Guan KL. 2013. "Regulation of PIK3C3/VPS34 Complexes by MTOR in Nutrient Stress-Induced Autophagy." *Autophagy* 9 (12): 1983–95.

Yue Z, Jin S, Yang C, Levine AJ and Heintz N. 2003. "Beclin 1, an Autophagy Gene Essential for Early Embryonic Development, Is a Haploinsufficient Tumor Suppressor." *Proceedings of the National Academy of Sciences of the United States of America* 100 (25): 15077–82.

Zhang WC, Shyh-Chang N, Yang H, Rai A, Umashankar S, Ma S, Soh BS, et al. 2012. "Glycine Decarboxylase Activity Drives Non-Small Cell Lung Cancer Tumor-Initiating Cells and Tumorigenesis." *Cell* 148 (1–2): 259–72.

Zimmermann S and Moelling K. 1999. "Phosphorylation and Regulation of Raf by Akt (Protein Kinase B)." *Science (New York, N.Y.)* 286 (5445): 1741–44.

CHAPTER 2:

**ABLATION OF INSULIN RECEPTOR SUBSTRATES 1 AND 2 SUPPRESSES *KRAS*-
DRIVEN LUNG TUMORIGENESIS AND REDUCES INTRACELLULAR AMINO
ACID LEVELS**

This chapter is adapted from:

Xu H, Curry NL, Challa S, Freinkman E, Hitchcock DS, Copps KD, *et al*. Ablation of insulin

receptor substrates 1 and 2 suppresses *Kras*-driven lung tumorigenesis and reduces

intracellular amino acid levels. Manuscript submitted.

2.1 <u>ABSTRACT</u>

Non-small cell lung cancer (NSCLC) is a leading cause of cancer death worldwide, with 25% of cases harboring oncogenic *KRAS*. Although KRAS direct binding to, and activation of PI3K is required for *KRAS*-driven lung tumorigenesis, the contribution of insulin receptor (IR) and IGF-1 receptor (IGF-1R) in the context of mutant *KRAS* remains controversial. Here we provide genetic evidence that lung-specific dual ablation of insulin receptor substrates 1/2 (*Irs1*/*Irs2*), which mediate insulin and IGF-1 signaling, strongly suppresses tumor initiation and dramatically extends the survival of a mouse model of lung cancer with *Kras* activation and *p53* loss. Mice with *Irs1*/*Irs2* loss eventually succumb to tumor burden, with tumor cells displaying suppressed Akt activation and strikingly diminished intracellular amino acid levels. Acute loss of *IRS1*/*IRS2* or inhibition of IR/IGF-1R in *KRAS*-mutant human NSCLC cells similarly decreases intracellular amino acid levels, while enhancing basal autophagy and sensitivity to autophagy and proteasome inhibitors. These findings demonstrate that insulin/IGF-1 signaling is required for *KRAS*-mutant lung cancer initiation, and identify decreased amino acid levels as a metabolic vulnerability in tumor cells with IR/IGF-1R inhibition. Consequently, combinatorial targeting of IR/IGF-1R with autophagy or proteasome inhibitors may represent an effective therapeutic strategy in *KRAS*-mutant NSCLC.

2.2 <u>INTRODUCTION</u>

Non-small cell lung cancer (NSCLC) accounts for the majority of lung cancer, which to-date remains the leading cause of cancer death in the United States and worldwide (Siegel et al. 2017; WHO 2017). About a quarter of NSCLC cases harbor *KRAS* activating mutations

(Imielinski et al. 2012; Project 2017). However, effective therapies targeting KRAS are still

lacking and alternative approaches are urgently needed (Stephen et al. 2014). Previous reports

showed that KRAS can directly bind to and activate the p110 catalytic subunit of PI3K and

that this interaction is required for *in vivo Kras*-driven tumor initiation and maintenance in

mouse models of lung cancer (Gupta et al. 2007; Castellano et al. 2013). However, the

sufficiency of KRAS-PI3K interaction in driving lung cancer development remains largely

controversial, with evidence from cell culture studies implicating additional input from insulin

receptor (IR) and insulin-like growth factor-1 receptor (IGF-1R) (Pollak 2012; Molina-Arcas

et al. 2013). Most insulin/IGF-1 signaling in the lungs converges intracellularly onto the

adaptor proteins insulin receptor substrates IRS1 and IRS2 (White et al. 1985) prior to

diverging to a complex network of downstream signaling effectors, including PI3K/AKT

(Engelman et al. 2006). Here, using a robust genetic approach, we provide evidence that

concomitant ablation of *Irs1* and *Irs2* in the lungs of a well-established genetically engineered

mouse model of lung cancer with conditional *Kras* activation and *p53* loss strongly

suppresses tumor initiation, doubling tumor latency and significantly extending survival.

Lung cells with *Irs1/Irs2* ablation eventually overcome this suppression, though at a

stochastic rate, forming advanced lung adenocarcinomas. Interestingly, cells derived from

these tumors not only display suppressed Akt activation in response to insulin/IGF-1

stimulation, but also significantly decreased intracellular amino acid levels. We find that acute

loss or knockdown of *IRS1*/*IRS2* in *KRAS*-mutant human NSCLC cells, or pharmacological

inhibition of IR/IGF-1R in *KRAS*-mutant NSCLC or murine lung cancer cells similarly results

in decreased amino acid levels, accompanied by enhanced basal autophagy. NSCLC cells

with acute loss of *IRS1*/*IRS2* also display increased sensitivity to lysosomal or proteasomal

inhibitors. Our findings provide evidence that *IRS1* and *IRS2* are required for *Kras*-mutant lung cancer formation. They further shed light on the metabolic vulnerabilities that arise in tumors treated with IR/IGF-1R inhibitors, pointing to potential combinatorial approaches for treating *KRAS*-driven NSCLC.

2.3 <u>RESULTS</u>

2.3.1 Lung-specific genetic ablation of *Irs1* and *Irs2* significantly delays tumor formation in a *Kras*-driven mouse model of lung cancer

The conditional genetically engineered mouse model of lung cancer *Lox-STOP-Lox* (*LSL*)-*Kras*$^{G12D/+}$;*p53*$^{fl/fl}$ (Jackson et al. 2001; Jonkers et al. 2001; Oliver et al. 2010) herein referred to as "KP" was bred to mice harboring floxed alleles for both *Irs1* and *Irs2* genes (Dong et al. 2006), leading to the generation of *LSL-Kras*$^{G12D/+}$;*p53*$^{fl/fl}$;*Irs1*$^{fl/fl}$;*Irs2*$^{fl/fl}$ or "KPI" mice. Intranasal administration of adenoviral Cre into KP or KPI mice at 5-6 weeks of age led to the concomitant expression of activated *Kras* and loss of *p53* alone (KP mice) or the triple loss of *p53*, *Irs1* and *Irs2* (KPI mice) in mouse lung cells (Fig. 2.1A). As previously reported (Oliver et al. 2010; Curry et al. 2013), 10 weeks post-Cre administration, KP mice developed extensive lung adenomas and adenocarcinomas (Fig. 2.1B, C) and succumbed to tumor burden by 140 days, with median survival of 107 or 103 days for males and females, respectively (Fig. 2.1D). In contrast, lungs of KPI mice were devoid of any tumors or hyperplasia at 8-10 weeks post-infection and retained normal histology (Fig. 2.1B, C, E, F). Surprisingly however, KPI mice eventually overcame the loss of *Irs1*/*Irs2*, and developed lung adenocarcinomas at a significantly extended and highly variable tumor latency (16-30 weeks for KPI compared to 8 weeks for KP, Fig. 2.1E, F). Moreover, both the median

survival (191 days for males and 209 days for females) and maximal survival (~300 days) of

KPI mice were twice as long as those of KP mice (Fig. 2.1D). Interestingly, when lung tumors

from moribund KP and KPI mice were analyzed and compared histopathologically, KPI

tumors displayed a significantly increased proportion of higher-grade adenocarcinomas and

carcinomas, characterized by nuclear pleomorphism and invasion of basement membrane

(Fig. 2.1G, H). These results indicate that *Irs1* and *Irs2* are required for *Kras*-driven lung

tumor initiation and that *Kras*-transformed cells can eventually bypass *Irs1*/*Irs2* loss,

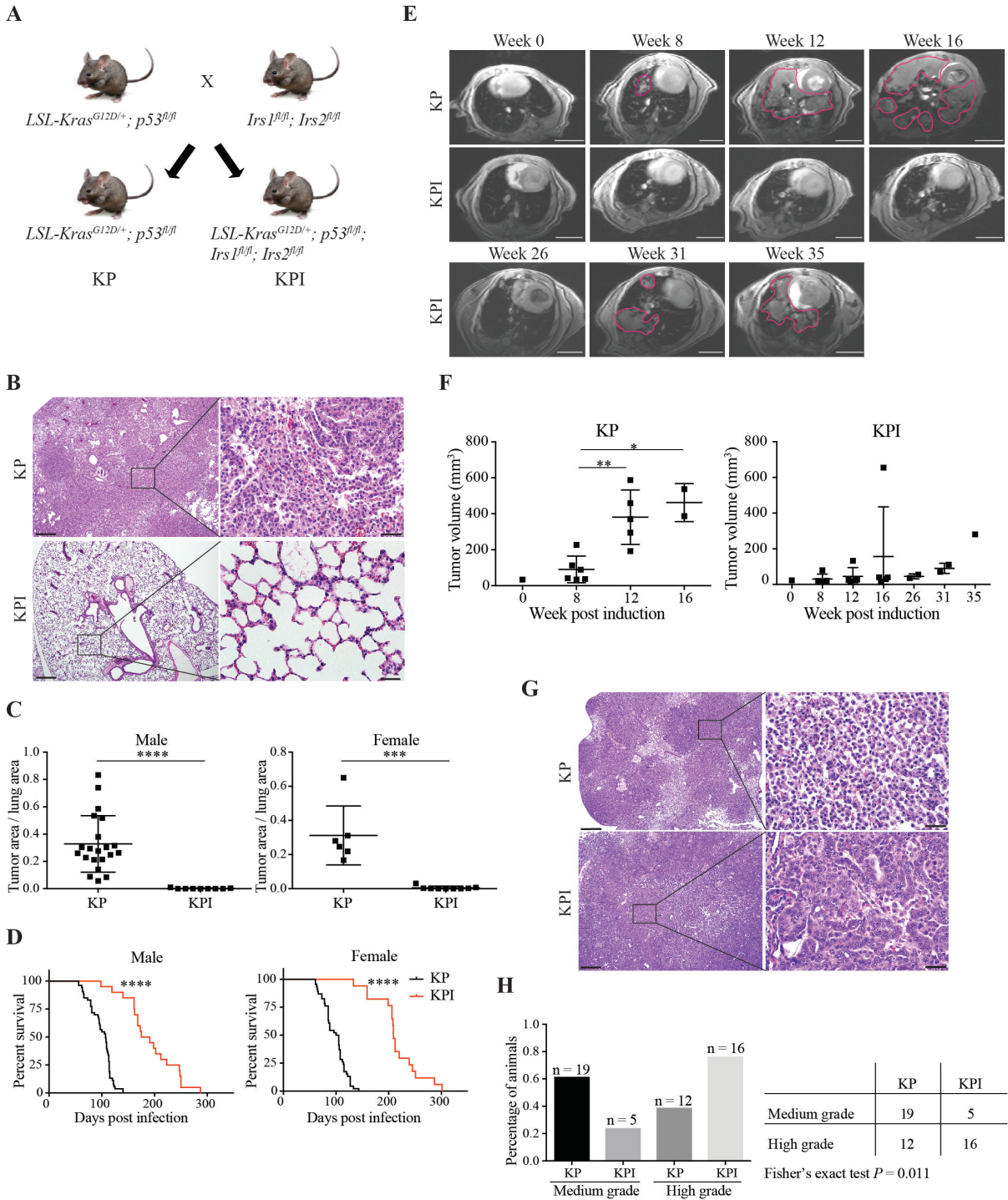developing more aggressive tumors at a highly variable and extended latency.

Figure 2.1. Loss of *Irs1* and *Irs2* significantly delays *Kras*-driven lung tumorigenesis.

(**A**) Breeding schematic for generating KP and KPI mice. (**B**) H&E staining of KP and KPI

lungs 10 weeks post-adenoviral Cre infection (left) with 10-fold magnification of the framed

Figure 2.1. (Continued)

area (right). Scale bars, 400 μm (left) and 40 μm (right). (**C**) Tumor burden representing

tumor area/total lung area in KP and KPI lungs 10 weeks post-adenoviral Cre infection.

Males, $n = 21$ (KP) and $n = 9$ (KPI); females, $n = 6$ (KP) and $n = 9$ (KPI); ***$P < 0.001$;

****$P < 0.0001$. (**D**) Kaplan-Meier survival curves for KP and KPI mice. Males, $n = 53$ (KP)

and $n = 20$ (KPI); females, $n = 46$ (KP) and $n = 17$ (KPI); ****$P < 0.0001$ by log-rank test

between KP and KPI for both genders. (**E**) MRI showing axial planes of representative KP

lungs at weeks 0 to 16, and KPI lungs at weeks 0 to 35 post-adenoviral Cre infection. Tumor

areas are delineated in red. (**F**) Volumes of KP and KPI tumors quantified from MRI images

represented in *E*. Each data point represents one animal; *$P < 0.05$; **$P < 0.01$. (**G**) H&E

staining of KP and KPI lungs from moribund mice (left) with 10-fold magnification of the

framed area (right). Scale bars, 400 μm (left) and 40 μm (right). (**H**) Percentage of KP and

KPI mice with medium grade or high grade tumors at moribund stage (left) with Fisher's

exact test (right). Mice with medium grade tumors are characterized by non-invasive grade 2

adenomas and grade 3 adenocarcinomas. Mice with high grade tumors harbor grade 3 and

invasive grade 4 adenocarcinomas as described in Methods; "*n*" indicates the number of mice

in each group. In C and F, data represent the mean ± SD. H&E, hematoxylin and eosin.

2.3.2 Loss of *Irs1* and *Irs2* suppresses Akt signaling and leads to decreased amino acid

levels in murine *Kras*-driven lung tumor cells

To characterize the signaling and metabolism of cells with *Irs1/Irs2* loss, KP and KPI

lung tumors were isolated and used to establish cell lines in culture. Genotyping confirmed

the concomitant excision of the STOP codon upstream of $Kras^{G12D}$ and loss of *p53* in both KP

and KPI cells, with the additional deletion of *Irs1* and *Irs2* in KPI but not KP cells (Fig.

2.2A). Although one of the KPI cell lines (KPI-6) seemed to harbor incomplete Cre-mediated

recombination, the faint genotyping bands for LSL-$Kras^{G12D}$ and floxed *Irs1* and *Irs2* were

due to the rare residual presence of non-transformed cells at this early cell line passage.

Indeed, in future passages, Irs1 and Irs2 proteins were completely lost in all KPI cell lines
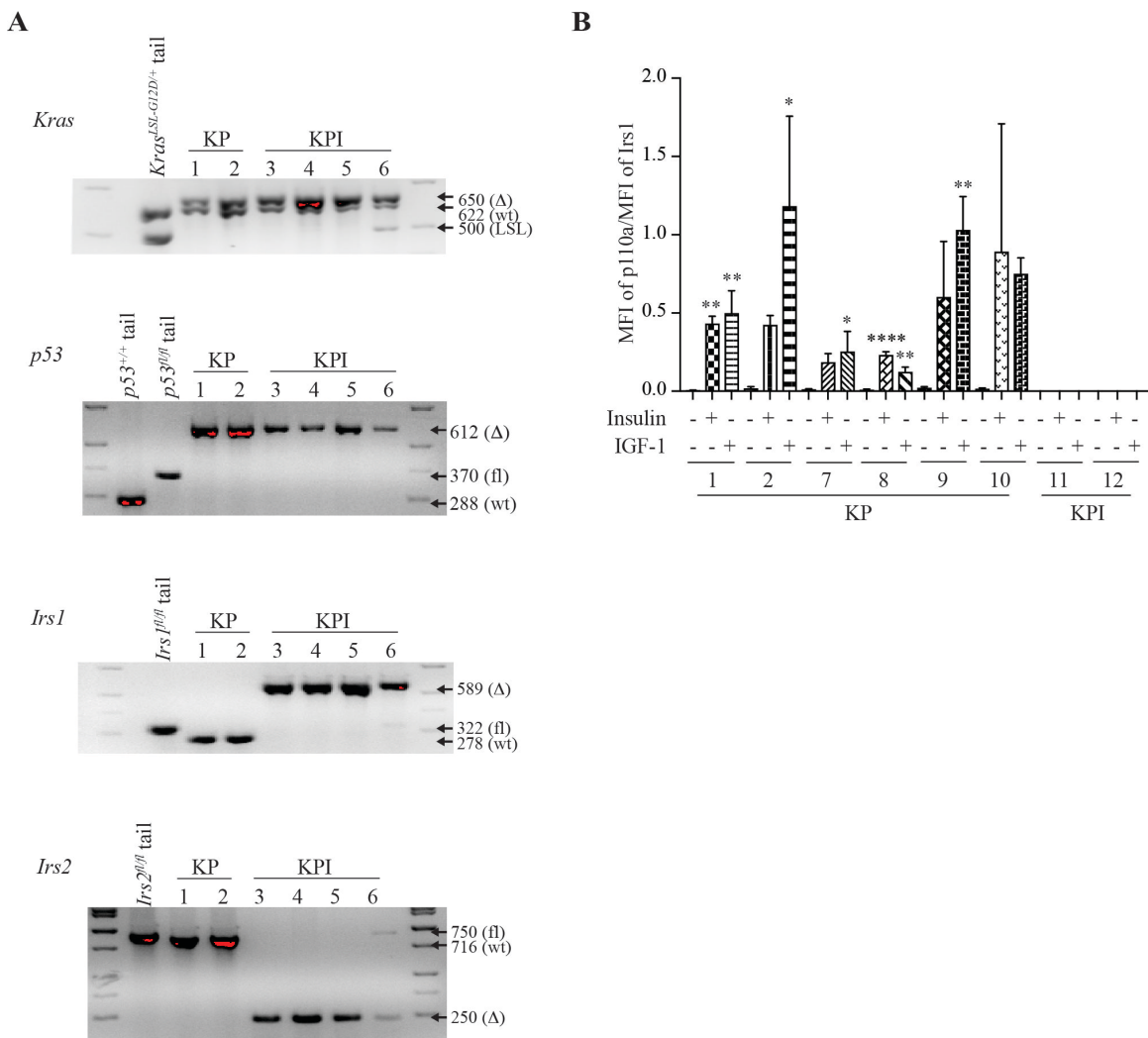
(Fig. 2.5A).

Figure 2.2. KPI but not KP cells demonstrate loss of *Irs1*/*Irs2* expression and loss of

insulin/IGF-1 signaling to Pi3k.

Figure 2.2. (Continued)

(**A**) Genotyping DNA gels showing recombined LSL-*Kras*^*G12D* and *p53*^*fl/fl* alleles in KP (1, 2) and KPI (3-6) cells, in addition to recombined *Irs1*^*fl/fl* and *Irs2*^*fl/fl* alleles in KPI, but not KP cells. KPI-6 shows presence of residual non-transformed cells at this earlier passage, evident by trace levels of non-recombined LSL-*Kras*^*G12D*, *Irs1* and *Irs2* alleles. Tail DNA was used as a control for wild-type and floxed alleles. (**B**) Luminex bead-based assay demonstrating Irs1-Pi3k p110α interaction in KP but not KPI cells. Cells were starved of serum for 1 hour and stimulated with insulin (500 ng/ml) or IGF-1 (50 ng/ml) for 10 minutes. Irs1-p110α interaction was quantified as median fluorescence intensity (MFI) of p110α over MFI of Irs1; Data indicate the mean ± SD and are representative of 3 independent experiments; *n*= 3 biological replicates per condition per cell line; *P < 0.05; **P < 0.01 and ****P < 0.0001.

To confirm the relevance and engagement of Irs1 and Irs2 in insulin/IGF-1 signaling in lung tumor cells, we first performed a Luminex bead-based immunoassay (Copps et al. 2016) in KP and KPI cell lines that is optimized to assess the interaction between Irs1 and Pi3k catalytic subunit p110⬜ (Fig. 2.2B). Acute stimulation of serum-starved KP but not KPI cells with either insulin or IGF-1 dramatically enhanced Irs1-p110⬜ interaction, confirming signal transduction from Ir and Igf1r to Pi3k in the lung cancer cells (Fig. 2.2B).

We then assessed alterations in Akt phosphorylation (pT308 and pS473) upon ligand stimulation in KP and KPI cells with single or double knockdown of *Irs1* and *Irs2*. Loss of either *Irs1* or *Irs2* alone did not significantly affect Akt activation in the murine KP cells (Fig. 2.3A, B) or in human *KRAS*-mutant NSCLC cells (Fig. 2.4A-D). In contrast, concomitant

69

silencing of both *Irs1* and *Irs2* strongly suppressed Akt activation in response to insulin or

IGF-1 stimulation (Fig. 2.5A). These results provide strong evidence of a functional

redundancy in Irs1 and Irs2 signal transduction in *Kras*-driven lung tumor cells, and are

consistent with a recent report demonstrating increased rather than decreased tumor formation

in a *Kras*-driven mouse model of lung cancer with loss of *Irs1* alone (Metz et al. 2016).

Intriguingly however, Erk1/2 activation (pT202/Y204) levels varied significantly among the

different cell lines upon ligand treatment, and did not correlate with the loss of *Irs1*/*Irs2*,

reflecting heterogeneity in the tumor cell populations (Fig. 2.3, 2.4, and 2.5A). This

observation is consistent with the previously reported intratumoral stage-heterogeneity in

Kras-driven lung tumors, where MAPK signal amplification, a driver of malignant

progression, was found to only mark a fraction of the tumor cell populations (Feldser et al.

2010).
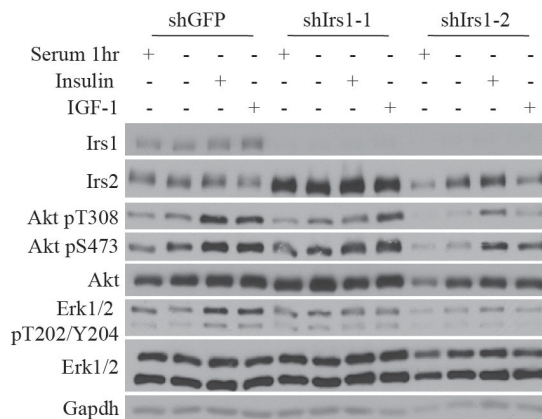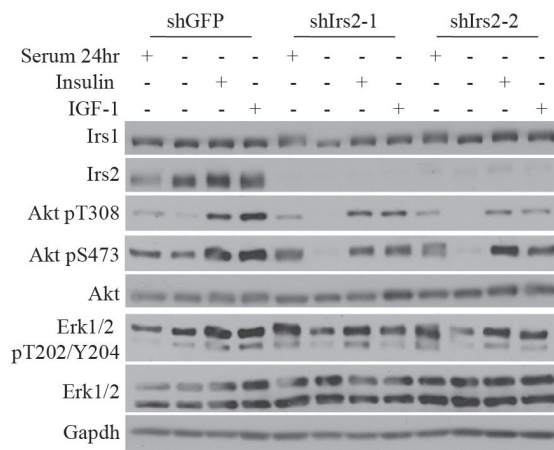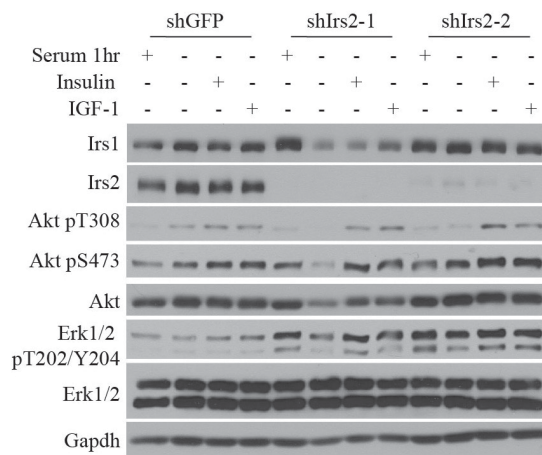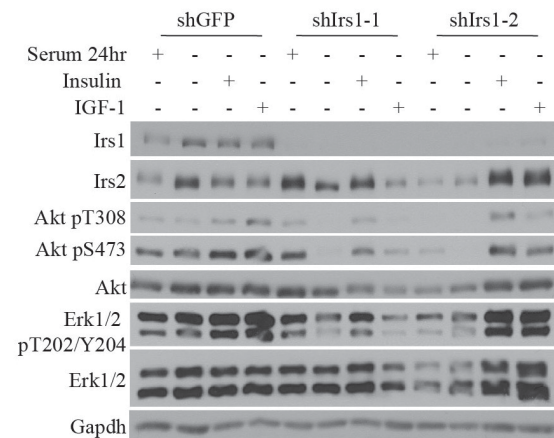
Figure 2.3. Single knockdown of *Irs1* or *Irs2* does not suppress Akt signaling in murine *Kras*-mutant lung cancer cells.

(**A, B**) Levels of Irs1, Irs2, total or phosphorylated Akt (pT308 or pS473) and Erk1/2 (pT202/Y204) in murine *p53*-null, *Kras*-mutant lung cancer cells (KP cells) with control *GFP* knockdown or single knockdown of *Irs1*, or *Irs2*. Cells were starved of serum for 1 hour (A) or 24 hours (B) and stimulated with insulin (1 µg/ml) or IGF-1 (100 ng/ml) for 10 minutes. Gapdh was used as a loading control.

Figure 2.4. Single knockdown of *IRS1* or *IRS2* does not suppress AKT signaling in human *KRAS*-mutant NSCLC cells.

(**A-D**) Levels of IRS1, IRS2, total or phosphorylated AKT (pT308 or S473) and ERK1/2 (pT202/Y204) in *KRAS*-mutant NSCLC A549 (A and B) and Calu-1 (C and D) cells with control *GFP* knockdown or single knockdown of *IRS1* or *IRS2*. Cells were starved of serum for 1 hour in A and C, and 24 hours in B and D, and stimulated with insulin (1 μg/ml for A549 cells, 100 ng/ml for Calu-1 cells) or IGF-1 (100 ng/ml for A549 cells, 10 ng/ml for Calu-1 cells) for 10 minutes. GAPDH was used as a loading control.

Figure 2.4. (Continued)

A

KP | KPI

| | KP | | | | KPI | | | |
Serum / IGF-1 panels...

Irs1
Irs2
Akt pT308
Akt pS473
Akt
Erk1/2 pT202/Y204
Erk1/2
Gapdh

C

	-log (P)	FDR
Pantothenate and CoA biosynthesis	27.832	3.93E-11
Ubiquinone and other terpenoid-quinone biosynthesis	23.755	9.41E-10
Phenylalanine, tyrosine and tryptophan biosynthesis	23.269	9.41E-10
Phenylalanine metabolism	23.269	9.41E-10
Valine, leucine and isoleucine degradation	22.969	1.02E-09
Valine, leucine and isoleucine biosynthesis	18.462	7.68E-08
Aminoacyl-tRNA biosynthesis	15.891	8.60E-07
Tyrosine metabolism	15.229	1.46E-06
D-Glutamine and D-glutamate metabolism	15.028	1.59E-06
Lysine biosynthesis	12.851	1.26E-05
Glycine, serine and threonine metabolism	12.591	1.42E-05
Tryptophan metabolism	12.549	1.42E-05
Nitrogen metabolism	12.289	1.70E-05
Alanine, aspartate and glutamate metabolism	10.245	1.22E-04

D

row min — row max

KP: 1 2   KPI: 3 4 5 6

methionine
threonine
phenylalanine
valine
tryptophan
leucine
glutamine
tyrosine
serine
isoleucine
aspartate
alanine
histidine

B

Igf1r pY1135/1136
Akt pT308
Akt pS473
Gsk3α/β pS21/29
Tsc2 pT1462
S6k1 pT389
β-catenin pT41/S45
β-Catenin
E-Cadherin

Serum / IGF-1
KP   KPI

Figure 2.5. Murine *Kras*-driven lung tumor cells with *Irs1/Irs2* loss have impaired Akt signaling and decreased intracellular amino acids.

Figure 2.5. (Continued)

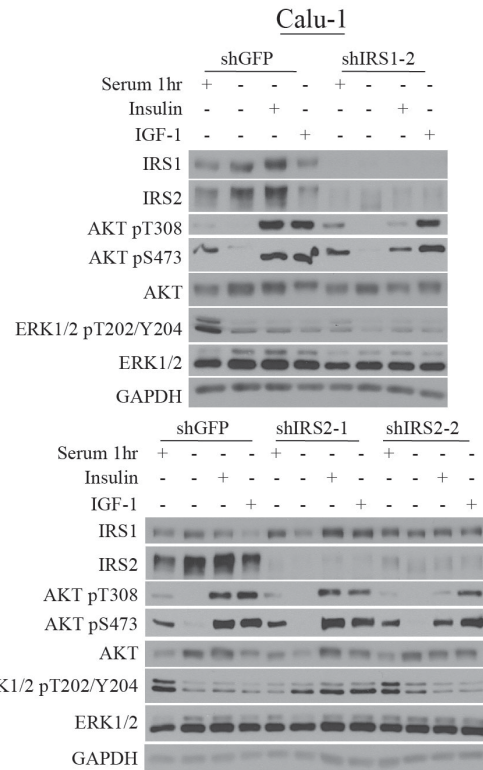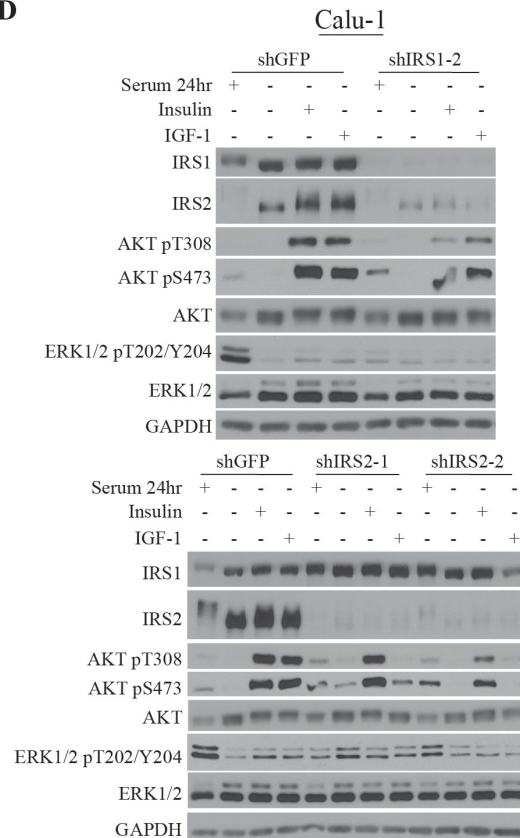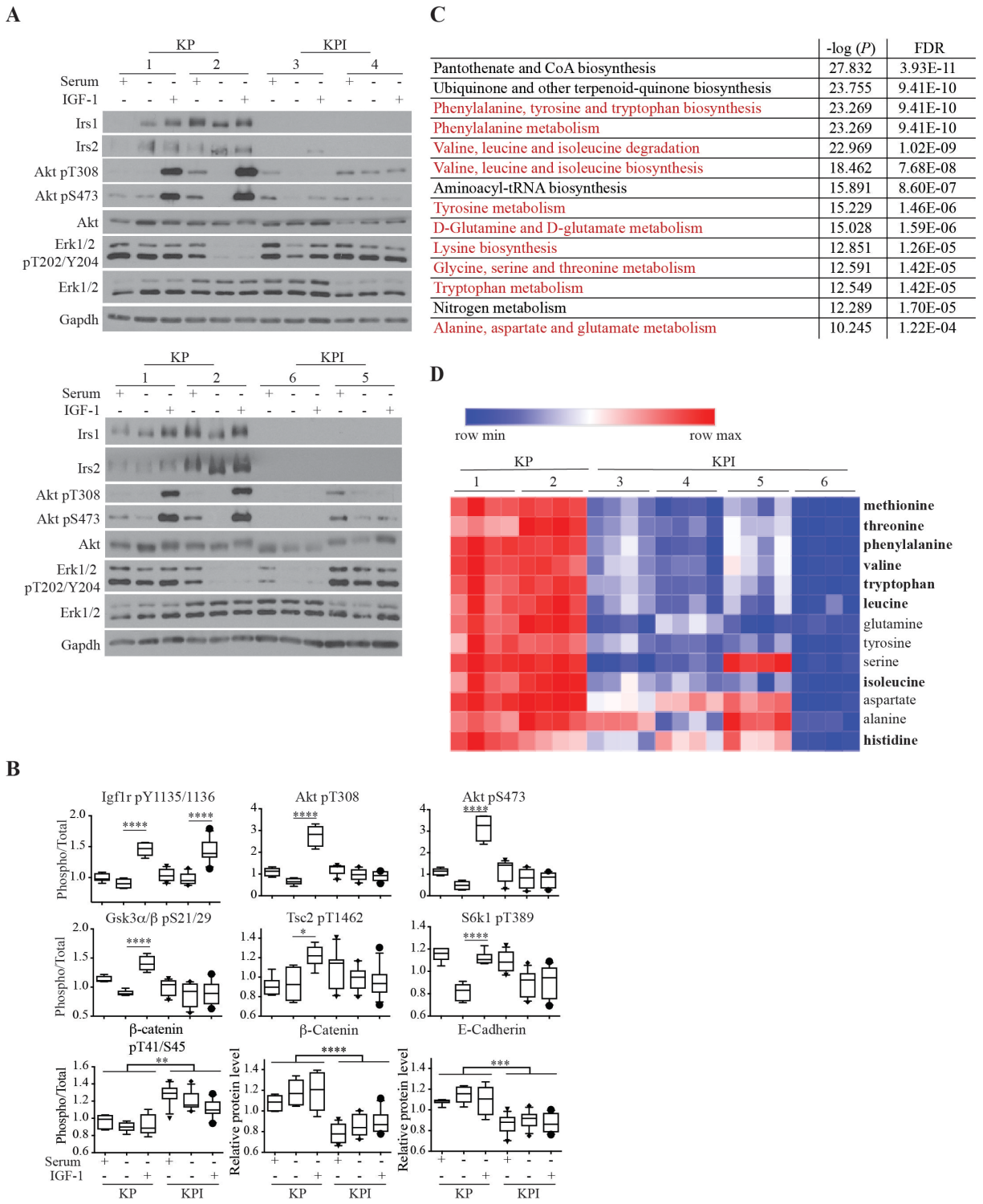(**A**) Levels of Irs1, Irs2, total or phosphorylated Akt (pT308 and pS473) and total or phosphorylated Erk1/2 (pT202/Y204) in KP (cell lines 1 and 2) and KPI (cell lines 3, 4, 5 and 6) cells that were grown in 10% serum or serum-starved for 1 hour with or without IGF-1 (50 ng/ml) stimulation for 10 minutes. Gapdh was used as a loading control. (**B**) Box plots representing total or phosphorylated levels of selected effectors of Akt signaling quantified by reverse phase protein array (RPPA) in KP and KPI cells treated as in *A*. Levels of phosphorylated proteins were normalized to total levels of the respective proteins. Data represent the median ± 10-90 percentile for each protein/phosphoprotein; $n = 3$ biological replicates per condition per cell line. In the top 2 rows, stars indicate significant changes in serum-starved cells with or without IGF-1 stimulation. In the bottom row, stars indicate the lowest degree of significance between KP and KPI cells under each condition. *$P < 0.05$; **$P < 0.01$; ***$P < 0.001$; ****$P < 0.0001$. (**C**) List of top 14 metabolic pathways that are significantly different between KP (1, 2) and KPI (3-6) cells grown in 10% serum. In red are pathways involved in amino acid metabolism. Data were processed by Metaboanalyst 3.0 and the pathways were ranked by –log of the *P*-value. FDR indicates false discovery rate. (**D**) Heatmap listing in descending order of statistical significance ($P < 0.05$ by t-test), all amino acids whose levels are different between KP and KPI cells described in *C*. In bold are essential amino acids. Red indicates higher expression, and blue indicates lower expression relative to the mean expression level within each group; $n = 4$ biological replicates per cell line.

To acquire a broader assessment of the effects of *Irs1* and *Irs2* loss on signaling networks, we performed reverse phase protein array (RPPA) analysis (Hennessy et al. 2010) of 300 proteins and phosphoproteins representing many major signaling pathways (Fig. 2B and Supplemental Table S1). We used protein lysates from KP and KPI cells that were either non-starved (10% serum), 1-hour serum-starved or serum-starved and acutely stimulated with IGF-1. The most striking differences were detected under acute IGF-1-stimulated conditions, representing significant suppression of Akt activation and its downstream signaling in KPI compared to KP cells. As expected, IGF-1 stimulation resulted in the phosphorylation of its receptor at Y1135/1136 in both KP and KPI cells (Fig. 2.5B). However, Akt activation (pT308 and pS473) upon IGF-1 stimulation was blunted in KPI, compared to KP cells. This was mirrored by the blunted inactivating phosphorylation of the Akt targets, Gsk-3□/□ (pS21/29) and Tsc2 (pT1462). Indeed, the increased activity in KPI cells, of Tsc2, a repressor of mTORC1 signaling, led to decreased phosphorylation of the mTORC1 target S6k1 (pT389) upon IGF-1 stimulation, as compared to KP cells (Fig. 2.5B). However, because mTORC1 can be activated by growth factor signaling independent of insulin/IGF-1 (Saxton and Sabatini 2017), S6k1 phosphorylation was maintained in KPI cells cultured in 10% serum, independent of *Irs1*/*Irs2* loss. Consistent with suppressed Akt signaling in KPI cells, an increase in Gsk-3 □/□ activity resulted in constitutive phosphorylation of β-catenin (pT41/S45), which leads to its proteasomal degradation (Fig. 2.5B). Indeed, lower levels of β-catenin were detected in KPI cells, accompanied by a decrease in the levels of its binding partner E-cadherin (Fig. 2.5B). Interestingly, this phenotype is known to correlate with tumor progression (Jeanes et al. 2008), consistent with the more aggressive nature of KPI tumors at a moribund stage (Fig. 2.1G, H) .

We then sought to explore the metabolic differences between KP and KPI cells, with the goal of identifying metabolic dependencies upon *Irs1/Irs2* loss. To that end, we profiled over 150 polar metabolites in the tumor cells grown for 24 hours under either non-serum-starved or serum-starved conditions. KP and KPI cells displayed no significant metabolic distinctions under serum-starved conditions, indicating that loss of *Irs1/Irs2* closely mimics conditions of growth factor deprivation. In contrast, striking differences were observed under non-starved conditions, with pathway enrichment analysis identifying amino acid synthesis or degradation as top impacted metabolic pathways between KP and KPI cells (Fig. 2.5C). In particular, KPI cells exhibited significantly lower intracellular levels of essential amino acids, including leucine, isoleucine, valine, methionine, phenylalanine, threonine, tryptophan, in addition to glutamine and tyrosine (Fig. 2.5D), suggesting a role for Irs1/Irs2 in amino acid metabolism.

2.3.3 Loss of *IRS1* and *IRS2* in human *KRAS*-mutant NSCLC cells leads to impaired AKT signaling and reduced intracellular amino acid levels

To investigate the relevance of IRS1 and IRS2 in human lung cancer, we extended our studies to established NSCLC cell lines that harbor activating *KRAS* mutations. Dual loss of *IRS1* and *IRS2* was engineered via CRISPR/Cas9 double knockout (DKO) in A549 cells (Fig. 2.6A), whereas *IRS1/IRS2* double knockdown (DKD) was achieved via stable small hairpin expression in both A549 and Calu-1 cells (Fig. 2.6A and Fig. 2.7). In A549 DKO, A549 DKD and Calu-1 DKD cells, AKT activation was severely mitigated in response to insulin or IGF-1 stimulation (Fig. 2.6A and Fig. 2.7A, B), consistent with the results obtained from murine KP

and KPI cells (Fig. 2.5A). Moreover, *in vitro* cellular proliferation was impaired by loss of *IRS1*/*IRS2* (Fig. 2.6B).

To assess the effects of loss of *IRS1* and *IRS2* on cellular metabolism, metabolite profiling was performed on A549 and Calu-1 cells cultured under non-serum starved conditions. Strikingly, and consistent with our findings in the mouse KPI cells, the levels of all essential amino acids, except for lysine, in addition to the semi-essential amino acids asparagine, glutamine, glycine and tyrosine, were significantly decreased or trended towards a decrease in A549 DKO and Calu-1 DKD cells compared to the control cells, further underscoring a role of IRS1/2 in amino acid metabolism (Fig. 2.6C).
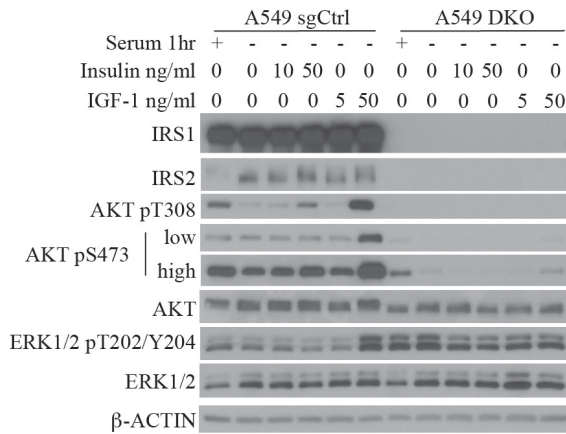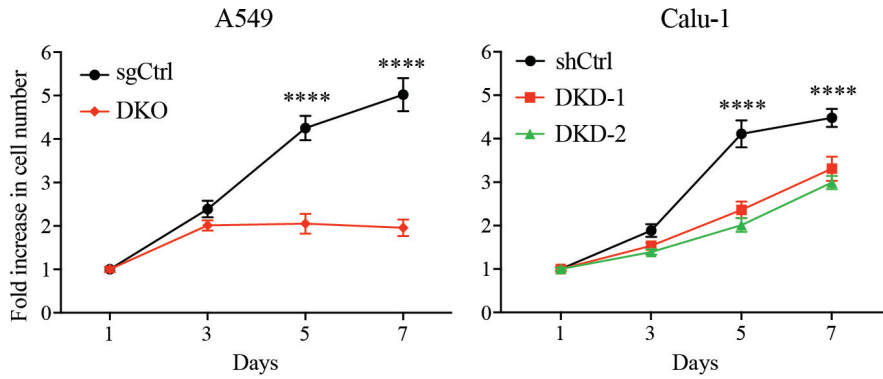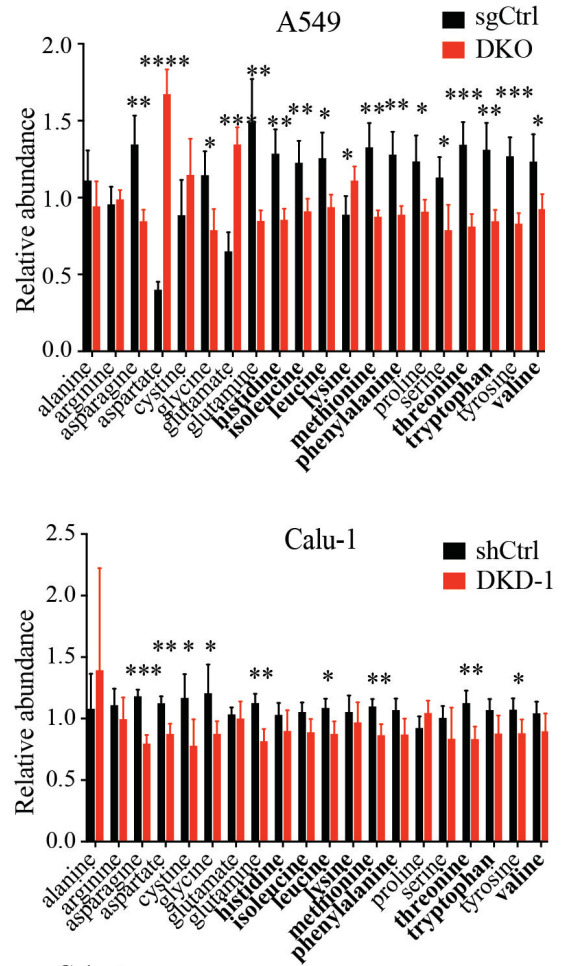
Figure 2.6. Loss of *IRS1* and *IRS2* in human *KRAS*-mutant NSCLC leads to impaired AKT signaling and reduced intracellular amino acid levels.

Figure 2.6. (Continued)

(**A**) Levels of IRS1, IRS2, total or phosphorylated AKT (pT308 and pS473) and total or phosphorylated Erk1/2 (pT202/Y204) in NSCLC A549 cells with *IRS1/IRS2* (A549 DKO) or control (A549 sgCtrl) double knockout as well as Calu-1 cells with *IRS1/IRS2* (Calu-1 DKD) or control (Calu-1 sh*GFP*/sh*Scramble*, termed shCtrl) double knockdown cells. Cells were serum-starved for 1 hour and then stimulated with insulin (0, 10 or 50ng/ml) or IGF-1 (0, 5 or 50ng/ml) for 10 minutes. (**B**) Proliferation curves of cells described in *A* that were grown under low serum conditions (0.1% serum for A549 and 2% serum for Calu-1) over 7 days; $n = 6$. (**C**) Levels of amino acids in NSCLC cells described in *A* that were first normalized to protein levels, and then normalized to the median of all samples for each amino acid; $n = 4$ biological replicates per cell line; data are representative of two independent experiments. In B and C, data represent the mean ± SD; *$P < 0.05$; **$P < 0.01$; ***$P < 0.001$; ****$P < 0.0001$. In bold are essential amino acids.
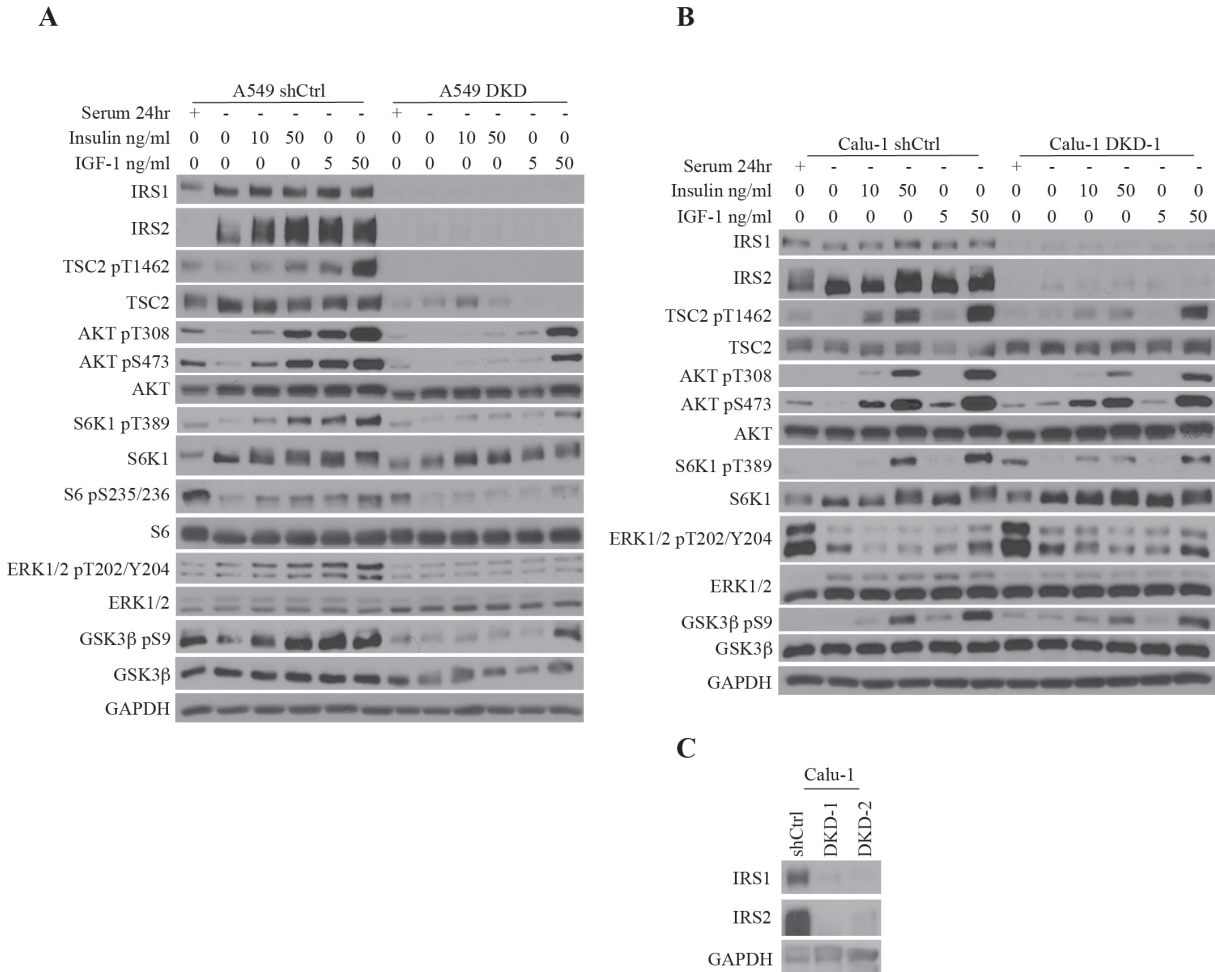
Figure 2.7. Concomitant silencing of *IRS1* and *IRS2* in human NSCLC cells impairs insulin/IGF-1-stimulated AKT signaling.

(**A, B**) Levels of IRS1, IRS2, total or phosphorylated ERK1/2 (pT202/Y204), S6K (pT389), S6 (pS235/236), AKT (pT308 or pS473) and its targets TSC-2 (pT1462) and GSK3β (pS9) in A549 (A) or Calu-1 (B) cells with control knockdown (sh*GFP*/sh*Scramble*, termed shCtrl) or *IRS1*/*IRS2* double knockdown (DKD). Cells were serum-starved for 24 hours and then stimulated with insulin or IGF-1 for 10 minutes. (**C**) Western blots confirming concomitant knockdown of *IRS1* and *IRS2* in Calu-1 cells using 2 distinct pairs of hairpins for *IRS1* and *IRS2* (DKD-1 and DKD-2). In A-C, GAPDH was used as a loading control.

2.3.4 Acute loss of *IRS1* and *IRS2* promotes autophagy in human *KRAS*-mutant lung cancer cells

Because amino acid levels were significantly decreased upon *IRS1*/*IRS2* loss, we investigated a potential effect on autophagy, a self-catabolic process induced by nutrient starvation and decreased mTORC1 activity (Perera and Zoncu 2016). We found that compared to control cells, both A549 DKO and Calu-1 DKD cells are more sensitive to chloroquine (CQ) treatment, indicating that loss of *IRS1*/*IRS2* sensitizes NSCLC cells to autophagy inhibition (Fig. 2.8A). Indeed, A549 DKO cells demonstrated higher basal autophagic flux than control cells, as evidenced by increased levels and enhanced accumulation, in the presence of full media, of the autophagosome marker LC3-II upon CQ treatment (Fig. 2.8B). Moreover, upon GFP-LC3 overexpression, these cells demonstrated significantly higher levels of GFP cleavage independent of CQ treatment (Fig. 2.8C). Consistently, compared to control cells, a higher percentage of A549 DKO cells displayed GFP-LC3 punctae, resulting from enhanced autophagosome formation (Fig. 2.8D, E). These results imply that NSCLC cells promote intracellular protein catabolic pathways to compensate for the sharp decrease in amino acid levels upon *IRS1*/*IRS2* loss. Indeed, compared to their respective control cells expressing *IRS1* and *IRS2*, both A549 DKO and Calu-1 DKD cells were more sensitive to the proteasome inhibitor MG-132 (Fig. 2.8F).
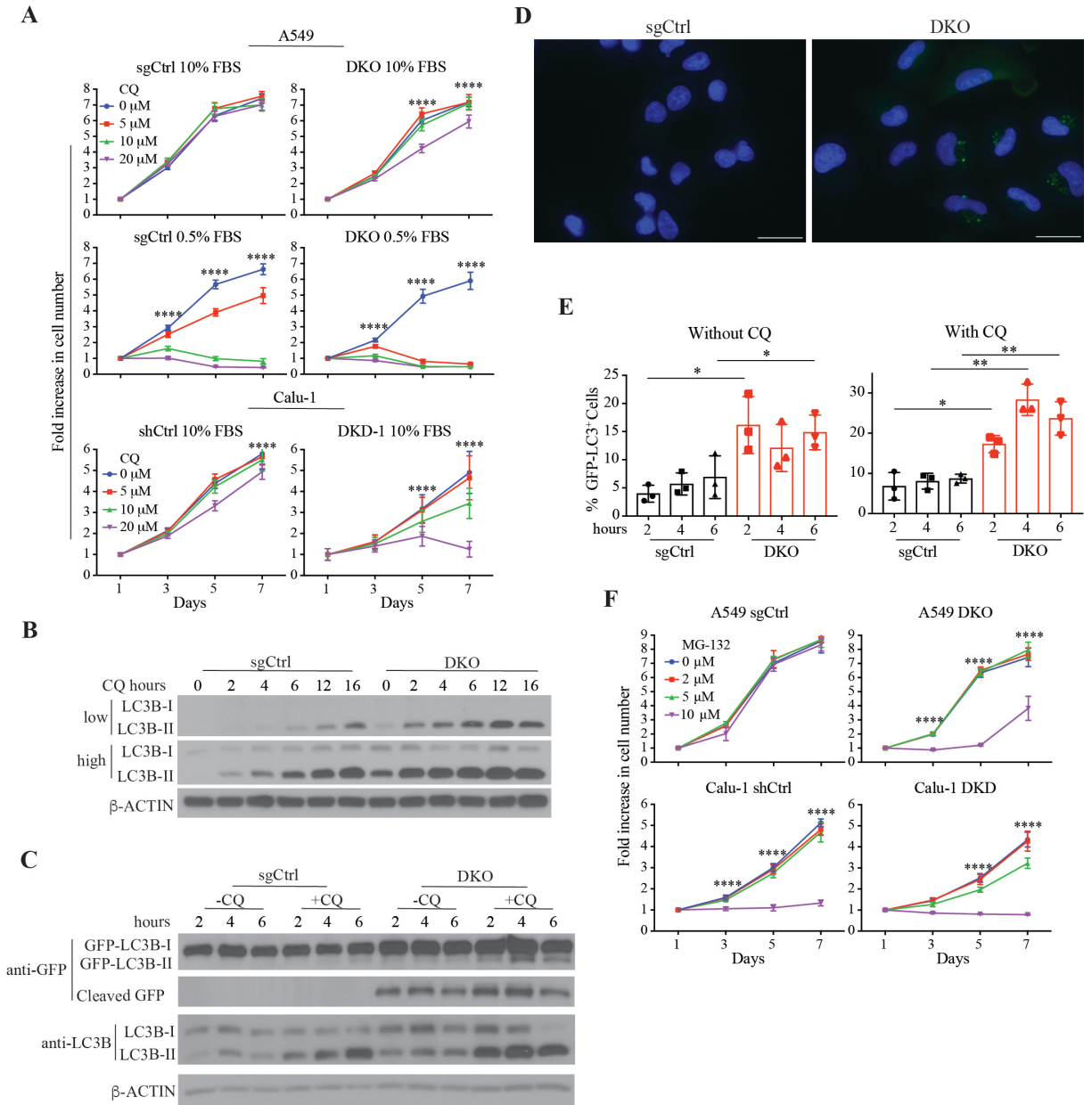
Figure 2.8. Acute loss of *IRS1* and *IRS2* induces autophagy in human *KRAS*-mutant NSCLC cells.

(**A**) Proliferation curves of NSCLC A549 cells with *IRS1/IRS2* (A549 DKO) or control (A549 sgCtrl) double knockout as well as Calu-1 cells with *IRS1/IRS2* (Calu-1 DKD) or control *GFP/Scramble* (shCtrl) double knockdown cells cultured in 10% serum and treated with chloroquine (CQ, 0, 5, 10 or 20 μM); *n* = 6; ****P < 0.0001 between 0 and 20 μM

Figure 2.8. (Continued)

conditions. (**B**) Levels of LC3B-I and LC3B-II in A549 cells described in *A* treated with 10 μM CQ for 0 to 16 hours. Compared to sgCtrl cells, A549 DKO cells have enhanced LC3B-II accumulation, indicating enhanced autophagic flux. (**C**) Increased accumulation with or without CQ treatment, of endogenous LC3B-II as well as GFP cleavage from exogenously expressed GFP-LC3B in A549 cells with *IRS1/IRS2* loss, compared to A549 sgCtrl cells. Cells were cultured in the presence of 10% serum with or without 10 μM CQ for 2, 4 or 6 hours. In B and C, β-ACTIN was used as a loading control. (**D**) Fluorescence microscopy images demonstrating increased GFP-LC3 punctae upon loss of *IRS1/IRS2* in A549 DKO cells compared to sgCtrl cells described in *C* that were treated with 10 μM CQ for 6 hours. Scale bars, 25 μM. (**E**) Quantification of GFP-LC3 punctae in cells from *D*; n = 15-20 images per condition; *$P < 0.05$; **$P < 0.01$; Data are pooled from three independent experiments. (**F**) Proliferation curves of A549 and Calu-1 cells described in *A*, that were grown in 10% serum and treated with MG-132 (0, 2, 5 and 10 μM) for 7 days; $n = 6$; ****$P < 0.0001$ between 0 and 10 μM conditions for A549 and between 0 and 5 μM as well as 0 and 10 μM for Calu-1. In A, E and F, data represent the mean ± SD.

2.3.5 Acute inhibition of insulin and IGF-1 receptors induces autophagy and loss of *IRS1/IRS2* hinders *in vivo* NSCLC growth

To assess whether acute inhibition of insulin/IGF-1 signaling can result in a similar metabolic phenotype, *KRAS*-mutant human NSCLC cells (Fig. 2.9A, B) and murine KP cells (Fig. 2.9C, D), were treated with the pharmacological IR/IGF-1R inhibitor NVP-AEW541.

The latter led to enhanced basal autophagy detected by rapid accumulation of LC3B-II and accompanied by decreased intracellular amino acid levels. These data indicate that suppressed insulin/IGF-1 signaling decreases amino acid availability, generating an increased dependency on protein catabolic pathways to compensate for lower nutrient levels.

Interestingly, the murine KPI cells, which overcame chronic rather than acute *Irs1*/*Irs2* loss *in vivo* following prolonged tumor latency (Fig. 2.1), did not display enhanced autophagic flux nor did they exhibit enhanced sensitivity to CQ treatment (Fig. 2.10A, B). This implied that the KPI cells have adapted alternative mechanisms to overcome the metabolic and growth impairment resulting from chronic loss of *Irs1* and *Irs2*. Indeed, RPPA results revealed that 3 out of 4 KPI cells had enhanced activation of growth factor receptors other than IR/IGF-1R (Fig. 2.10C). In particular, increased phosphorylation of epidermal growth factor (Egfr) on Y1173 and Y1068 was found in both KPI-3 and KPI-5 cells. Moreover, KPI-6 cell line displayed significantly increased phospho-Y1289 Her3 (Fig. 2.10C). On the other hand, KPI-5 cells exhibited increased levels of platelet-derived growth factor-beta (Pdgf- []). Upregulation or activation of these alternative receptor tyrosine kinases may have enabled KPI cells to overcome the loss of *Irs1* and *Irs2* and the resulting suppression of lung tumor growth.

Figure 2.9. Acute inhibition of insulin/IGF-1 signaling in *KRAS*-mutant lung cancer cells leads to decreased intracellular amino acid levels, enhanced autophagy and *in vivo* growth suppression.

(**A, C**) Levels of total and phosphorylated IGF1R (pY1135/1136) and IR (pY1150/1151), total and phosphorylated (pT308 and pS473) AKT, as well as LC3B-I and LC3B-II in NSCLC A549 and Calu-1 cells (A) or murine *Kras*-mutant, *p53*-null lung cancer (KP) cells (C) grown in 10% serum and treated with 2 μM NVP-AEW541 for 0, 4 or 24 hours; ⏵-ACTIN was used as a loading control. (**B, D**) Levels of amino acids in Calu-1 cells (B) or KP cells (D) treated with 2 μM NVP-AEW541 for 24 hours. Cells were cultured in media with 10% serum and with or without 2 μM of NVP-AEW541 for 24 hours; Metabolite levels were normalized to the amount of protein in each sample, and then normalized to the median of all samples for each amino acid; *n* =4 biological replicates per condition. Bolded amino acids are essential amino acids. In bold are essential amino acids. (**E**) Growth of individual subcutaneous xenograft tumors derived from A549 cells over 67 days (1 mouse had to be euthanized at 51 days) and Calu-1 over 84 days (left) with end-point average tumor volume (right); *n* = 12 for A549 sgCtrl; *n* = 11 for A549 DKO; *n* = 10 for Calu-1 shCtrl; *n* = 12 for Calu-1 DKD-1 cells. In B, D and E (right*)*, data represent the mean ± SD. In B, D and E, *P < 0.05; **P < 0.01; ***P < 0.001.

Figure 2.9. (Continued)
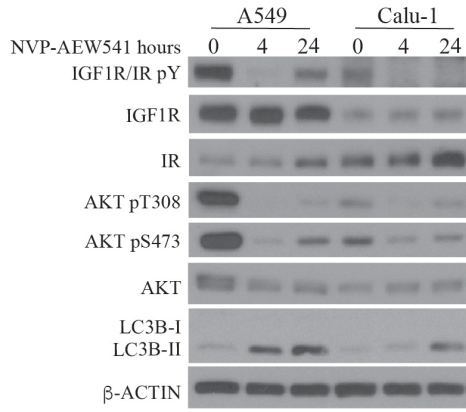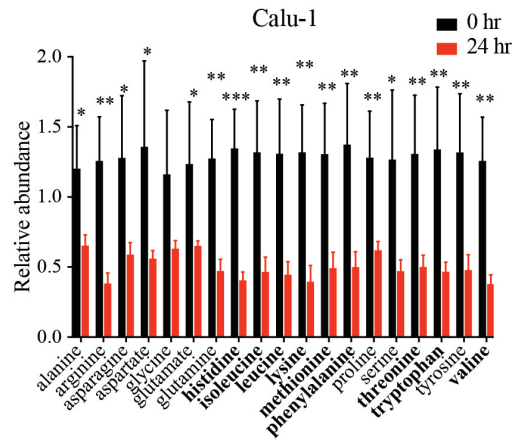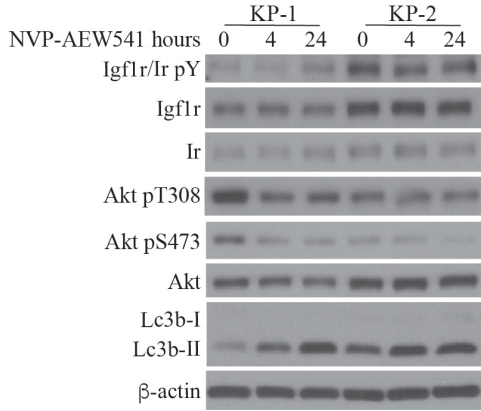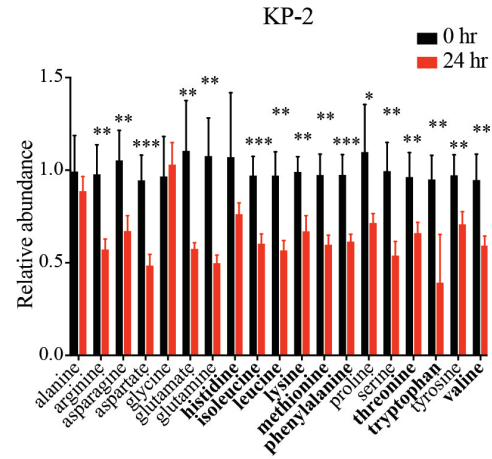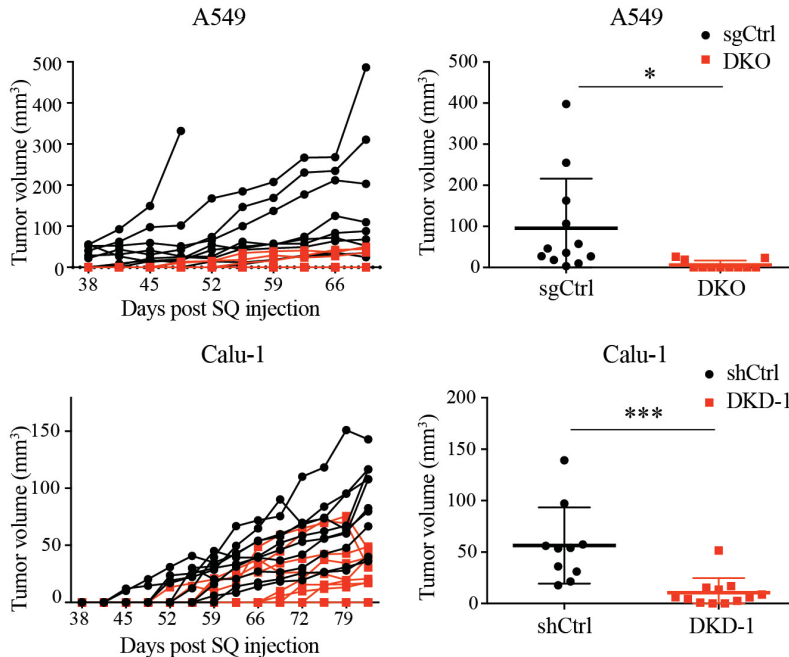
Recently, *Kras*-driven lung cancer was shown to be dependent on branched chain amino acid metabolism for nucleotide synthesis and *in vivo* tumor growth (Mayers et al. 2016). Consistently, we found that loss of *IRS1/IRS2*, which results in decreased intracellular amino acid levels, significantly hinders the ability of NSCLC cells to form tumors *in vivo*. Whereas all A549 control cells formed tumors over a period of 10 weeks, only 3 out of 11 A549 DKO cell injections yielded tumors that however grew to a significantly lesser extent than controls (Fig. 2.9E). Similarly, the growth of all Calu-1 tumors was mitigated upon *IRS1/IRS2* knockdown (Fig. 2.9E). Altogether, these results indicate that loss of *IRS1/IRS2* suppresses *in vivo* growth of *KRAS*-mutant NSCLC along with decreased AKT signaling and intracellular amino acid levels.
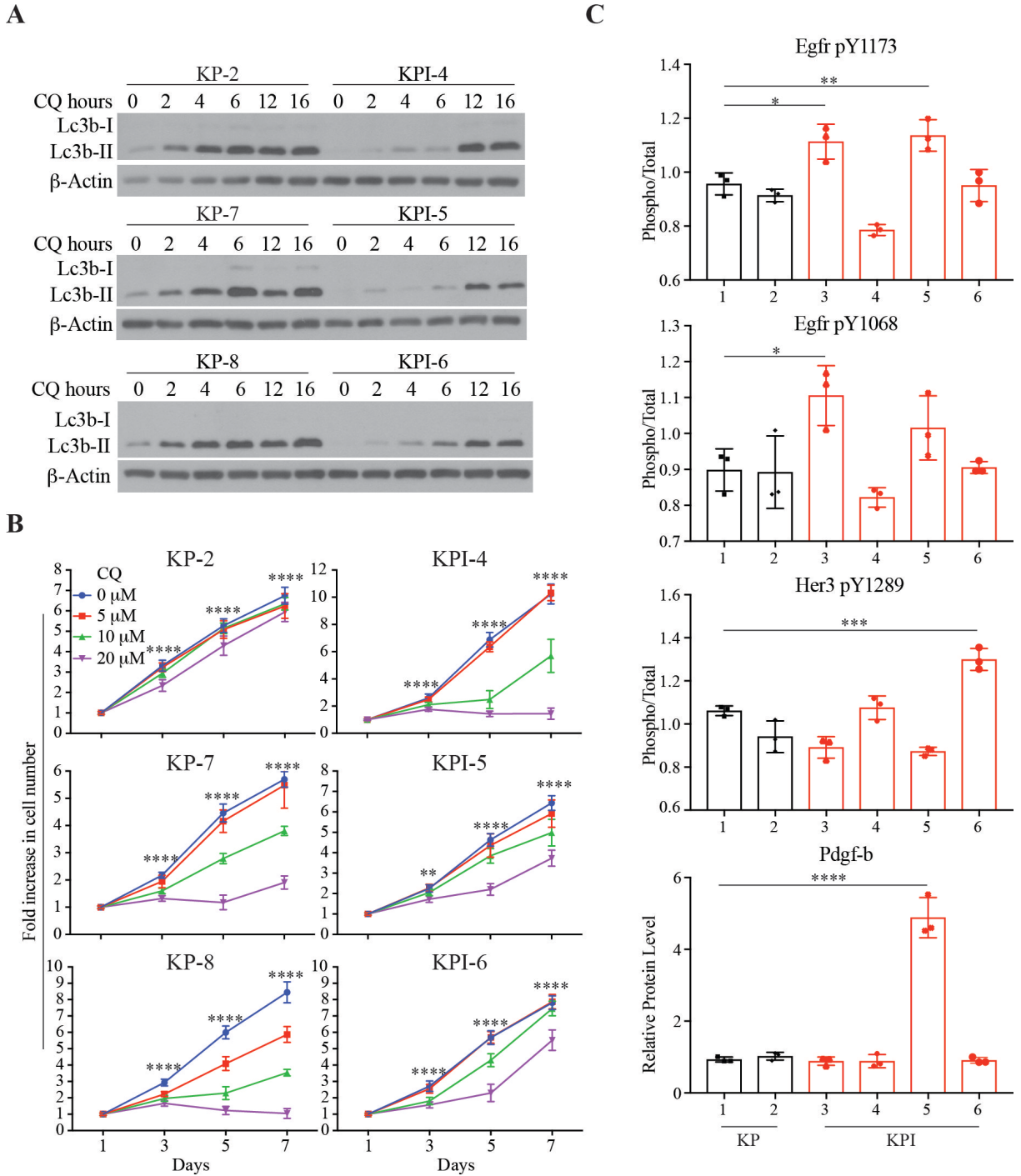
Figure 2.10. Murine *Kras*-mutant KPI lung cancer cells with *Irs1*/*Irs2* loss display compensatory induction of alternative receptor tyrosine kinases.

(**A**) Levels of Lc3b-I and Lc3b-II in *Kras*-mutant lung cancer cells with *Irs1*/*Irs2* loss (KPI cells) compared to control KP cells with wild-type *Irs1*/*Irs2*. Cells were cultured in the

Figure 2.10. (Continued)

presence of 10% serum and 10 μM chloroquine (CQ) for 0 to 16 hours. Compared to KP cells, KPI cells have reduced Lc3b-II accumulation, indicating decreased autophagic flux. β-actin was used as a loading control. (**B**) Proliferation curves of KP and KPI cells treated with CQ (0, 5, 10 or 20 μM); $n = 6$; ****$P < 0.0001$ between 0 and 20 μM conditions. (**C**) Levels of phosphorylated Egfr (pY1173, pY1068), Her3 (pY1289) and total Pdgf-□, as measured by reverse-phase protein array (RPPA) in 1-hour serum-starved KP and KPI cell lines. Levels of phosphorylated proteins were normalized to total levels of the respective proteins; $n = 3$ biological replicates; *$P < 0.05$; **$P < 0.01$, ***$P < 0.001$; ****$P < 0.0001$. In *B* and *C*, data represent the mean ± SD.

2.4 <u>DISCUSSION</u>

Previous work demonstrated that KRAS can bind to and activate PI3K p110□, and that this interaction is required for *KRAS*-driven transformation. Disrupting the Kras-p110□ interaction in genetically engineered mouse models of lung cancer suppresses tumor initiation and causes partial regression of established tumors (Gupta et al. 2007; Castellano et al. 2013). However, despite its requirement, the sufficiency of KRAS-p110□ interaction in driving *KRAS*-driven lung tumor formation, and the need for additional input from growth factor receptors upstream of KRAS and PI3K has remained largely controversial (Molina-Arcas et al. 2013).

Here, using a conditional genetically engineered mouse model of lung cancer with *Irs1/Irs2* loss, we provide robust evidence that insulin/IGF-1 signaling is required for *Kras*-

driven lung tumor initiation. We show that concomitant expression of *Kras* oncogene and the triple loss of *p53, Irs1* and *Irs2* specifically in lung cells, strongly suppresses *Kras*-driven lung tumor formation. Moreover, we show that *Kras*-transformed lung cells can eventually overcome this suppression, albeit at a stochastic rate and with extended latency.

It is noteworthy that genetic loss of *Irs1* alone in a similar *Kras*-driven mouse model of lung cancer, which however expresses wild-type *p53*, resulted in increased rather than decreased tumor burden and reduced survival (Metz et al. 2016). This seemingly contradictory result is however not surprising, given that the tumor cells had retained wild-type *Irs2* expression. Although the report did not mention or discuss *Irs2* expression, we find that Irs2 protein levels are significant in both mouse and human *Kras*-mutant lung cancer cells, and that knockdown of *Irs1* either does not affect or rather causes a compensatory increase in the expression of *Irs2* (Figs. 2.3 and 2.4). As a result, Akt activation remains intact in *Irs1* knockdown cells, in response to insulin/IGF-1 stimulation (Figs. 2.3 and 2.4). Thus, dual genetic ablation of *Irs1* and *Irs2* but not *Irs1* alone, is required for suppression of Akt activation upon ligand stimulation and suppression of tumor growth.

Importantly, whereas preclinical studies indicated a role for insulin/IGF-1 signaling in lung tumor growth, clinical trials showed adverse effects of systemic IGF-1R inhibition in unselected patients (Fidler et al. 2012; Pollak 2012), leaving questionable the relevance of therapeutic targeting of IR/IGF-1R in NSCLC patients. Our study highlights the translational relevance of blocking IR/IGF-1R signaling specifically in the lungs, leading to strong suppression of tumor formation. Furthermore, it provides a metabolic link between IR/IGF-1R signaling and amino acid utilization, as inhibition of such signaling results in decreased intracellular amino acid levels, generating a metabolic dependency of *KRAS*-driven lung

tumors on protein catabolic pathways. Consequently, combinatorial targeting of IR/IGF-1R

and either autophagy or the proteasome may represent a valuable therapeutic strategy in

treating *KRAS*-mutant NSCLC.

2.5 <u>MATERIALS AND METHODS</u>

Mouse studies

All animal studies and procedures were approved by the Institutional Animal Care and

Use Committee at Boston Children's Hospital. KP and KPI mice were generated by crossing

LSL-Kras$^{G12D/+}$; *p53*$^{fl/fl}$ (Jackson et al. 2001; Jonkers et al. 2001) to *Irs1*$^{fl/fl}$, *Irs2*$^{fl/fl}$ (Dong et al.

2006) mice. Five to 6-week-old mice were infected by a single 67.5 µl intranasal instillation

of 3 x 10^7 infectious particles of adenovirus-Cre (University of Iowa), following isoflurane

anesthesia (DuPage et al. 2009). In survival studies, mice were euthanized when they reached

moribund stage. For xenograft studies, human NSCLC cells were subcutaneously injected into

the flanks of 6-week-old female athymic nude mice (Jax # 002019) in 100 µl RPMI with 15%

phenol red-free, growth factor reduced Matrigel (BD Biosciences). Tumors were measured in

live mice twice per week using a digital caliper and tumor volumes were estimated using the

formula: V= (L x W^2)/2, where V is the volume, L is the length and W the width. Following

euthanasia and tumor harvest, tumor volumes were estimated according to the ellipsoid

formula (Wapnir et al. 1996).

Tumor burden quantification and grading

For genetically engineered mouse model studies (KP and KPI mice), formalin-fixed

lung lobes were bisected, embedded in paraffin, transversely sectioned and stained with

hematoxylin and eosin (H&E). Lung tumor burden was measured in the H&E-stained sections using cellSens software by quantifying total tumor area in each bisected lobe and normalizing it to the corresponding lobe area. Values represent averages of whole lung tumor burden from at least 6 mice. Tumor grading was performed by a pathologist in a blinded fashion, using H&E-stained lung sections, based on the following criteria: Grade 1 and 2 tumors are adenomas with nuclei of uniform size and shape. Grade 1 tumors are open and lacy with air spaces between cords of tumor cells. Grade 2 tumors are solid. Grade 3 and 4 tumors are adenocarcinomas with pleiomorphic nuclei that vary in size and shape. Grade 4 tumors show nuclear pleomorphism with invasion of stroma in the spaces around bronchi and blood vessels. Grade 4 tumors metastasize to mediastinal lymph nodes. Mice harboring only grade 1 and 2 lung tumors were categorized as having "low grade" tumors; those harboring grade 2 and grade 3 tumors, "medium grade" and those with grade 3 and grade 4 tumors, "high grade". At moribund stage (Fig. 2.1H), all mice harbored either medium or high grade tumors.

Magnetic Resonance Imaging (MRI)

MRI experiments were carried out with a Bruker 7T 30 cm scanner, equipped with a 450 mT/m gradient system (Bruker-Biospin, Billerica, MA, USA). The 1H Larmor frequency was 300.3 MHz. Animals were anesthetized by inhalation of isoflurane, initially at 2-3% and maintained at 1.0-2.5%, through a nose cone for the duration of the scanning. Mice were placed on a Bruker cardiac array receive-only probe mounted to the scanner animal table, and moved inside an 86 mm Bruker transmit-only resonator and the bore of the scanner. Respiration rates were monitored and observed in a range of 25 to 70 per minute throughout the scanning. Black blood magnetic resonance images were acquired with a Bruker IntraGate

Flash sequence, a retrospective imaging method utilizing additional navigator signals for image reconstruction and eliminating motion artifact without physically using ECG or respiration gating. The following parameters were used: FOV = 30 mm x 18 mm, matrix = 256 x 256, echo time = 2.112 ms, repetition time = 45.211 ms, number of repetition = 100 (from which, 10 cardiac frames were reconstructed for each slice). Ten to twelve 1 mm thick consecutive axial slices were acquired for each mouse with an acquisition time of 20 minutes. Digital Imaging and Communications in Medicine (DICOM) files of the MRI images were loaded into 3D Slicer software for tumor volume quantification. Tumor volume was assessed by the sum of all identified tumor areas in 30 consecutive frames for each mouse.

Tumor dissociation and cell culture

Tumors from KP and KPI mice were dissociated in Calcium/Magnesium-free Hank's Buffered Salt Solution (HBSS, Invitrogen) containing 0.025% trypsin-EDTA (Invitrogen) and 1 mg/ml collagenase IV (Worthington Biochemicals). Following a 2-hour incubation with rotation at 37°C, the samples were triturated and centrifuged. The resulting pellets were re-suspended in culture medium and filtered through 40 μm cell strainers (BD Falcon) prior to *in vitro* culture. Human NSCLC cell lines A549 and Calu-1 were obtained from the American Type Culture Collection (ATCC). ATCC cell lines are routinely authenticated by STR profiling. All cells were cultured in RPMI supplemented with 10% fetal bovine serum (FBS).

Cell line genotyping

KP and KPI cells were trypsinized, washed twice in ice-cold phosphate buffered saline (PBS) and incubated overnight at 50°C in digestion buffer containing 100 mM NaCl, 10 mM

TrisCl, pH8, 25 mM EDTA, pH8, 0.5% SDS and 0.1 mg/ml proteinase K. Samples were extracted with an equal volume of phenol, chloroform and isoamyl alcohol and centrifuged. Aqueous top layer was transferred to a new tube and DNA was precipitated with 1:10 volume of 3M Sodium Acetate and 2 volumes of 100% ethanol. Primers and protocols used for genotyping are listed below: *Kras* F1 - 5'- GTCTTTCCCCAGCACAGTGC - 3'; *Kras*-R1: 5'-CTCTTGCCTACGCCACCAGCTC-3', *Kras*-SD5: 5'-AGCTAGCCACCATGGCTTGAGTAAGTCTGCA-3'. *Kras*-F1 and *Kras*-R1 detect wild-type and recombined *Kras* alleles, yielding products that are 622 bp and 650 bp, respectively. *Kras*-R1 and *Kras*-SD5 detect floxed *Kras* allele, yielding a product that is 500 bp. Genotyping protocol for *Kras* (Jackson et al. 2001): 2 min at 95°C for initial denaturation; 30 cycles of 30s at 95°C, 30s at 59.2°C, and 50s at 72°C; 10 min at 72°C for final extension. *Tp53*-A: 5'-CACAAAAACAGGTTAAACCCAG-3'; *Tp53*-B: 5'-AGCACATAGGAGGCAGAGAC-3'; *Tp53*-C: 5'-GAAGACAGAAAAGGGGAGGG-3'. *Tp53*-A and *Tp53*-B detect wild-type and floxed *Tp53* alleles, yielding products that are 288 bp and 370 bp, respectively. *Tp53*-A and *Tp53*-C detect recombined *Tp53* allele, yielding a product that is 612 bp. Genotyping protocol for *Tp53* (Jonkers et al. 2001): 2 min at 94°C for initial denaturation; 29 cycles of 30s at 94°C, 30s at 58°C, and 50s at 72°C; 5 min at 72°C for final extension. *Irs1*-Nhe7: 5'-GCTAATAGTGCCAGGTGTGAGATC-3'; *Irs1*-Nhe10: 5'-GGACGCGGGTGACCTGCTAG-3'; *Irs1*-UTRRev1: 5' -AGAGAGAAGCCCTTCTGTGGCTGCTCCAAACACA-3'. *Irs1*-Nhe7 and *Irs1*-Nhe10 detect wild-type and floxed *Irs1* alleles, yielding products that are 278 bp and 322 bp, respectively. *Irs1*-Nhe7 and *Irs1*-UTRRev1 detect recombined *Irs1* allele, yielding a product that is 589 bp. Genotyping protocol for *Irs1*: 2 min at 95°C for initial denaturation; 35 cycles

of 30s at 94°C, 20s at 64°C, and 45s at 72°C; 10 min at 72°C for final extension. *Irs2*-5p

Outer Fwd: 5'-TCCGATCATATTCAATAACCCTTA-3'; *Irs2*-Inner Fwd: 5' -

ACGTCGTCGCCACAGTTCAGAG-3'; *Irs2*-3p Outer Rev: 5'-

TACACTGAGACAGAAGGTTAGG-3'. *Irs2*-Inner Fwd and *Irs2*-3p Outer Rev detect wild-

type and floxed *Irs2* alleles, yielding products that are 716 bp and 750 bp, respectively. *Irs2*-

5p Outer Fwd and *Irs2*-3p Outer Rev detect recombined *Irs2* allele, yielding a product that is

250 bp. Genotyping protocol for *Irs2* (Lin et al. 2004): 2 min at 95°C for initial denaturation;

35 cycles of 30s at 94°C, 20s at 60°C, and 45s at 72°C; 10 min at 72°C for final extension.

Generation of cells with stable gene knockout, knockdown or overexpression

For generation of human *IRS1* and *IRS2* or mouse *Irs1* and *Irs2* stable knockdown

lung cancer cells, lentiviral supernatants produced from pLKO plasmids each encoding the

corresponding hairpins were used, and infected cells were selected for at least 7 days with

either puromycin (pLKO.TRC005, 4 μg/ml, for mouse *Irs1*, *Irs2* hairpins, human *IRS2* or

control *GFP* hairpins) and/or blasticidin (pLKO.TRC016, 10-20 μg/ml, for human *IRS1* and

control *Scramble* hairpins). Mouse *Irs1* hairpins: sh*Irs1*-1

(TACCGCAACTGCCGAAGATTC) and sh*Irs*1-2 (CGGAACAATTAGTGTGCATAA).

Mouse *Irs*2 hairpins: sh*Irs2*-1 (TCATGTCCCTTGACGAGTATG) and sh*Irs2*-2

(TCTCCACTCTCTGACTATATG); Human *IRS1* hairpins: sh*IRS1*-1

(ACTCATTGCCAAGATCCTTTA) and sh*IRS1*-2 (GGGTTTGGAGAATGGTCTTAA);

Human *IRS2* hairpins: sh*IRS2*-1 (TCTCCGCTCTCCGACTACATG); sh*IRS2*-2

(GTGAAGATCTGTCTGGCTTTA); sh*IRS2-3* (CCCAGAGGACTACGGAGACAT) and

control *GFP* hairpins: sh*GFP* (CTACAACAGCCACAACGTCCT and

TCTCGGCATGGACGAGCTGTA); control *Scramble* hairpin: sh*Scr*

(CCTAAGGTTAAGTCGCCCTCG). A549 DKD cells were infected with sh*IRS1*-1 and

sh*IRS2*-1; Calu-1 DKD-1 cells were infected with sh*IRS1*-1 and sh*IRS2*-1; Calu-1 DKD-2

cells were infected with sh*IRS1*-1 and sh*IRS2*-2. For generation of A549 *IRS1* and *IRS2*

double knockout cells, single targeting guide RNAs were cloned into the empty backbone

construct pSpCas9(BB)-2A-Puro. Empty pSpCas9(BB)-2A-Puro plasmid was used as

negative control. Lentiviral supernatants were produced and cells were infected and selected

for at least 7 days with puromycin (4 µg/ml). Human *IRS1*-targeting guide RNA: Forward: 5'-

GGCTTCTCGGACGTGCGCA - 3', Reverse: 5'- TGCGCACGTCCGAGAAGCC - 3'.

Human *IRS2*-targeting guide RNA: Forward 5'- ACCACAGCGTGCGCAAGTG - 3',

Reverse: 5'- CACTTGCGCACGCTGTGGT - 3'. Individual clones that survived selection

were validated via QPCR and western blot. A single *IRS1* and *IRS2* double knockout clone

was expanded and used for subsequent experiments. For GFP-LC3 expression, cells were

lentivirally infected with pBABEpuro GFP-LC3 (Addgene #22405) and selected with

puromycin as described above.

Cell proliferation assay

     The assay was performed using XTT Cell Viability Kit (Cell Signaling Technology)

according to the manufacturer's protocol. Eight hundred cells were plated per well in 96-well

plates one day prior to subjecting them to treatment conditions, as described in the figure

legends.

GFP-LC3 expression and punctae quantification

Cells stably expressing GFP-LC3 were seeded on cover glasses (Bellco Glass #1943-10025) in 6-well plates in media with 10% serum, with or without chloroquine treatment (10 uM) for the indicated periods of time. After media removal, the cells were washed 3 times with ice-cold PBS and fixed in 4% EM-grade paraformaldehyde (VWR Cat# 15710) in PBS for 30 minutes at room temperature. Cells were then stained with 1 µg/ml DAPI (Thermo Scientific, Cat# D3571) in PBS for 15 minutes at room temperature. Cells were then rinsed 5 times with PBS before being mounted on glass slides (VWR Cat# 48311-703) with Fuoroshield^{TM} (Sigma Cat# F6182). Image acquisition was performed using a Nikon Eclipse 90i Advanced Automated Research Microscope equipped with a standard optical filter set including DAPI and FITC. Images were captured with a 60x objective and the NIS-Elements Advanced Research Microscope Imaging Software (Nikon). Exposure time for DAPI acquisition was 20 ms and that for FITC acquisition was 200 ms. For each condition and each cell line, 15-20 representative images were captured and used for quantification. The total number of cells as well as the number of cells positive for GFP-LC3 punctae were visually counted. The data represent averages of three independent experiments.

Luminex assay

The IRS1 capture antibody (rabbit monoclonal clone 58-10C-31, Millipore #05-784R) was coupled to magnetic carboxylated microspheres (Luminex Magplex-C beads) as described (Copps et al. 2016). Antibodies used for the detection of captured IRS1 and associated p110α were biotinylated using reagents from Thermo Fisher (EZ-Link NHS-PEG4-Biotin kit, cat# 21330) following the manufacturer's guidelines and keeping the antibody

concentrations between 1.5 and 2.0 mg/ml. The antibody used for detection of IRS1 was from

Millipore (mouse monoclonal, cat #05-1085) and that for p110α was from Cell Signaling

Technology (rabbit monoclonal clone C73F8, CST #4249). KP and KPI cells were treated

with indicated conditions before protein lysates were collected as described below in the

Immunoblotting section. Protein lysates (60 µg) were incubated with Irs1 capture beads (2500

beads/well) in a total volume of 50 µl/well of Milliplex MAP Assay Buffer 2 (Millipore #43-

041) in 96-well plates and the assay was performed as described (Copps et al. 2016).

Fluorescence signals from captured Irs1 and p110α were read by a Luminex FlexMap 3D

instrument. Median fluorescence intensities (MFIs) were reported by the instrument. The

degree of interaction between p110α and Irs1 was measured as the ratio of MFI of p110α over

MFI of Irs1. Triplicates were used per condition for each cell line.

Reverse phase protein array (RPPA)

Cells were rinsed twice with ice-cold PBS and collected in lysis buffer containing 1%

Triton X-100, 50 mM HEPES, pH7.4, 150 mM NaCl, 1.5 mM $MgCl_2$, 1mM EGTA, 100 mM

NaF, 10 mM Na pyrophosphate, 1mM Na_3VO_4, 10% glycerol, and protease and phosphatase

inhibitors (Roche). Protein lysates were shipped to the RPPA Core Facility at University of

Texas MD Anderson Cancer Center (Houston, TX) where RPPA was performed as previously

described (Hennessy et al. 2010).

Immunoblotting

Cells were rinsed once with ice-cold PBS and collected in lysis buffer containing 50

mM HEPES, pH 7.4, 40 mM NaCl, 2 mM EDTA, 50 mM NaF, 10 mM sodium

pyrophosphate, 10 mM sodium beta-glycerophosphate, EDTA-free protease inhibitors (Roche), and 1% Triton X-100. Proteins were resolved by 6% - 15% SDS-PAGE, and transferred to polyvinylidene difluoride (PVDF) membrane (Merck Millipore). Membranes were blocked with 5% nonfat dry milk in PBS with Tween (PBS-T) and then incubated with primary antibody overnight at 4ºC. Following PBS-T washing, membranes were incubated with peroxidase-conjugated secondary antibody for 1 hour at room temperature and exposed on film using Enhanced Chemiluminescence (ECL) Detection System (Thermo Scientific). Antibodies were from Cell Signaling Technology: AKT (1:2000, CST #4691), AKT pS473 (1:2000, CST #4058), AKT pT308 (1:1000, CST #4056), ERK (1:5000, CST #4695), ERK pT202/Y204 (1:1000, CST #4376), GSK3β (1:1000, CST #9315), GSK3β pS9 (1:1000, CST #9322), IGF-1R (1:1000, CST #9750), IR (1:1000, CST #3025), LC3B (1:2000, CST #2775), IGF-1R pY1135/1136 / IR pY1150/1151 (1:1000, CST #3024), S6 (1:2000, CST #2217), S6 pS235/236 (1:1000, CST #2211), S6K pT389 (1:1000, CST #9205), TSC2 (1:1000, CST #4308), TSC2 pT1462 (1:1000, CST #3617); Santa Cruz Biotechnology: β-actin (1:20000, sc-47778), GAPDH (1:5000, sc-25778), S6K (1:1000, sc-230). Antibodies for western blot detection of IRS1 and IRS2 (1:1000) were a gift of Dr. Morris White. IRS1 was detected using a protein G-purified mouse monoclonal antibody raised against residues surrounding S439 of mouse Irs1 (Hancer et al. 2014). IRS2 was detected using a protein G-purified rabbit monoclonal antibody raised against a His-tagged protein containing residues 818-1323 of mouse Irs2.

Metabolite extraction and quantification

For all metabolite analysis (except Fig. 2.9B, D): Cells were rinsed once with ice-cold 0.9% NaCl and placed on dry ice. All metabolites were extracted with extraction solution (80% methanol containing a mixture of internal amino acid standards at 90.9 nM each), vortexed for 10 minutes at 4°C and centrifuged (10 min, 10,000 x g, 4°C). Supernatants were then transferred to fresh eppendorf tubes and dried with Speedvac. Dried extracts were suspended in 100 µl water. After centrifugation at top speed for 10 min, 2 µl of supernatant was injected for LC/MS analysis as described (Birsoy et al. 2015). For Figure 2.5C, D: data representing raw peak areas normalized to internal standards were uploaded to Metaboanalyst 3.0 (Xia and Wishart 2016), median-normalized, log-transformed, mean-centered and divided by the standard deviation of each variable. For Fig. 2.9B, D: Metabolites were extracted with 80% methanol as described above. Data were acquired using a hydrophilic interaction liquid chromatography method (HILIC) with positive ion mode Mass Spectrometry (MS) operated on Nexera X2 UHPLC (Shimadzu Scientific Instruments, Marlborough, MA) coupled to a Q Exactive orbitrap mass spectrometer (Thermo Fisher Scientific, Waltham, MA) as described previously (Townsend et al. 2013).

Statistical analyses

Data are presented as mean ± standard deviation (SD), unless otherwise indicated. A log-rank test was used for analysis of survival curves and a nonparametric two-tailed Fisher's exact test was used for analysis of tumor grade. For all other data, when comparing two groups, a two-tailed nonpaired Student's t-test was conducted. For three or more groups, two-

way ANOVA was conducted, followed by post-hoc Tukey's multiple comparison test. $P <$ 0.05 was considered statistically significant.

REFERENCES

Birsoy K, Wang T, Chen WW, Freinkman E, Abu-Remaileh M, Sabatini DM. 2015. An Essential Role of the Mitochondrial Electron Transport Chain in Cell Proliferation Is to Enable Aspartate Synthesis. *Cell* 162: 540-551.

Castellano E, Sheridan C, Thin MZ, Nye E, Spencer-Dene B, Diefenbacher ME, Moore C, Kumar MS, Murillo MM, Gronroos E et al. 2013. Requirement for interaction of PI3-kinase p110alpha with RAS in lung tumor maintenance. *Cancer Cell* 24: 617-630.

Copps KD, Hancer NJ, Qiu W, White MF. 2016. Serine 302 Phosphorylation of Mouse Insulin Receptor Substrate 1 (IRS1) Is Dispensable for Normal Insulin Signaling and Feedback Regulation by Hepatic S6 Kinase. *The Journal of biological chemistry* 291: 8602-8617.

Curry NL, Mino-Kenudson M, Oliver TG, Yilmaz OH, Yilmaz VO, Moon JY, Jacks T, Sabatini DM, Kalaany NY. 2013. Pten-null tumors cohabiting the same lung display differential AKT activation and sensitivity to dietary restriction. *Cancer Discov* 3: 908-921.

Dong X, Park S, Lin X, Copps K, Yi X, White MF. 2006. Irs1 and Irs2 signaling is essential for hepatic glucose homeostasis and systemic growth. *J Clin Invest* 116: 101-114.

DuPage M, Dooley AL, Jacks T. 2009. Conditional mouse lung cancer models using adenoviral or lentiviral delivery of Cre recombinase. *Nat Protoc* 4: 1064-1072.

Engelman JA, Luo J, Cantley LC. 2006. The evolution of phosphatidylinositol 3-kinases as regulators of growth and metabolism. *Nat Rev Genet* 7: 606-619.

Feldser DM, Kostova KK, Winslow MM, Taylor SE, Cashman C, Whittaker CA, Sanchez-Rivera FJ, Resnick R, Bronson R, Hemann MT et al. 2010. Stage-specific sensitivity to p53 restoration during lung cancer progression. *Nature* 468: 572-575.

Fidler MJ, Shersher DD, Borgia JA, Bonomi P. 2012. Targeting the insulin-like growth factor receptor pathway in lung cancer: problems and pitfalls. *Therapeutic advances in medical oncology* 4: 51-60.

Gupta S, Ramjaun AR, Haiko P, Wang Y, Warne PH, Nicke B, Nye E, Stamp G, Alitalo K, Downward J. 2007. Binding of ras to phosphoinositide 3-kinase p110alpha is required for ras-driven tumorigenesis in mice. *Cell* 129: 957-968.

Hancer NJ, Qiu W, Cherella C, Li Y, Copps KD, White MF. 2014. Insulin and metabolic stress stimulate multisite serine/threonine phosphorylation of insulin receptor substrate 1 and inhibit tyrosine phosphorylation. *The Journal of biological chemistry* 289: 12467-12484.

Hennessy BT, Lu Y, Gonzalez-Angulo AM, Carey MS, Myhre S, Ju Z, Davies MA, Liu W, Coombes K, Meric-Bernstam F et al. 2010. A Technical Assessment of the Utility of Reverse Phase Protein Arrays for the Study of the Functional Proteome in Non-microdissected Human Breast Cancers. *Clin Proteomics* 6: 129-151.

Imielinski M, Berger AH, Hammerman PS, Hernandez B, Pugh TJ, Hodis E, Cho J, Suh J, Capelletti M, Sivachenko A et al. 2012. Mapping the hallmarks of lung adenocarcinoma with massively parallel sequencing. *Cell* 150: 1107-1120.

Jackson EL, Willis N, Mercer K, Bronson RT, Crowley D, Montoya R, Jacks T, Tuveson DA. 2001. Analysis of lung tumor initiation and progression using conditional expression of oncogenic K-ras. *Genes Dev* 15: 3243-3248.

Jeanes A, Gottardi CJ, Yap AS. 2008. Cadherins and cancer: how does cadherin dysfunction promote tumor progression? *Oncogene* 27: 6920-6929.

Jonkers J, Meuwissen R, van der Gulden H, Peterse H, van der Valk M, Berns A. 2001. Synergistic tumor suppressor activity of BRCA2 and p53 in a conditional mouse model for breast cancer. *Nat Genet* 29: 418-425.

Lin X, Taguchi A, Park S, Kushner JA, Li F, Li Y, White MF. 2004. Dysregulation of insulin receptor substrate 2 in beta cells and brain causes obesity and diabetes. *J Clin Invest* 114: 908-916.

Mayers JR, Torrence ME, Danai LV, Papagiannakopoulos T, Davidson SM, Bauer MR, Lau AN, Ji BW, Dixit PD, Hosios AM et al. 2016. Tissue of origin dictates branched-chain amino acid metabolism in mutant Kras-driven cancers. *Science* 353: 1161-1165.

Metz HE, Kargl J, Busch SE, Kim KH, Kurland BF, Abberbock SR, Randolph-Habecker J, Knoblaugh SE, Kolls JK, White MF et al. 2016. Insulin receptor substrate-1 deficiency drives a proinflammatory phenotype in KRAS mutant lung adenocarcinoma. *Proc Natl Acad Sci U S A* 113: 8795-8800.

Molina-Arcas M, Hancock DC, Sheridan C, Kumar MS, Downward J. 2013. Coordinate direct input of both KRAS and IGF1 receptor to activation of PI3 kinase in KRAS-mutant lung cancer. *Cancer Discov* 3: 548-563.

Oliver TG, Mercer KL, Sayles LC, Burke JR, Mendus D, Lovejoy KS, Cheng MH, Subramanian A, Mu D, Powers S et al. 2010. Chronic cisplatin treatment promotes enhanced damage repair and tumor progression in a mouse model of lung cancer. *Genes Dev* 24: 837-852.

Perera RM, Zoncu R. 2016. The Lysosome as a Regulatory Hub. *Annu Rev Cell Dev Biol* 32: 223-253.

Pollak M. 2012. The insulin and insulin-like growth factor receptor family in neoplasia: an update. *Nat Rev Cancer* 12: 159-169.

Project CG. 2017. Catalogue of Somatic Mutations in Cancer (COSMIC), version 80. Wellcome Trust Sanger Institute.

Saxton RA, Sabatini DM. 2017. mTOR Signaling in Growth, Metabolism, and Disease. *Cell* 168: 960-976.

Siegel RL, Miller KD, Jemal A. 2017. Cancer Statistics, 2017. *CA Cancer J Clin* 67: 7-30.

Stephen AG, Esposito D, Bagni RK, McCormick F. 2014. Dragging ras back in the ring. *Cancer Cell* 25: 272-281.

Townsend MK, Clish CB, Kraft P, Wu C, Souza AL, Deik AA, Tworoger SS, Wolpin BM. 2013. Reproducibility of metabolomic profiles among men and women in 2 large cohort studies. *Clinical chemistry* 59: 1657-1667.

Wapnir IL, Wartenberg DE, Greco RS. 1996. Three dimensional staging of breast cancer. *Breast Cancer Res Treat* 41: 15-19.

White MF, Maron R, Kahn CR. 1985. Insulin rapidly stimulates tyrosine phosphorylation of a Mr-185,000 protein in intact cells. *Nature* 318: 183-186.

WHO. 2017. Cancer, Fact sheet N° 297. World Health Organization.

Xia J, Wishart DS. 2016. Using MetaboAnalyst 3.0 for Comprehensive Metabolomics Data Analysis. *Curr Protoc Bioinformatics* 55: 14 10 11-14 10 91.

CHAPTER 3:

DISCUSSION AND CONCLUSIONS

3.1 Overview

In this dissertation, I investigated the role of Ir/Igf-1r signaling, mediated by adaptor proteins Irs1 and Irs2, in *Kras*-driven lung tumorigenesis. Using a conditional genetically engineered mouse model (GEMM), I demonstrated that *Irs1* and *Irs2* are required for *Kras*-driven lung tumor initiation. Intriguingly, the dual loss of *Irs1* and *Irs2* imparts specific metabolic vulnerabilities regarding amino acid metabolism on *Kras*-mutant lung cancer cells, rendering them dependent on catabolic sources of amino acids such as autophagy and proteasomal degradation. In this chapter I highlight some of the implications of my research findings, share unpublished data from work in progress, as well as discuss future directions that will shed light on some of the unanswered questions.

3.2 Loss of *Irs1* or *Irs2* alone does not suppress *Kras*-driven lung tumor initiation

It has been shown that loss of *Irs1* in a conditional *Kras*-driven mouse model of lung cancer did not result in suppression, but rather enhancement of tumor growth (Metz et al. 2016). The authors discovered that mechanistically loss of IRS1 in human NSCLC cells results in increased membrane-association of p85, the regulatory subunit of PI3K, which subsequently becomes activated by mutant *KRAS* and leads to enhanced AKT activation and GSK3β phosphorylation in *KRAS*-mutant cells. They concluded that phospho-GSK3β then prolongs the half-life of IL-22 receptor A1, which results in enhanced proinflammatory cytokine production and IL22 signaling that contributes to enhanced tumorigenesis. The authors claimed that Irs1 protein interacts mainly with p85 in the cytoplasm when actively transducing signal from upstream receptors. Therefore with loss of *Irs1* p85 is free to relocate predominantly to the cell membrane. This explanation raises controversies on the spatial

control of IR/IGF-1R signaling, where adaptor proteins IRS1 and IRS2 are recruited to phosphorylated tyrosine residues on activated IR or IGF-1R in cell membrane, as discussed in Chapter 1.3.2. Moreover, it was not discussed in this study the potential role of Irs2 in recruiting p85 to cell membrane and in mediating the tumor-promoting effects. Enhanced membrane-association of p85 could alternatively have been mediated by compensatory overexpression of Irs2 protein, similar to what I have observed in my research (Figs. 2.3 and 2.4).

Consistently, I have found that loss of either IRS1 or IRS2 protein alone does not affect AKT activation or downstream effector signaling in human and mouse lung cancer cells (Figs. 2.3 and 2.4). In the breeding process to generate KP and KPI mice, 3 mice with floxed *Irs1* and wild-type *Irs2* alleles were generated (*LSL-Kras$^{G12D/+}$, p53$^{fl/fl}$, Irs1$^{fl/fl}$*, termed KP-Irs1), and were subjected to intranasal Cre as described in Chapter 2. These mice develop lung tumor at a similar pace to KP mice, reaching substantial tumor burden 10 weeks post Cre infection (Fig. 3.1). Therefore, Irs1 and Irs2 share significant functional redundancy in activating downstream Akt signaling in lung epithelial cells, and loss of either adaptor protein is not sufficient for tumor suppression in the context of mutant *Kras* and loss of *p53*.
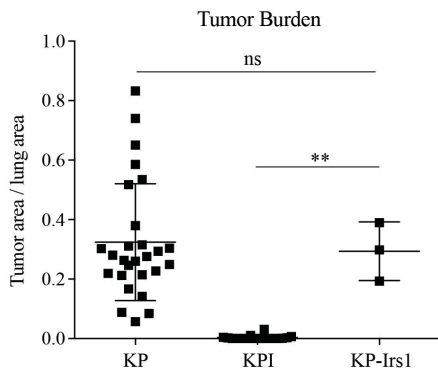

Figure 3.1. Loss of *Irs1* alone does not inhibit *Kras*-driven lung tumorigenesis.

Figure 3.1. (Continued)

Tumor burden representing tumor area/total lung area in KP, KPI, and KP-Irs1 (*Kras* $^{G12D/+}$, *p53*$^{-/-}$, *Irs1*$^{-/-}$) lungs 10 weeks post-adenoviral Cre infection. $N = 27$ (KP), $n = 18$ (KPI), and $n = 3$ (KP-Irs1); **$P < 0.01$ (One-way ANOVA followed by Tukey's test).

3.3 Are *Foxo1* and *Foxo3* partial mediators of tumor suppression by loss of *Irs*1 and *Irs*2?

FOXO transcription factors are effectors downstream of PI3K/AKT signaling that promote cell cycle arrest and apoptosis (Coomans de Brachène and Demoulin 2016; Eijkelenboom and Burgering 2013). It has been shown that Foxo transcription factors are bona fide tumor suppressors. Conditional deletions of *Foxo1*, *Foxo3* and *Foxo4* in adult mice result in development of thymic lymphomas and hemangiomas (Paik et al. 2007). Active Akt directly phosphorylates Foxo transcription factors, resulting in their nuclear export and cytoplasmic sequestration. Conversely, we hypothesized that loss of *Irs1* and *Irs2* leads to nuclear localization and constitutive activation of Foxos as a result of suppressed Akt signaling in the lungs of KPI mice following Cre exposure. In order to investigate whether active Foxo transcription factors contribute to tumor suppression conferred by loss of *Irs1* and *Irs2*, KP mice were bred to mice with homozygously floxed *Irs1*, *Irs2*, as well as *Foxo1* and *Foxo3* alleles to generate mice with floxed *Foxo1* alleles (*LSL-Kras*$^{G12D/+}$, *p53*$^{fl/fl}$, *Irs1*$^{fl/fl}$, *Irs2*$^{fl/fl}$, *Foxo1*$^{fl/fl}$, termed KPI-Foxo1), mice with floxed *Foxo3* alleles (*LSL-Kras*$^{G12D/+}$, *p53*$^{fl/fl}$, *Irs1*$^{fl/fl}$, *Irs2*$^{fl/fl}$, *Foxo3*$^{fl/fl}$, termed KPI-Foxo3), as well as mice with both floxed *Foxo1* and floxed *Foxo3* alleles (*LSL-Kras*$^{G12D/+}$, *p53*$^{fl/fl}$, *Irs1*$^{fl/fl}$, *Irs2*$^{fl/fl}$, *Foxo1*$^{fl/fl}$, *Foxo3*$^{fl/fl}$, termed KPI-

Foxo1/3). KPI-Foxo1, KPI-Foxo3 and KPI-Foxo1/3 animals will be called KPI-Foxo animals in general. Upon exposure to intranasally delivered Cre, mutant *Kras* is expressed in the lungs concomitantly with loss of *p53*, *Irs1*, *Irs2*, and one or both of *Foxo1* and *Foxo3* in KPI-Foxo mice. KPI-Foxo1 and KPI-Foxo3 animals exhibit minimal tumor development histologically by 10 weeks post Cre delivery, and have tumor burden similar to that of KPI animals, indicating that loss of either *Foxo1* or *Foxo3* is not sufficient to rescue tumor initiation (Fig. 3.2A). However, small tumor nodules are present in the lungs of some KPI-Foxo1/3 animals, albeit not reaching the extent in KP animals, suggesting that loss of *Foxo1* and *Foxo3* partially but not completely rescues tumor initiation (Fig. 3.2B). KPI-Foxo animals eventually succumb to tumor development stochastically and form high-grade adenocarcinomas (Fig. 3.2B, C). For both males and females, KPI-Foxo1/3 animals exhibit a significantly shorter latency compared to KPI animals (15-20 weeks for KPI-Foxo1/3, compared to 16 - 30 weeks for KPI) and a survival profile closer to that of KP mice. Surprisingly, there is an appreciable difference between the median survival of male and female KPI-Foxo1/3 animals, with males exhibiting a median survival of 111 days while females exhibiting a median survival of 157 days. However, there is no corresponding difference in maximal survival of KPI-Foxo1/3 mice between the sexes, with the maximal survival for males being 212 days and that for females being 196 days. This points to subtle differences in tumor progression between male and female KPI-Foxo1/3 animals, with females succumbing more rapidly to tumor-associated death than males do once tumor growth is under way. It could also indicate the more sporadic nature of tumor initiating events in male KPI-Foxo1/3 mice, resulting in a more variable tumor latency compared to female KPI-Foxo1/3 mice. Loss of *Foxo3* in addition to loss of *Foxo1* results in a substantial reduction of tumor latency and mouse survival in males,

whereas loss of *Foxo1* alone has minimal effect. Conversely in females loss of either *Foxo1* or *Foxo3* results in some reduction in tumor latency and survival. These differences between genders could indicate potentially differential expression, activity and/or function of *Foxo1* and *Foxo3* transcription factors in the lungs of male versus female mice. Alternatively this could be due to other gender-specific pleiotropic effects of the mouse model.

In summary, these preliminary results are consistent with previous reports that demonstrated the functional redundancy among the members of the *Foxo* transcription factor family, while implicating *Foxo1* and *Foxo3* in mediating tumor suppression by loss of *Irs1* and *Irs2*. However, given that the survival of KPI-Foxo1/3 animals is not fully restored to that of the KP mice, other mechanisms are likely to contribute to tumor suppression as well. One possibility is the remaining *Foxo4* transcription factor that shares partial functional redundancy with *Foxo1* and *Foxo3*. In a previous report, only loss of all 3 Foxo transcription factors resulted in thymic lymphoma and hemangioma development in mice (Paik et al. 2007). Therefore it remains to be investigated whether loss of *Foxo4* in addition to loss of *Foxo1* and *Foxo3* would fully rescue tumor development in KPI mice.
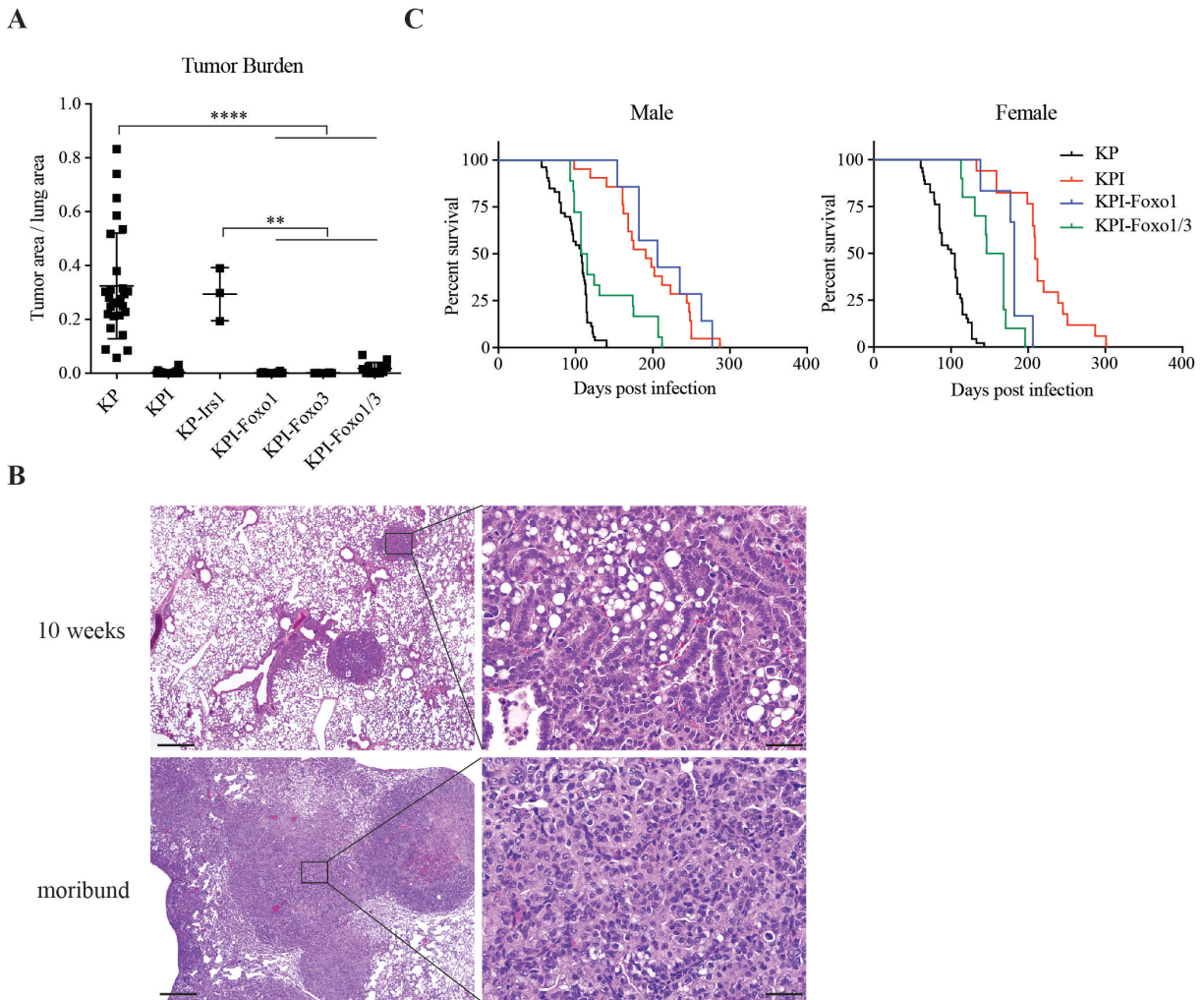
Figure 3.2. Loss of *Foxo1* and *Foxo3* partially rescues tumor development and reduces survival of KPI mice.

(**A**) Tumor burden representing tumor area/total lung area in KP, KPI, KP-Irs1, KPI-Foxo1 (*Kras* $^{G12D/+}$, *p53* $^{-/-}$, *Irs1* $^{-/-}$, *Irs2* $^{-/-}$, *Foxo1* $^{-/-}$), KPI-Foxo3 (*Kras* $^{G12D/+}$, *p53* $^{-/-}$, *Irs1* $^{-/-}$, *Irs2* $^{-/-}$, *Foxo3* $^{-/-}$), and KPI-Foxo1/3 (*Kras* $^{G12D/+}$, *p53* $^{-/-}$, *Irs1* $^{-/-}$, *Irs2* $^{-/-}$, *Foxo1* $^{-/-}$, *Foxo3* $^{-/-}$) lungs 10 weeks post-adenoviral Cre infection. $N = 27$ (KP), $n = 18$ (KPI), $n = 3$ (KP-Irs1), n = 14 (KPI-Foxo1), n = 5 (KPI-Foxo3), n = 12 (KPI-Foxo1/3). **$P < 0.01$ and ****$P < 0.0001$ (One-way ANOVA followed by Tukey's test). (**B**) H&E staining of KPI-Foxo1/3 lungs 10 weeks post-adenoviral Cre infection and from moribund mice (left), with 10-fold magnification of the framed area (right). Scale bars, 400 μm (left) and 40 μm (right). (**C**) Kaplan-Meier

Figure 3.2. (Continued)

survival curves for KP, KPI, KPI-Foxo1 and KPI-Foxo1/3 mice. Males, $n = 53$ (KP), $n = 21$ (KPI), n = 7 (KPI-Foxo1), n = 18 (KPI-Foxo1/3); females, $n = 46$ (KP), $n = 17$ (KPI), n = 6 (KPI-Foxo1), n = 10 (KPI-Foxo1/3); Males, $P = 0.0021$ (KP vs. KPI-Foxo1/3), $P < 0.0001$ (KP vs. KPI, KP vs. KPI-Foxo1), $P = 0.0006$ (KPI vs. KPI-Foxo1/3), $P = 0.004$ (KPI-Foxo1 vs. KPI-Foxo1/3). Females, $P < 0.0001$ (KP vs. KPI, KP vs. KPI-Foxo1, KP vs. KPI-Foxo1/3, KPI vs. KPI-Foxo1/3), $P = 0.003$ (KPI vs. KPI-Foxo1). $P = 0.04$ (KPI-Foxo1 vs. KPI-Foxo1/3). All comparisons were performed by log-rank test for both genders.

3.4 Does loss of IRS1 and IRS2 result in decreased amino acid uptake in *KRAS*-mutant NSCLC cells?

One of the most striking findings of my research is the dramatically reduced intracellular amino acid levels in cells with loss of IRS1 and IRS2. IGF-1 is known to regulate fetal growth, in part by regulating amino acid transport across the placenta (Agrogiannis et al. 2014). It was shown that IGF-1 stimulates amino acid uptake and protein synthesis in a variety of experimental contexts including cultured human placental trophoblast, BeWo human choriocarcinoma cells, as well as chicken muscle satellite cells (Duclos et al, 1993; Karl, 1995; Fang et al. 2006). IGF-1 expression also results in increased mRNA levels of amino acid transporters SLC7A5 (LAT1) and SLC3A2 (4F2hc) in BeWo human choriocarcinoma cells, and restores protein levels of these transporters in a murine model of placental insufficiency (Jones, Crombleholme, and Habli 2014). Moreover, in MCF7 breast cancer cells overexpressing IGF-1 or IGF-2, half of the genes upregulated were involved in

amino acid transport and biosynthesis, including SLC7A11, SLC7A5 (LAT1) and SLC3A2 (4F2hc) involved in transport of branched chain amino acids (BCAAs) and aromatic amino acids (Pacher et al. 2007).

Given the pre-established link between IGF-1 signaling and amino acid transport, I investigated whether the diminished amino acid levels in NSCLC cells were a result of decreased amino acid uptake with loss of IRS1 and IRS2. Human *KRAS*-mutant A549 cells with *IRS1/IRS2* (A549 DKO) or control (A549 sgCtrl) double knockout were cultured in media with U-^{13}C-leucine for 1 hour and levels of intracellular labeled leucine was measured. A549 DKO cells exhibited significantly lower amount of intracellular labeled leucine compared to A549 sgCtrl cells, suggesting that leucine uptake is diminished with loss of IRS1 and IRS2 in A549 cells (Fig. 3.3A). However, after 1 hour of labeling, the intracellular U-^{13}C-leucine level is strictly speaking the result of leucine uptake, secretion as well as catabolism. Therefore, acute labeling could be performed at 5 minutes, 10 minutes and 15 minutes to more accurately gauge the kinetics of leucine uptake of A549 sgCtrl and A549 DKO cells. Additionally, A549 DKO cells have strongly suppressed protein expression of the BCAA and aromatic amino acid transporter, a heterodimer of SLC7A5 (LAT1) and SLC3A2 (4F2hc) (Fig. 3.3B). However, protein levels of the amino acid transporter are not affected by acute pharmacological inhibition of IR/IGF-1R in A549 sgCtrl cells (Fig. 3.3B). These results suggest that loss of IRS1 and IRS2 leads to decreased protein expression of certain amino acid transporters in some human *KRAS*-mutant NSCLC cells, which results in decreased amino acid uptake that contributes to reduction of intracellular amino acid levels. However, amino acid transporters may be specifically regulated by the adaptor proteins IRS1 and IRS2, rather than by the IR/IGF-1R signaling pathway in general. It remains to be fully characterized

whether this suppressive effect applies to other amino acid transporters, whether decreased

import of amino acids drives the observed depletion of cellular amino acid pool, as well as

how this differs between cell lines and affects tumor growth *in vivo*. Additionally, how IRS1

and IRS2 mechanistically regulate amino acid transporters remains to be investigated.

A   **B**
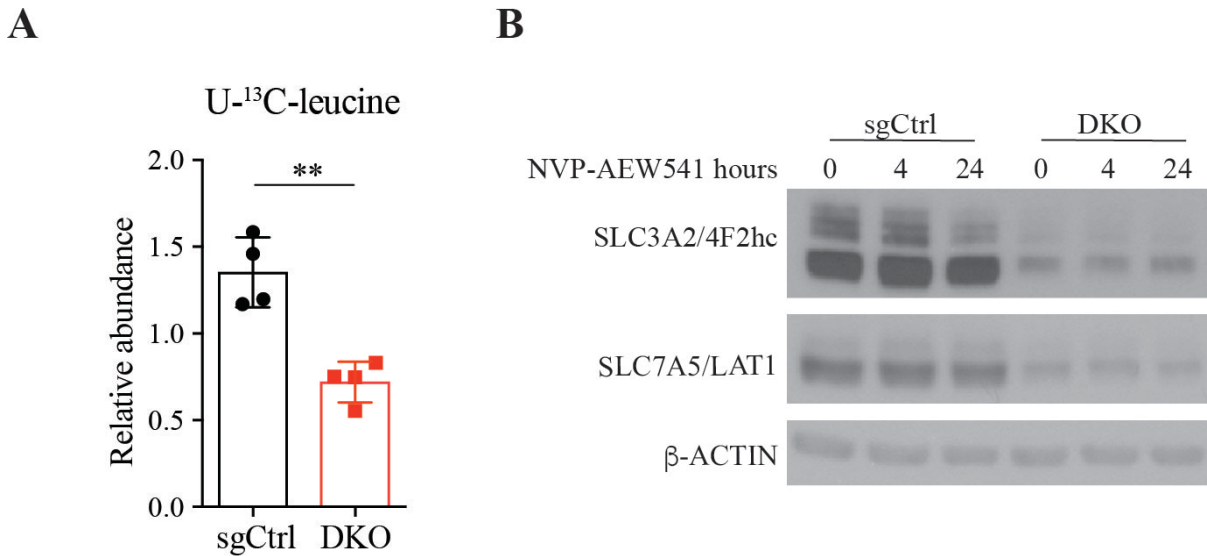
Figure 3.3. **A549 cells demonstrate decreased leucine uptake and reduced protein levels of amino acid transporters.**

(**A**) Levels of U -^{13}C-leucine in NSCLC A549 cells with *IRS1*/*IRS2* (A549 DKO) or control

(A549 sgCtrl) double knockout, that were first normalized to protein levels, and then

normalized to the median of all samples; n = 4 biological replicates per cell line. Cells were

cultured in media with U -^{13}C-leucine (50 mg/L) and 10% serum for 1 hour. (**B**) Levels of

SLC3A2/4F2hc and SLC7A5/LAT1 in A549 cells described in A. Cells were grown in media

with 10% serum and treated with 2 μM NVP-AEW541 for 0, 4 or 24 hours; ⬜-ACTIN was

used as a loading control. Representative results from two independent experiments are

shown. In A, **$P < 0.01$; ***$P < 0.001$; ****$P < 0.0001$ (two-tailed nonpaired Student's t-

test).

3.5 How do reduced cellular amino acid levels affect amino acid metabolism and contribute to suppression of tumor growth?

It has been shown that NSCLC tumors display increased uptake of BCAAs to incorporate into tissue proteins and to use as a nitrogen source (Mayers et al. 2016). During the first step of BCAA catabolism, branched-chain α-ketoacids (BCKAs) and glutamate are produced from BCAAs and α-ketoglutarate (α-KG) in a transamination reaction where the amino nitrogen of BCAAs is transferred to glutamate and can be subsequently incorporated into other amino acids or nucleotides. This transamination reaction is reversibly catalyzed by branched-chain amino acid transaminase 1 and 2 (Bcat1/2) in the cytosol and mitochondria, respectively. When this metabolic adaptation is inhibited via genetic ablation of *Bcat1/2*, NSCLC allograft growth was significantly hindered *in vivo* (Mayers et al. 2016). In addition to BCAAs, other amino acids including glutamine, aspartate, serine and glycine have been demonstrated to support tumor growth by contributing to nucleotide synthesis, maintaining redox balance and meeting cellular energetic demands in various contexts (see Chapter 1.4 for a detailed discussion and references). My research shows BCAAs, other essential amino acids with the exception of lysine, as well as serine, glycine and glutamine are all dramatically reduced by inhibition of IR/IGF-1R signaling, either pharmacologically or genetically. It has not been investigated whether, and how this global depletion of cellular amino acids contributes to tumor growth suppression in the context of loss of *Irs1* and *Irs2*. Tracing experiments with labeled cocktails of essential amino acids could be performed to dissect the perturbation of amino acid metabolism in human NSCLC cells with loss of IRS1 and IRS2, and identify metabolic nodes that could be potential targets forming combinatorial therapies with IR/IGF-1R signaling inhibitors in *KRAS*-mutant human NSCLC.

**3.6 Is perturbed amino acid metabolism a feature of *in vitro* culturing?**

It has been shown that cancer cells exhibit distinct metabolic features when grown in cell culture compared to when grown *in vivo*. When NSCLC cells are cultured in media, they display aerobic glycolysis and glutamine-dependent growth (Davidson et al. 2016). However, both lung tumors and normal lung tissue demonstrate minimal glutamine utilization, with lung tumors showing increased glucose contribution to the TCA cycle compared to normal lung tissue (Davidson et al. 2016; Hensley et al. 2016; Sellers et al. 2015). Genetic ablation of enzymes involved in glucose oxidation severely impairs lung tumor growth *in vivo*, while having no effect on lung tumor cell proliferation *in vitro* (Davidson et al. 2016). In another study where NSCLC is shown to rely on enhanced uptake of BCAAs as a nitrogen source, inhibition of BCAA catabolism only suppressed tumor growth *in vivo* while having minimal effect on cell proliferation in culture (Mayers et al. 2016). Therefore, I investigated whether the depletion of intracellular amino acids, so far observed in both murine and human lung cancer cells with loss of IRS1 and IRS2 grown in culture, is also observed *in vivo*. Metabolites extracted from human *KRAS*-mutant NSCLC xenografts, as well as from the plasma of xenograft-bearing nude mice were assayed for their amino acid contents. Surprisingly, we did not see a dramatic decrease in amino acid levels in tumors derived from either A549 or Calu-1 cells with loss of IRS1 and IRS2 (Fig. 3.4A). In contrast, aspartate level is significantly higher in A549 DKO tumors than in sgCtrl tumors, similar to what we observed in cells grown in culture (Fig. 2.6C). However, glycine level is also significantly enhanced in A549 DKO tumors than in sgCtrl tumors, contrary to what we saw in culture (Fig. 2.6C). Intriguingly, a group of amino acids including arginine, asparagine, BCAAs, methionine, phenylalanine, proline, serine and threonine are significantly lower in the plasma

of mice bearing Calu-1 DKD tumors compared to mice bearing shCtrl tumors (Fig. 3.4B). The lower circulating level of BCAAs in this case is consistent with what was reported before, as NSCLC tumors have increased BCAAs uptake that results in lower plasma levels of BCAAs (Mayers et al. 2016). The inconsistency between what we see in cell culture and in xenografts could be yet another example of the distinct metabolic dependencies of cells when cultured in media and when grown *in vivo*. Moreover, as the majority of injections of A549 DKO and Calu-1 DKD cells either did not form tumors or formed very small tumors, samples used for metabolic analysis were in a sense outliers that formed tumors from A549 DKO cells or formed sizable tumors from Calu-1 DKD cells, and they may have very well found ways to replenish their intracellular amino acids in order to grow. To truly assess whether loss of *IRS1* and *IRS2* would lead to depletion of intracellular amino acids *in vivo*, xenografts derived from human *KRAS*-mutant NSCLC cells that express inducible small hairpins targeting *IRS1* and *IRS2* or control small hairpins could be established. Loss of *IRS1* and *IRS2* could be induced acutely in established tumors and its impact on tumor amino acid levels could be measured.

A
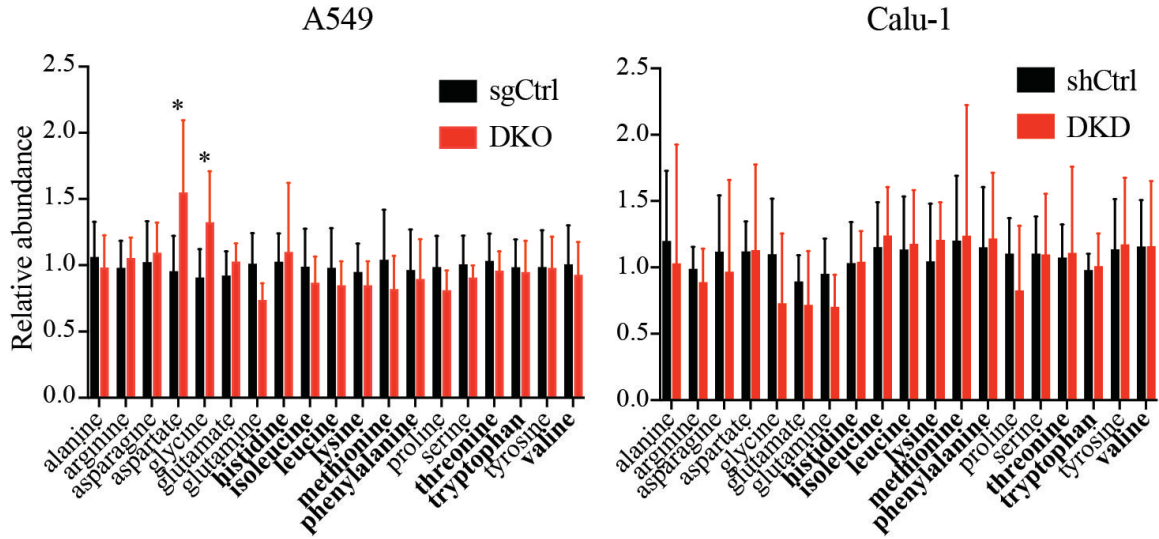
B
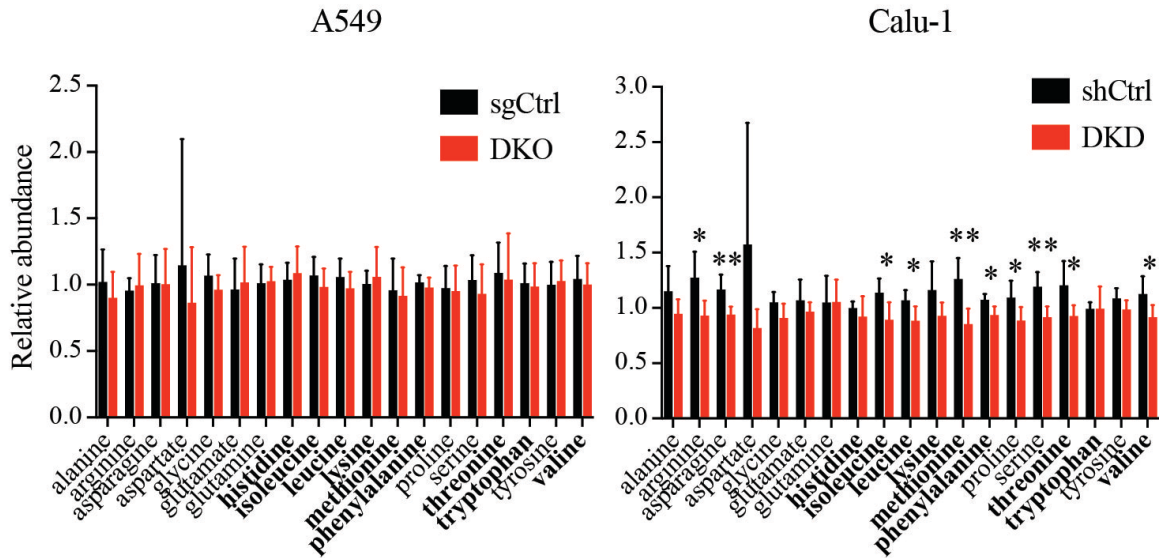
Figure 3.4. Human NSCLC xenograft tumors with loss of IRS1 and IRS2 do not demonstrate depletion of intracellular amino acids.

(**A**) Levels of intracellular amino acids in NSCLC A549 xenograft tumors with *IRS1*/*IRS2* (A549 DKO) or control (A549 sgCtrl) double knockout as well as Calu-1 xenograft tumors with *IRS1*/*IRS2* (Calu-1 DKD) or control (Calu-1 sh*GFP*/sh*Scramble*, termed shCtrl) double knockdown. $N = 10$ for A549 sgCtrl; $n = 3$ for A549 DKO; $n = 9$ for Calu-1 shCtrl; $n = 4$ for

120

Figure 3.4. (Continued)

Calu-1 DKD-1 cells. (**B**) Levels of plasma amino acids at the time of sacrifice from mice

bearing xenograft tumors described in A. $N = 6$ for A549 sgCtrl and DKO; $n = 5$ for Calu-1

shCtrl; $n = 6$ for Calu-1 DKD-1 cells. In A and B, data represent mean ± SD. *$P < 0.05$; **P

< 0.01 (two-tailed unpaired Student's t-test).

3.7 Is depletion of cellular amino acids the main driver of basal autophagy activation in NSCLC cells with loss of IRS1 and IRS2?

It is known that autophagy is induced by nutrient starvation, such as reduction of

intracellular amino acid levels. Decreased amino acid levels induce autophagy primarily

through inhibition of mTORC1 signaling (Feng, Yao, and Klionsky 2015). In my research,

Human *KRAS*-mutant NSCLC cells with loss of IRS1 and IRS2 have elevated autophagy,

despite displaying similar levels of mTORC1 signaling under basal, nutrient-replete condition

(Fig. 2.7). Therefore, alternative mechanisms of autophagy activation may be playing a role

here. It has been shown that ammonia generated from glutaminolysis is sufficient to induce

basal autophagy independent of mTORC1 signaling or nutrient deprivation in both non-

transformed and cancer cells (Eng et al. 2010). In my research glutamine is significantly

diminished in cells with loss of IRS1 and IRS2. However, glutamate levels are either

increased or unchanged (Fig 2.6C). Therefore, whether loss of IRS1 and IRS2 leads to

enhanced glutaminolysis, and whether glutamine-derived ammonia contributes to activation

of autophagy is worth investigating. Further, depletion of cellular amino acids could induce

autophagy via transcriptional regulation. Leucine deprivation alone in mouse embryonic

fibroblasts (MEFs) results in inhibition of protein synthesis via GCN2-mediated phosphorylation of eIF2α, which simultaneously leads to preferential translation of the transcription factor ATF4 that in turn increases expression of multiple genes involved in autophagosome formation (B'chir et al. 2013). Therefore whether decreased cellular amino acid levels transcriptionally induce autophagy via the GCN2- eIF2α- ATF4 axis in NSCLC cells with loss of IRS1 and IRS2 remains to be investigated. Additionally, autophagy can be induced by AMPK under conditions of increased cellular AMP/ATP ratio, discussed in detail in Chapter 1.5.3 (Hardie, Ross, and Hawley 2012; Inoki, Zhu, and Guan 2003; Gwinn et al. 2008). Loss of IRS1 and IRS2 in human *KRAS*-mutant NSCLC A549 cells results in decreased contribution of glucose-derived carbon to glycolysis, serine and glycine synthesis, as well as TCA cycle (Fig. 3.5). It should be noted that the M+3 labeled fractions of malate and aspartate reflect flux from glucose through pyruvate carboxylase (PC) to replenish the TCA cycle, consistent with findings by other groups showing dependence of NSCLC tumors on PC-mediated anaeplerosis from glucose for cell proliferation and tumor growth (Sellers et al. 2015; Davidson et al. 2016). Given the diminished glucose oxidation and anaeplerosis in A549 DKO cells, it remains a possibility that loss of IRS1 and IRS2 perturbs cellular energy status that culminates in autophagy activation via AMPK signaling.
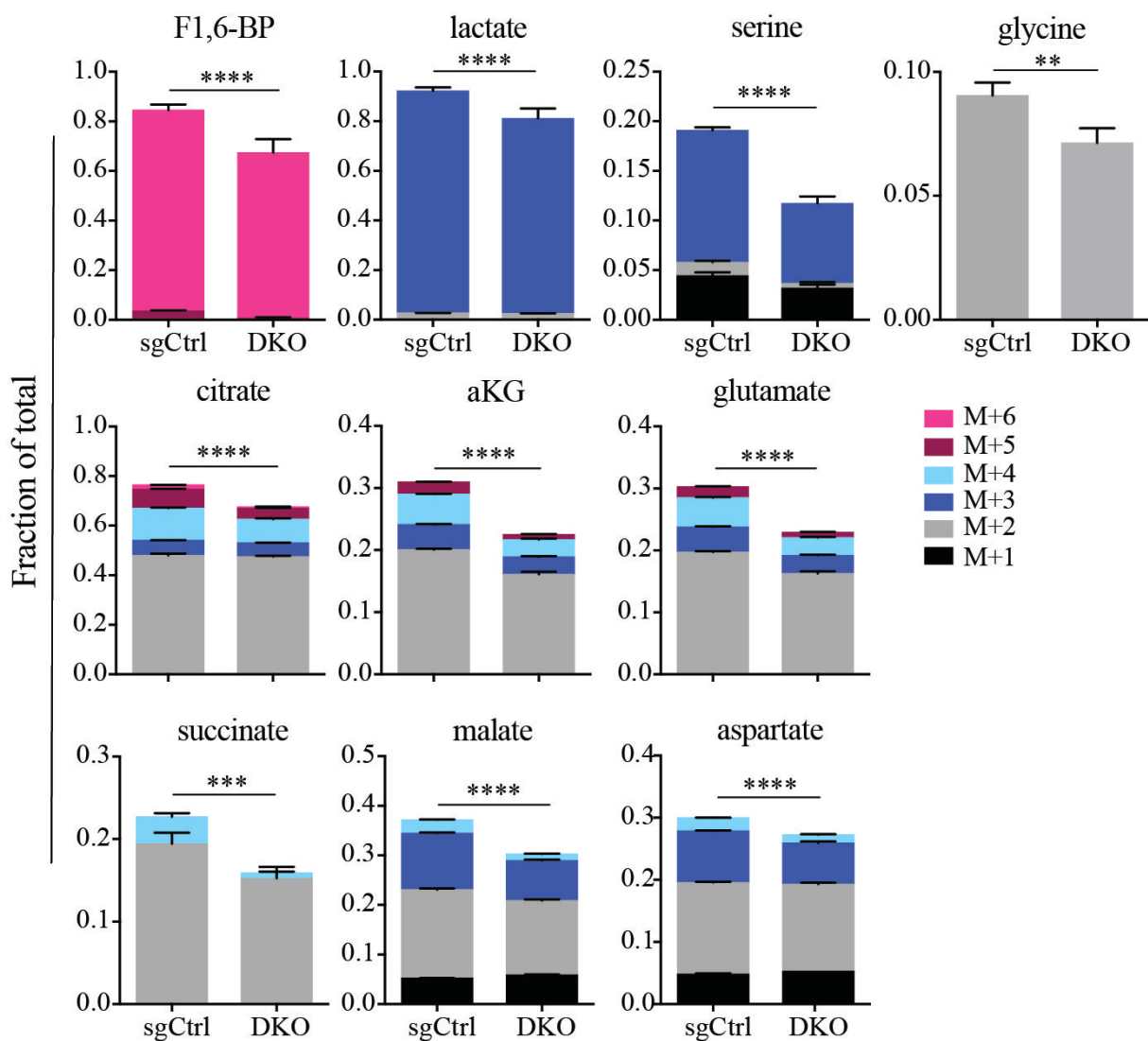
Figure 3.5. A549 cells demonstrate decreased glucose metabolism with loss of IRS1 and IRS2.

Labeled isotopomers of glycolytic intermediates, serine, glycine and TCA cycle intermediates from U-^{13}C-glucose as fractions of total metabolites. NSCLC A549 cells described in A were cultured in media with 10% serum and U-^{13}C-glucose (11 μM) for 25 hours. Fractional labeling was determined as the ratio of raw peak areas of labeled isotopomers to total raw peak areas of the corresponding metabolites. $N = 4$ biological replicates per cell line. **P <

Figure 3.5. (Continued)

0.01; ***P < 0.001; ****P < 0.0001 (two-tailed nonpaired Student's t-test). Highest level of statistical significance among the isotopomers was indicated.

3.8 Is inhibition of autophagy or proteasome synergistic with IR/IGF-1R targeting in treating *KRAS*-mutant NSCLC?

My research demonstrates that cells with acute loss of IRS1 and IRS2, or under acute pharmacological inhibition of IR/IGF-1R signaling, are more sensitive to autophagy and proteasome inhibition *in vitro* due to their dependency on these catabolic pathways to compensate for depletion of cellular amino acids. It is important to note that chloroquine was used as a standard inhibitor of autophagy in my research to both assay for its effects on cell proliferation and to block autophagic flux and visualize accumulation of LC3B-II (Fig. 2.8). However, it has been shown that *ATG7*-deficient and -proficient human *KRAS*-mutant cancer cells are equally sensitive to chloroquine treatment, indicating that chloroquine is not a specific inhibitor for autophagy and its cytotoxic effects may not stem from its inhibition of autophagy (Eng et al. 2016). As a pH neutralizer of the lysosome, chloroquine inhibits all cellular processes that involve lysosomal degradation including macropinocytosis. Mutant *Kras* stimulates macropinocytosis in pancreatic cancer cells to scavenge for extracellular nutrients (Commisso et al. 2013; Kamphorst et al. 2015; Davidson et al. 2016). However, in my research *Kras*-mutant murine and human lung cancer cells demonstrate minimal macropinocytosis via TMR-dextran uptake assay (data not shown). Therefore it is not clear to what extent the suppressive effect of chloroquine on proliferation of *Kras*-mutant murine and

human lung cancer cells stems from its inhibition of autophagy specifically (Fig. 2.8A, 2.10B). Caution should be employed when drawing conclusions about autophagy from studies that utilize chloroquine alone as an autophagy inhibitor. Genetic means of autophagy inhibition should be employed to complement studies using chloroquine.

To determine the translational relevance of combinatorial targeting of IR/IGF-1R signaling and autophagy/proteasome in *KRAS*-mutant NSCLC, it remains to be investigated whether autophagy or proteasome inhibition would elicit growth suppression of tumors with loss of *IRS1* and *IRS2 in vivo*. To that end, KP and KPI mice could be bred to an inducible model of lung-specific autophagy inhibition through genetic ablation of *Atg7*. The effects of induced loss of autophagy on KP and KPI tumors could be assessed. Similarly, patient-derived *KRAS*-mutant NSCLC xenografts could be established to assess efficacy of combinatorial targeting of IR/IGF-1R and autophagy/proteasome in a preclinical model.

Importantly, clinical trials have shown that systemic IGF-1R inhibition leads to compensatory signaling from GHR, which results in unintended adverse effects (Haluska et al. 2010; Moody et al. 2014). Similarly, whole-body inhibition of autophagy in adult mice by genetic ablation of *Atg7* leads to adipose loss, muscle wasting, liver damage and eventual death from neurodegeneration (Karsli-Uzunbas et al. 2014). Remarkably, lung specific loss of autophagy is well tolerated in mice without affecting lifespan, and *Kras*-mutant lung tumors are substantially more sensitive to autophagy inhibition than untransformed lung tissue (Guo et al. 2013; Karsli-Uzunbas et al. 2014). Therefore, combinatorial therapies targeting IR/IGF-1R and autophagy specifically delivered to the lungs would achieve the clinical benefits without generating the undesirable side effects for patients.

3.9 How do compensatory mechanisms enable KPI cells to bypass Ir/Igf-1r signaling and form tumors without activating autophagy and restoring amino acid levels?

In contrast to the acute inhibition of IR/IGF-1R signaling in human and mouse NSCLC cells, chronic loss of *Irs1* and *Irs2* in KPI cells led to compensatory mechanisms that allowed them to form tumors despite exhibiting depletion of cellular amino acid levels and lower autophagic flux. These cells display aberrant activation or amplification of alternative RTKs including Egfr, Her3 and Pdgf that may allow them to bypass the need for Ir/Igf-1r signaling (Fig. 2.10C). Activation of EGFR signaling is frequently found to lead to resistance against therapies targeting other RTKs such as ALK and MET kinases (Katayama et al. 2012; McDermott et al. 2010; Qi et al. 2011; Sasaki et al. 2011). Therefore it remains to be investigated whether Egfr signaling and possibly other RTK signaling result in Ir/Igf-1r-independent tumor formation by KPI cells, as well as how these alternative signaling pathways promote cell growth in the presence of amino acid depletion.

Specifically, KPI - 3 and 5 cell lines display Akt phosphorylation when grown in 10% serum despite not showing IGF-1 -induced Akt activation (Fig. 2.5A). This suggests that some KPI cells respond to other growth factors in serum to compensate for the lack of Ir/Igf-1r signaling. Alternative RTK signaling that activates Pi3k and Akt downstream, such as G protein-coupled receptors (GPCRs), Egfr and Pdgf-r signaling, is worth investigating. On the other hand, KPI-4 cells display constitutive activation of Akt regardless of whether serum is present, suggesting that they have compensatory mechanisms upstream of Akt that results in constitutive Akt activation, such as secondary activating mutations in Pi3k or Akt, or inactivating mutations in pathway suppressors such as Pten and PHLPP. More intriguingly, KPI - 6 cell line has adapted to proliferate without the need for activated Akt altogether,

which could be made possible by rewiring effectors downstream of Akt that activate

mitogenic and pro-survival signals. It should be noted that despite the alternative means KPI

cells have adopted to activate Akt signaling, the level of Akt phosphorylation is dramatically

reduced compared to KP cells under IGF-1 stimulation (Fig. 2.5A). Therefore, KPI cells have

adapted to grow and proliferate with a strongly reduced capability to activate Akt in response

to growth factor signaling.

Except for their shared suppression of Akt and downstream effector signaling in

response to IGF-1 stimulation, KPI cells demonstrate distinct signaling profiles that share

very little commonality, indicating the extraordinary flexibility cancer cells possess to

circumvent obstacles and thrive (Fig. 3.6). This flexibility poses a significant challenge to our

efforts in identifying novel therapeutic targets and developing viable treatments to fight

cancer clinically.
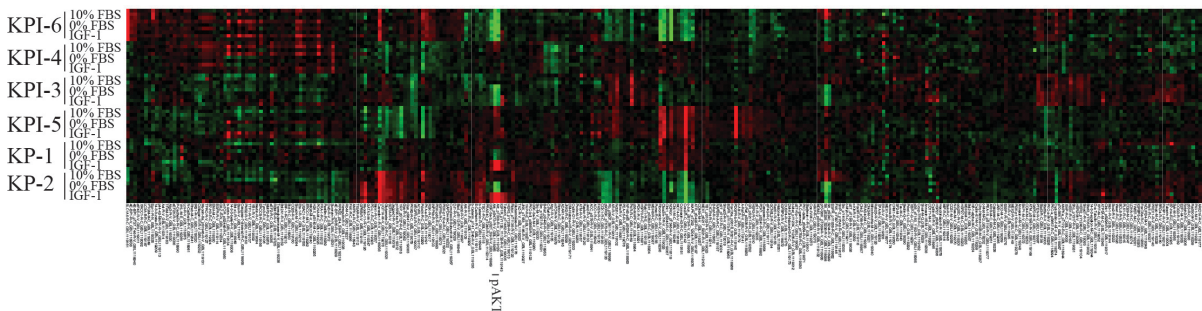
Figure 3.6. KPI cells demonstrate distinct signaling profiles.

Heatmap of relative abundance of 308 proteins and phophoproteins between KP cells (cell

lines 1 and 2) and KPI cells (lines 3-6). Cells were either non-serum starved (10% fetal bovine

serum or FBS), serum-starved (0% FBS) for 1 hour or serum-starved for 1 hour and

stimulated with 50 ng/ml IGF-1 for 10 minutes (indicated as IGF1). Rows indicate the

specific cell line and treatment. Columns indicate different proteins and phosphoproteins.

Protein loading-normalized values were Log2 transformed and median-centered for heatmap

Figure 3.6. (Continued)

generation. Heatmap was generated in Cluster 3.0 and visualized in Treeview. Red indicates

higher expression, and green indicates lower expression relative to the median expression

level of each protein. Data represent mean ± SD; $n = 3$ biological replicates per condition per

cell line. Distinct differences regarding Akt activation in response to IGF-1 stimulation can be

seen between KP and KPI cell lines.

3.10 Does loss of *Irs1* and *Irs2* suppress *Kras*-driven tumor maintenance and progression?

My research has demonstrated the requirement for *Irs1* and *Irs2* in *Kras*-driven lung

tumor initiation. However, it has been shown that tumor maintenance and progression may

depend on signaling pathways distinct from those required for initiation (Genovese et al.

2017; Kapoor et al. 2014; Lim and Counter 2005). To investigate the role of *Irs1* and *Irs2* in

Kras-driven lung tumor maintenance, we obtained a different conditional mouse model that

expresses *Frt-STOP-Frt (FSF)-Kras$^{G12D/+}$; p53$^{frt/frt}$*, and bred it to mice harboring *Irs1$^{fl/fl}$* and

Irs2$^{fl/fl}$ alleles to generate *FSF-Kras$^{G12D/+}$; p53$^{frt/frt}$; Irs1$^{fl/fl}$; Irs2$^{fl/fl}$* mice (Young, Crowley, and

Jacks 2011; Lee et al. 2012; Dong et al. 2006). In order to initiate tumor development driven

by mutant *Kras* and loss of *p53* while temporally inducing the loss of *Irs1* and *Irs2* at a later

stage, I designed a construct that expresses FlpO-IRES-CreERT2, where intranasal exposure

to the mammalian codon-optimized Flippase recombinase (FlpO) would initiate tumorigenesis

in the lungs while later exposure to tamoxifen would activate Cre recombinase and induce

loss of *Irs1* and *Irs2* specifically in cells that have been exposed to the construct and hence

transformed. However, we did not see sufficient Cre-mediated recombination of floxed alleles

in KP MEFs upon tamoxifen exposure using this construct *in vitro*, and therefore pursued a second strategy to tackle this problem.

We obtained an inducible dual-recombinase mouse model that expresses *Col1a1$^{FSF-CreERT2}$; FSF-Kras$^{G12D/+}$; p53$^{frt/frt}$* and bred them to *Irs1$^{fl/fl}$; Irs2$^{fl/fl}$* mice to generate *Col1a1$^{FSF-CreERT2}$; FSF-Kras$^{G12D/+}$; p53$^{frt/frt}$; Irs1$^{fl/fl}$; Irs2$^{fl/fl}$* mice (Zhang and Kirsch 2015). Upon intranasal exposure to Flippase, lung tumorigenesis would be initiated by mutant *Kras* and loss of *p53* with concomitant expression of CreERT2 in transformed cells. Later exposure to tamoxifen would activate Cre recombinase and induce loss of *Irs1* and *Irs2* specifically in tumor cells. However, characterization of the model revealed insufficient expression of CreERT2 in *Kras*-mutant, *p53*-null lung tumor cells. Similar findings were also reported by the authors (Zhang and Kirsch 2016).

To circumvent the problem of insufficient CreERT2 expression, a slightly different inducible dual-recombinase model could be used, where CreERT2 expression is under the control of the CAG promoter from the endogenous ROSA26 locus (*FSF-R26$^{CAG-CreERT2}$; FSF-Kras$^{G12D/+}$*)(Schönhuber et al. 2014). The robust expression and activity of Cre following Flippase and tamoxifen exposure were validated in a number of different models where induced deletion of *p53, Pdpk1* and other genes as well as induced expression of *lacZ* in *Kras*-transformed pancreatic cancer cells were successful (Schönhuber et al. 2014). Therefore, to investigate whether *Irs1* and *Irs2* are required for *Kras*-mutant lung tumor maintenance, *FSF-R26$^{CAG-CreERT2}$; FSF-Kras$^{G12D/+}$* mice could be bred to *p53$^{frt/frt}$* mice and to *p53$^{frt/frt}$; Irs1$^{fl/fl}$; Irs2$^{fl/fl}$* mice to generate *FSF-R26$^{CAG-CreERT2}$; FSF-Kras$^{G12D/+}$; p53$^{frt/frt}$* mice as well as *FSF-R26$^{CAG-CreERT2}$; FSF-Kras$^{G12D/+}$; p53$^{frt/frt}$; Irs1$^{fl/fl}$; Irs2$^{fl/fl}$* mice. Upon intranasal exposure to Flippase, mutant *Kras* and loss of *p53* would initiate lung tumor development and CreERT2

would be expressed in transformed cells. Later exposure to tamoxifen would induce the loss of *Irs1* and *Irs2*, allowing us to assess its impact on tumor maintenance and progression. This will identify novel signaling and metabolic vulnerabilities unique to estalibshed *Kras*-mutant lung tumors following acute inhibition of Ir/Igf-1r signaling, as well as better shed light on the therapeutic potential of targeting IR/IGF-1R signaling in established *KRAS*-mutant NSCLC in patients.

3.11 Conclusions

This dissertation has established the requirement for *Irs1* and *Irs2* in *Kras*-driven lung tumorigenesis. It has identified amino acid metabolism as a metabolic vulnerability of *KRAS*-mutant NSCLC cells and revealed their dependency on autophagy and proteasomal degradation upon loss of IRS1 and IRS2, as well as pharmacological IR/IGF-1R inhibition. The research presented here has deepened our understanding of the intricate interplay between signaling and metabolism in *KRAS*-mutant NSCLC, as well as uncovered novel avenues for further investigation. We hope the research presented here, together with the future work outlined above, will unveil innovative targets and therapeutic strategies to combat NSCLC clinically.

REFERENCES

Agrogiannis, Georgios D, Stavros S, Patsouris ES, and Konstantinidou AE. 2014. "Insulin-like Growth Factors in Embryonic and Fetal Growth and Skeletal Development (Review)." *Molecular Medicine Reports* 10 (2). Spandidos Publications: 579–84.

B'chir W, Maurin AC, Carraro V, Averous J, Jousse C, Muranishi Y, Parry L, Stepien G, Fafournoux P, and Bruhat A. 2013. "The eIF2α/ATF4 Pathway Is Essential for Stress-Induced Autophagy Gene Expression." *Nucleic Acids Research* 41 (16): 7683–99.

Commisso C, Davidson SM, Soydaner-Azeloglu RG, Parker SJ, Kamphorst JJ, Hackett S, Grabocka E, et al. 2013. "Macropinocytosis of Protein Is an Amino Acid Supply Route in Ras-Transformed Cells." *Nature* 497 (7451): 633–37.

Coomans de Brachène A and Demoulin JB. 2016. "FOXO Transcription Factors in Cancer Development and Therapy." *Cellular and Molecular Life Sciences : CMLS* 73 (6): 1159–72.

Davidson SM, Papagiannakopoulos T, Olenchock BA, Heyman JE, Keibler MA, Luengo A, Bauer MR, et al. 2016. "Environment Impacts the Metabolic Dependencies of Ras-Driven Non-Small Cell Lung Cancer." *Cell Metabolism* 23 (3): 517–28.

Davidson SM, Jonas O, Keibler MA, Hou HW, Luengo A, Mayers JR, Wyckoff J, et al. 2016. "Direct Evidence for Cancer-Cell-Autonomous Extracellular Protein Catabolism in Pancreatic Tumors." *Nature Medicine* 23 (2): 235–41.

Dong X, Park S, Lin X, Copps K, Yi X, and White MF. 2006. "Irs1 and Irs2 Signaling Is Essential for Hepatic Glucose Homeostasis and Systemic Growth." *The Journal of Clinical Investigation* 116 (1): 101–14.

Astrid E and Burgering BMT. 2013. "FOXOs: Signalling Integrators for Homeostasis Maintenance." *Nature Reviews Molecular Cell Biology* 14 (2): 83–97.

Eng CH, Wang Z, Tkach D, Toral-Barza L, Ugwonali S, Liu S, Fitzgerald SL, et al. 2016. "Macroautophagy Is Dispensable for Growth of KRAS Mutant Tumors and Chloroquine Efficacy." *Proceedings of the National Academy of Sciences of the United States of America* 113 (1): 182–87.

Eng CH, Yu K, Lucas J, White E, and Abraham RT. 2010. "Ammonia Derived from Glutaminolysis Is a Diffusible Regulator of Autophagy." *Science Signaling* 3 (119): ra31.

Fang J, Mao D, Smith CH, and Fant ME. 2006. "IGF Regulation of Neutral Amino Acid Transport in the BeWo Choriocarcinoma Cell Line (b30 Clone): Evidence for MAP Kinase-Dependent and MAP Kinase-Independent Mechanisms." *Growth Hormone and IGF Research*.

Feng Y, Yao Z, and Klionsky DJ. 2015. "How to Control Self-Digestion: Transcriptional, Post-Transcriptional, and Post-Translational Regulation of Autophagy." *Trends in Cell Biology* 25 (6): 354–63.

Genovese G, Carugo A, Tepper J, Robinson FS, Li L, Svelto M, Nezi L, et al. 2017. "Synthetic Vulnerabilities of Mesenchymal Subpopulations in Pancreatic Cancer." *Nature* 542 (7641): 362–66.

Guo JY, Karsli-Uzunbas G, Mathew R, Aisner SC, Kamphorst JJ, Strohecker AM, Chen G, et al. 2013. "Autophagy Suppresses Progression of K-Ras-Induced Lung Tumors to Oncocytomas and Maintains Lipid Homeostasis." *Genes & Development* 27 (13): 1447–61.

Gwinn DM, Shackelford DB, Egan DF, Mihaylova MM, Mery A, Vasquez DS, Turk BE, and Shaw RJ. 2008. "AMPK Phosphorylation of Raptor Mediates a Metabolic Checkpoint." *Molecular Cell* 30 (2): 214–26.

Haluska P, Worden F, Olmos D, Yin D, Schteingart D, Batzel GN, Paccagnella ML, de Bono JS, Gualberto A, and Hammer GD. 2010. "Safety, Tolerability, and Pharmacokinetics of the Anti-IGF-1R Monoclonal Antibody Figitumumab in Patients with Refractory Adrenocortical Carcinoma." *Cancer Chemotherapy and Pharmacology* 65 (4): 765–73.

Grahame HD, Ross FA, and Hawley SA. 2012. "AMPK: A Nutrient and Energy Sensor That Maintains Energy Homeostasis." *Nature Reviews Molecular Cell Biology* 13 (4): 251–62.

Hensley CT, Brandon F, Yuan Q, Lev-Cohain N, Jin E, Kim J, Jiang L, et al. 2016. "Metabolic Heterogeneity in Human Lung Tumors." *Cell* 164 (4): 681–94.

Inoki K, Zhu T, and Guan KL. 2003. "TSC2 Mediates Cellular Energy Response to Control Cell Growth and Survival." *Cell* 115 (5): 577–90.

Jones H, Crombleholme T, and Habli M. 2014. "Regulation of Amino Acid Transporters by Adenoviral-Mediated Human Insulin-like Growth Factor-1 in a Mouse Model of Placental Insufficiency In vivo and the Human Trophoblast Line BeWo In vitro." *Placenta* 35: 132–38.

Kamphorst JJ, Nofal M, Commisso C, Hackett SR, Lu W, Grabocka E, Vander Heiden MG, et al. 2015. "Human Pancreatic Cancer Tumors Are Nutrient Poor and Tumor Cells Actively Scavenge Extracellular Protein." *Cancer Research* 75 (3): 544–53.

Kapoor A, Yao W, Ying H, Hua S, Liewen A, Wang Q, Zhong Y, et al. 2014. "Yap1 Activation Enables Bypass of Oncogenic Kras Addiction in Pancreatic Cancer." *Cell* 158 (1): 185–97.

Karsli-Uzunbas G, Guo JY, Price S, Teng X, Laddha SV, Khor S, Kalaany NY, et al. 2014. "Autophagy Is Required for Glucose Homeostasis and Lung Tumor Maintenance." *Cancer Discovery* 4 (8): 914–27.

Katayama, R, Shaw AT, Khan TM, Mino-Kenudson M, Solomon BJ, Halmos B, Jessop NA, et al. 2012. "Mechanisms of Acquired Crizotinib Resistance in ALK-Rearranged Lung Cancers." *Science Translational Medicine* 4 (120).

Lee CL, Moding EJ, Huang X, Li YF, Woodlief LZ, Rodrigues RC, Ma Y, and Kirsch DG. 2012. "Generation of Primary Tumors with Flp Recombinase in FRT-Flanked p53 Mice." *Disease Models & Mechanisms* 5 (3): 397–402.

Lim KH, and Counter CM. 2005. "Reduction in the Requirement of Oncogenic Ras Signaling to Activation of PI3K/AKT Pathway during Tumor Maintenance." *Cancer Cell* 8 (5): 381–92.

Mayers JR, Torrence ME, Danai LV, Papagiannakopoulos T, Davidson SM, Bauer MR, Lau AN, et al. 2016. "Tissue of Origin Dictates Branched-Chain Amino Acid Metabolism in Mutant Kras-Driven Cancers." *Science* 353 (6304): 1161–65.

McDermott U, Pusapati RV, Christensen JG, Gray NS, and Settleman J. 2010. "Acquired Resistance of Non–Small Cell Lung Cancer Cells to MET Kinase Inhibition Is Mediated by a Switch to Epidermal Growth Factor Receptor Dependency." *Cancer Research* 70 (4).

Metz HE, Kargl J, Busch SE, Kim KH, Kurland BF, Abberbock SR, Randolph-Habecker J, et al. 2016. "Insulin Receptor Substrate-1 Deficiency Drives a Proinflammatory Phenotype in KRAS Mutant Lung Adenocarcinoma." *Proceedings of the National Academy of Sciences of the United States of America* 113 (31): 8795–8800.

Gordon M, Beltran PJ, Mitchell P, Cajulis E, Chung YA, Hwang D, Kendall R, Radinsky R, Cohen P, and Calzone. FJ 2014. "IGF1R Blockade with Ganitumab Results in Systemic Effects on the GH-IGF Axis in Mice." *The Journal of Endocrinology* 221 (1): 145–55.

Pacher M, Seewald MG, Mikula M, Oehler S, Mogg M, Vinatzer U, Eger A, et al. 2007. "Impact of Constitutive IGF1/IGF2 Stimulation on the Transcriptional Program of Human Breast Cancer Cells." *Carcinogenesis* 28 (1): 49–59.

Paik JH, Kollipara R, Chu G, Ji H, Xiao Y, Ding Z, Miao L, et al. 2007. "FoxOs Are Lineage-Restricted Redundant Tumor Suppressors and Regulate Endothelial Cell Homeostasis." *Cell* 128 (2): 309–23.

Qi J, McTigue MA, Rogers A, Lifshits E, Christensen JG, Jänne PA, and Engelman JA. 2011. "Multiple Mutations and Bypass Mechanisms Can Contribute to Development of Acquired Resistance to MET Inhibitors." *Cancer Research* 71 (3).

Sasaki T, Koivunen J, Ogino A, Yanagita M, Nikiforow S, Zheng W, Lathan C, et al. 2011. "A Novel ALK Secondary Mutation and EGFR Signaling Cause Resistance to ALK Kinase Inhibitors." *Cancer Research* 71 (18).

Schönhuber N, Seidler B, Schuck K, Veltkamp C, Schachtler C, Zukowska M, Eser S, et al. 2014. "A next-Generation Dual-Recombinase System for Time- and Host-Specific Targeting of Pancreatic Cancer." *Nature Medicine* 20 (11): 1340–47.

Sellers K, Fox MP, Bousamra M, Slone SP, Higashi RM, Miller DM, Wang Y, et al. 2015. "Pyruvate Carboxylase Is Critical for Non-Small-Cell Lung Cancer Proliferation." *The Journal of Clinical Investigation* 125 (2): 687–98.

Young NP, Crowley D, and Jacks T. 2011. "Uncoupling Cancer Mutations Reveals Critical Timing of p53 Loss in Sarcomagenesis." *Cancer Research* 71 (11): 4040–47.

Zhang M and Kirsch DG. 2015. "The Generation and Characterization of Novel *Col1a1* $^{FRT\text{-}Cre\text{-}ER\text{-}T2\text{-}FRT}$ and *Col1a1* $^{FRT\text{-}STOP\text{-}FRT\text{-}Cre\text{-}ER\text{-}T2}$ Mice for Sequential Mutagenesis." *Disease Models & Mechanisms* 8 (9): 1155–66.

Zhang M and Kirsch DG. 2016. "Retraction: The Generation and Characterization of Novel *Col1a1* $^{FRT\text{-}Cre\text{-}ER\text{-}T2\text{-}FRT}$ and *Col1a1* $^{FRT\text{-}STOP\text{-}FRT\text{-}Cre\text{-}ER\text{-}T2}$ Mice for Sequential Mutagenesis." *Disease Models & Mechanisms* 9 (12): 1513–1513.

APPENDIX (Please see supplemental material)

Supplemental Table S1. Reverse Phase Protein Array (RPPA) data. List of relative abundance of total proteins and phophoproteins between KP cells (cell lines 1 and 2) and KPI cells (lines 3-6). Cells were either non-serum starved (10% fetal bovine serum or FBS), serum-starved (0% FBS) for 1 hour or serum-starved for 1 hour and stimulated with 50 ng/ml IGF-1 for 10 minutes (indicated as IGF1). Rows indicate the specific cell line and treatment. Columns indicate the levels of the specific protein/phosphoprotein. All values are normalized for protein loading. Data represent the mean ± SD; $n = 3$ biological replicates per condition per cell line.